August 2021

Transcriptomics and Toxcast Data Identify Bioeffects in Zebrafish Embryos Exposed to Chemical Mixtures in an Effluent-dominated Stream

Emma Meade
University of Wisconsin-Milwaukee

TRANSCRIPTOMICS AND TOXCAST DATA IDENTIFY BIOEFFECTS IN ZEBRAFISH EMBRYOS EXPOSED TO CHEMICAL MIXTURES IN AN EFFLUENT-DOMINATED STREAM

by

Emma Bramfeld Meade

A Thesis Submitted in

Partial Fulfillment of the

Requirements for the Degree of

Master of Science

in Freshwater Sciences and Technology

at

The University of Wisconsin-Milwaukee

August 2021

ABSTRACT

TRANSCRIPTOMICS AND TOXCAST DATA IDENTIFY BIOEFFECTS IN ZEBRAFISH EMBRYOS EXPOSED TO CHEMICAL MIXTURES IN AN EFFLUENT-DOMINATED STREAM

by

Emma Bramfeld Meade

The University of Wisconsin-Milwaukee, 2021
Under the Supervision of Professor Rebecca Klaper

Wastewater treatment plant (WWTP) effluent-dominated streams provide critical habitat for aquatic organisms but also continually expose them to complex mixtures of pharmaceuticals and other contaminants of emerging concern (CECs) that can potentially impair growth, behavior, and reproduction. Limited toxicity data on the adverse biological impacts of *in vivo* exposure to these mixtures make it difficult to assess risk for aquatic organisms, particularly with respect to pharmaceuticals whose designed bioactivity often extends beyond conventionally monitored biological pathways. To address this knowledge gap, the goal of this thesis was to identify biomarkers of exposure to complex CEC mixtures relevant to specific chemicals and mixtures in an effluent-dominated stream. RNA sequencing and targeted gene expression were used to identify novel gene and pathway-based impacts of exposure to complex mixtures of pharmaceuticals and other CECs as they related to developmental stage in zebrafish (*Danio rerio*) larvae and seasonal changes in the chemical

mixture composition of the stream. High throughput screening data from the ToxCast database were used to predict biological impacts based on measured chemical concentrations. Together, these data suggest several associations between chemicals (diphenhydramine and thiabendazole) and impacts observed in zebrafish exposures (histaminergic and cardiovascular). While some pathway-based impacts observed in zebrafish exposures were also predicted by ToxCast, many were not (e.g., visual system, musculoskeletal, and metabolic). The results of this work demonstrate a need to expand the ToxCast assay library to encompass bioeffects specific to fish and relevant to pharmaceutical mixtures in WWTP effluent.

TABLE OF CONTENTS

LIST OF FIGURES

LIST OF TABLES

LIST OF ABBREVIATIONS

5-HT	Serotonin
AC50	Half-Maximal Activity Concentration
ACC	Activity Concentration at Cutoff
AMPK	AMP Kinase
AR	Androgen receptor
B-H	Benjamini-Hochberg
BLYES	Bioluminescent Yeast Estrogen Assay
BP	Biological Process
BPA	Bisphenol-A
CC	Cellular Component
cDNA	Complimentary DNA
CEC	Contaminants of Emerging Concern
COX	Cyclooxygenase
DET	Differentially expressed transcript
dpf	Days post fertilization
DS1	Downstream 1
DS2	Downstream 2
DWTP	Drinking Water Treatment Plant
$E_2Eq_{(BLYES)}$	17-Beta Estradiol Equivalents
EAR	Exposure-Activity Ratio
ECM	Extracellular Matrix
EPA	Environmental Protection Agency
GO	Gene Ontology
H1	Histamine receptor 1
H2	Histamine receptor 2
hdc	Histidine decarboxylase
hpf	Hours post fertilization
HPG	Hypothalamus-Pituitary-Gonadal Axis

HRH1	H1 Histamine receptor
HTS	High Throughput Screening
KEGG	Kyoto Encyclopedia of Genes and Genomes
KT	11-ketotestosterone
LC50	Lethal Concentration 50%
LOD	Limit of Detection
LOEC	Lowest Observed Effect Concentration
MAPK	Mitogen Activated Protein Kinase
MF	Molecular Function
mRNA	Messenger RNA
NWQL	National Water Quality Laboratory
PLS-DA	Partial Least Squares Discriminant Analysis
PNOEC	Predicted No Observed Effect Concentration
PPAR	Peroxisomal Proliferator-Activated Receptor
qPCR	Quantitative Polymerase Chain Reaction
RIN	RNA Integrity Number
SERT	Serotonin Transporter
SSNRI	Selective Serotonin-Norepinephrine Reuptake Inhibitor
SSRI	Selective Serotonin Reuptake Inhibitor
Tm CP	Capture Probe Melting Temperature
Tm RP	Reporter Probe Melting Temperature
ToxCast	Toxicity ForeCaster
TQ	Toxicity Quotient
US1	Upstream 1
USGS	United States Geological Survey
vst	variance stabilizing transformation
WWTP	Wastewater Treatment Plant

ACKNOWLEDGEMENTS

I am grateful to many people who have helped make this thesis possible. First, I would like to thank my advisor, Dr. Rebecca Klaper, for her enthusiastic support every step along the way. From lab-work to paper-writing, I learned from her creativity and ability to shape big ideas around complex data and benefitted immensely. I would also like to thank my committee members, Dr. Tim Grundl and Dr. Greg LeFevre for their interest and suggestions throughout my project. This work was supported by grants from the U.S. Geological Survey Grant (Grant 2017IA01G) and programmatic support from the U.S. Geological Survey's Toxic Substances Hydrology Program. I am very grateful to Greg, the PI of this project, for making this research possible and for his extensive feedback throughout the writing process. I would also like to express my gratitude to Dana Kolpin and Luke Iwanowicz for their support during the conceptualization and revision processes. I would also like to acknowledge and thank the many other people who contributed substantially to this project. Dana Kolpin, Shannon Meppelink, Hui Zhi, and Greg LeFevre collected the stream water samples I used for zebrafish exposures and generated the chemical data used in this thesis. Rachael Lane performed the chemical extractions for water samples used in the yeast estrogenicity screen and Luke Iwanowicz generated the estrogenicity data. I am immensely grateful to Angie Schmoldt for sharing her genomics expertise, teaching me best practices in RNA lab work, and preparing my samples for RNA sequencing. I would also like to acknowledge the work of Aurash Mohaimani and Olaf Mueller in processing the RNA sequencing data. My thesis would not have been possible without the instrumental help and support of members of the Klaper Lab: Becky Curtis, Eric

Ostovich, Nicholas Niemuth, Katie Schulz, and Peter Schumann. I would like to thank Becky Curtis, in particular, for her daily check-ins and many collaborations in learning. I would also like to thank and acknowledge the work of Nicklaus Neureuther, who preceded me on this project and established a protocol for the zebrafish embryo exposures. To Jackie Brown, who fueled my interest in science, taught me how to write, and modeled authenticity, I am forever grateful. Finally, I would like to express my enormous gratitude to my wife and my parents for believing in me and patiently supporting me through the many twists and turns of this journey. And to my daughter, Saia, who now loves to feed fish, I am grateful for the many reminders of how interesting and fun this work is!

Chapter 1: Introduction

Contaminants of emerging concern (CECs), which include pharmaceuticals, food additives, flame-retardants, and plasticizers, are largely unregulated but have potential to enter the environment and cause adverse biological effects at environmentally relevant concentrations. Like many emerging contaminants, pharmaceuticals have poorly understood ecotoxicological impacts and are detected globally in surface water,[1–5] groundwater,[6,7] and wastewater treatment plant (WWTP) effluent and influent.[8,9] The occurrence of pharmaceuticals in surface water is of particular concern with respect to aquatic species for several key reasons: (1) their designed bioactivity can effect off-target species,[10] (2) sublethal impacts, which can be consequential to population health but difficult to measure, include altered behavior, reproductive success, and disease resilience, and (3) complex mixtures can result in synergistic toxicities and other interactive effects.[11–13] Ability to detect environmental contaminants at very low concentrations (ng-µg/L) has vastly outpaced ability to interpret their biological significance,[14] and ecotoxicological data relevant to aquatic organisms is not available for most pharmaceuticals.[15] Thus, the task of characterizing potential effects and risks of adverse outcomes that stem from exposure to pharmaceutical residues in aquatic environments is enormously complex.

The primary route of entry into the environment for pharmaceuticals is through WWTP effluent discharged into surface water,[16] often small, lower-order streams.[1] Conventional wastewater treatment processes, which achieve removal of biodegradable organic matter through adsorption to activated sludge and microbial breakdown, are not designed to remove

pharmaceuticals. Pharmaceuticals tend not be metabolized by microbes[17] and may not sorb to solids during filtration due to hydrophilicity,[18] thus removal efficiencies in conventional facilities can be quite low.[8,19,20] Pharmaceuticals encompass compounds with an enormous range of chemical and physical properties, but for many their resistance to degradation is by design. The stability of pharmaceuticals within the body often allows for greater efficiency and specificity in reaching the therapeutic target. For example, the addition of a fluoro-group, which increases the potency and bioavailability of a drug, is common in many highly used pharmaceuticals known to be persistent in the environment including antibiotics (ciprofloxacin) and antidepressants (fluoxetine, citalopram).[21] Although most pharmaceuticals tend not to be highly persistent, continuous input from WWTP effluent can create chronic exposure conditions for aquatic organisms,[22] particularly in small streams where minimal dilution occurs. Consistent detections of pharmaceuticals in remote streams further illustrate the persistence and mobility of many CECs in surface water[23,24] and make it imperative to characterize the biological risks of exposure in effected aquatic ecosystems.

In addition to poor removal efficiencies, widespread detections of pharmaceuticals in surface water can also be attributed to increased consumption[25] and population growth in areas where effluent release occurs away from major rivers and tributaries with high dilution capacity.[26,27] Pharmaceutical consumption has been on the rise globally for the past several decades with 39% growth in antibiotic usage between 2000 and 2015.[28] While most of the recent growth is driven by countries in South America, Asia, and Africa,[29] the United States retains its place near the top in per capita consumption of pharmaceuticals. Nearly half of U.S. Americans reported taking one or more prescription drugs in the past 30 days in a 2007-2010

survey with 10% taking 5 or more prescribed drugs.[30] In 2011-2014, 12.7% of the US population aged 12 and over reported use of antidepressants in the past month.[25] Population growth and the urbanization of watersheds also contributes to the dispersal of pharmaceuticals in surface water, particularly in arid and semi-arid regions without major river systems and stressed groundwater reserves. In these areas, WWTP effluent release is likely to dominate receiving waters which provide the critical ecosystem service of maintaining aquatic and riparian habitat and also supply drinking water intakes.[26]

Aquatic species have often served as sentinels of pollution that can impact human populations, and another motivation for characterizing the sublethal impacts of wastewater exposure is the occurrence of pharmaceuticals and CECs in treated drinking water. Like conventional WWTPs, conventional drinking water treatment plants (DWTPs) provide insufficient removal of pharmaceuticals. Although advanced secondary treatments that use granular activated carbon and membrane filtration can improve removal efficiencies,[31] the separation of wastewater effluent release from DWTP intakes provides the most protection. It is estimated that more than 50% of DWTPs serving populations of 10,000 or more are positioned downstream of at least one WWTP discharge,[32] which presents the possibility of wastewater CECs emerging in finished drinking water.[33] In effluent-dominated streams, the volume of WWTP effluent tends to be consistent regardless of the baseflow in the receiving stream, so drought has the effect of increasing the effluent portion of streamflow. In decreased streamflow conditions projected by climate change models, the median effluent portion of water entering drinking water intakes positioned downstream of WWTPs in the US would rise from 3.6% (current) to 46%.[32] While impact of CECs on watersheds receiving WWTP effluent is

likely to become more pronounced with climate change throughout the arid and temperate U.S,[32] disparities in the impact of *de facto* wastewater reuse are already evident. In Texas, small communities (pop. < 3300) are both more likely to experience high *de facto* reuse of wastewater (greater than 20%) and less likely to have DWTPs with advanced treatment capability.[34] Without national health-based water quality standards for pharmaceuticals and CECs, pharmaceutical levels in drinking water and surface water remain unregulated. The increasing *de facto* reuse of WWTP effluent should inspire serious investment in understanding and managing the potential public health consequences of CEC persistence in surface freshwater. In many parts of the US, water shortages make *de facto* reuse of WWTP effluent inevitable.[35]

Over 900 streams across the U.S. are composed of at least 50% effluent.[32] These effluent-dominated streams provide important habitat for aquatic organisms but continually expose them to complex mixtures pharmaceuticals and CECs. The concentrations at which pharmaceuticals and other CECs are typically found in the surface water are such that acute toxicity is rare, yet many studies have shown that chronic low level exposures in aquatic organisms can alter endocrine system functioning and result diminished reproductive success, changes in offspring sex ratios, and impaired reproductive behavior.[36–38] A dramatic example of endocrine disruption in wild fish populations across the US the widespread occurrence of testicular oocytes in males, which has been associated with exposure to WWTP effluent and other non-point pollution sources such as agricultural run-off and human waste input from septic tank failures.[39,40]

Endocrine disruption effects in fish are well documented among pharmaceuticals across many drug classes, including neuro-pharmaceuticals, antibiotics, and diabetes medications.[41] Initially, the study of endocrine disruption in xenobiotics emphasized the structural similarity of a compound to estrogen or other endogenous hormones to establish potential for interference with hormone receptor binding.[42] Compounds with estrogen-like ring structures such as bisphenol-A (BPA) and phthalates are examples. However, endocrine system responses to xenobiotic exposures are not based solely on interference with hormone receptors, but rather may result from many interconnected biological pathways as is the case with many pharmaceuticals.

The ecotoxicological effects of antidepressants and other neuro-pharmaceuticals on neuroendocrine signaling pathways has received a great deal of attention in the past two decades.[43] Neurotransmitters modulated by antidepressants in the selective serotonin reuptake inhibitor (SSRI) class, for example, are responsible for the stimulation of reproductive hormone pathways. Increased serotonin levels that result from SSRI inhibition of serotonin reuptake may inappropriately activate the hypothalamus-pituitary-gonadal (HPG) axis in fish.[44,45] Amplified stimulation of the HPG axis is likely a factor in the over expression of estrogen-responsive genes, including the egg yolk protein vitellogenin, which has been observed in fish exposed environmentally relevant concentrations of fluoxetine (0.028 μg/L).[46] At a slightly higher environmentally relevant concentration of 1 μg/L, fluoxetine alters behaviors important for successful reproduction in fish including nest-building in fathead minnows (*Promelas pimephales*),[47] and social interactions in medaka (*Orzyzias latipes*).[48]

Metformin, prescribed for management of diabetes and polycystic ovarian syndrome, also impacts reproductive functioning through a variety of interconnected pathways. Metformin acts as an insulin sensitizer through activation of the AMP kinase (AMPK) pathway and bears no structural resemblance to estrogen.[49] Yet, it has also been linked to adverse reproductive impacts in fish including reduced fecundity and induction of testicular oocytes in males.[50–52] These endocrine disruption responses highlight the interconnected nature of the metabolic, neurological, and hormonal pathways that impact behavior and physiology.

Reproductive impairments can be devastating to wild fish populations[53] and the attention endocrine disruption has received in ecotoxicology of pharmaceuticals is warranted. However, there are many more biological pathways relevant to pharmaceutical exposures in fish that are poorly understood. Pharmaceuticals are often designed to target specific receptors in humans that have close homologs in other species, including fish. Examples of pharmaceuticals with protein targets (e.g., enzymes, receptors, and ion channels) that are homologous in fish include antidepressants (serotonin receptors),[54] beta-blockers (β-adrenergic receptors),[55–57] non-steroidal anti-inflammatory drugs (cyclooxygenase (COX) enzymes),[58] and cholesterol-lowering drugs (peroxisomal proliferator-activated receptors).[59] Although the protein targets of pharmaceuticals may be structurally similar across species, their specific functions can vary. For example, cyclooxygenase enzymes, which synthesize prostaglandins used to respond to injury and are homologous across many species, also has additional functions like eggshell formation in birds.[58]

Beyond therapeutic design, many other factors also shape and mediate the biological effects of pharmaceuticals on fish, particularly with respect to experience when exposed to

pharmaceuticals, environmental samples containing pharmaceutical mixtures. These factors include the duration, intensity, and developmental timing of an exposure; the interactive effects of chemicals within a mixture and additional off-target mechanisms of action; the mobility of chemicals across tissue types; and an individual's compensatory response to exposure. In real world exposure scenarios, the chemical composition of mixtures evolves spatially over the reach of a receiving stream and seasonally with changing patterns of human pharmaceutical use.[1] While lab-based exposures to select chemicals are critical, field and lab-based exposures using environmental samples capture more realistic exposure responses. The use of 'omics data, which identifies and quantifies the global the entirety of given biomolecule (e.g., RNA, protein, metabolite) detected within a sample, provides a broad view of exposure responses and allows for the identification of impacts across all mapped biological pathways. Establishing transcriptomic signatures of exposure to chemical mixtures in effluent can identify biological pathways with potential relevance to chemicals within mixtures.[60,61] This approach to identifying potential exposure impacts from complex pharmaceutical mixtures is taken in Chapter 2 of this thesis.

Change across the transcriptome can help identify biologically meaningful responses in chemical mixture exposures, and chemicals in single and multiple contaminant exposures can be distinguished through barcode-like responses within the transcriptome.[62] However, gene expression alone does not yet provide the specificity needed to prioritize chemicals, mixtures, and effects for further investigation.[63] Few genes are specific to single biological functions and many act widely across many different biological pathways. Another approach to interpreting the potential risks of biological impacts from exposure to complex chemical mixtures involves

leveraging high throughput screening (HTS) *in vitro* assay data relating chemical concentrations to biological effects as an interpretive lens. The Toxicity Forecaster (ToxCast) database from the US EPA is one such tool.[64] The database is comprised of hundreds of thousands of data points representing dose-response curves for over 9,000 chemicals screened in highly standardized biochemical and cell-based assays targeting a wide range of biomolecular and cell-based functions. Because of the highly standardized nature of these assays, activity with respect to specific biological targets can be compared across chemicals and across assay platforms. In Chapter 3 of this thesis ToxCast assay data is used to predict the bioeffects of exposure to pharmaceuticals and other CECs detected in an effluent-dominated stream. ToxCast assay data has been used in this way to prioritize contaminants and mixtures for future study in a wide range of contexts.[65–67]

The broad objective of this thesis was to identify the potential biological impacts of exposure to complex pharmaceutical and CEC mixtures in Muddy Creek, an effluent-dominated stream in Iowa, and to relate those impacts to spatial and seasonal changes in chemical composition. The research presented in Chapter 2 profiles the transcriptome-level changes in larval zebrafish at two developmental stages exposed to water samples taken above, at, and below the WWTP effluent outfall in Muddy Creek during the months of January and May. Transcriptome signatures unique to each month and developmental stage were identified, as were genes with consistent expression patterns between months. Chapter 3 of this thesis uses ToxCast assay data to predict bioeffects of exposure to chemical mixtures detected over seven monthly sampling events along an effluent dominated stream. Predicted effects were compared to the gene and pathway level effects identified in targeted and non-target gene

expression from *in vivo* fish embryo exposures to environmental stream water samples of the same months.

Chapter 2: Zebrafish embryo exposure to effluent-dominated stream water reveals transcriptome signatures specific to developmental stage and seasonal changes related to emerging contaminants

2.1 Introduction

Wastewater effluent containing complex mixtures of pharmaceuticals and other contaminants of emerging concern (CECs) poses an increasing threat to environmental health, and small effluent-dominated streams with minimal dilution are particularly at risk. Conventional wastewater treatment plants (WWTPs) were not designed to remove these chemicals, resulting in their frequent detection and wide distribution in surface water including drinking water sources.[23,24,68] Although effluent discharged into small streams typically undergoes substantial dilution once released into higher order waterways, small receiving streams provide important habitat in aquatic and riparian ecosystems.[69] The continual presence of bioactive chemical inputs can produce exposure conditions at concentrations with documented harm to aquatic organisms,[70] particularly during early life stages.[71,72]

Fundamental knowledge gaps still limit current understanding of how complex chemical mixtures impact aquatic organisms. Substantial research has focused on interference with steroidal reproductive hormones;[41,73,74] however, pharmaceuticals have many targets and act upon multiple biological pathways. Embryonic exposures can be particularly consequential and can lead to physiological and behavioral impacts later in development[75,76] and across generations.[77,78] Furthermore, pharmaceutical bioactivity often extends beyond the chemically-engineered therapeutic design, causing sublethal impacts at low concentrations (ng/L-µg/L

range)[79] that traditional toxicological endpoints are not designed to measure.[73,80,81] For example, the insulin-sensitizing diabetes drug, metformin, impairs growth in fish (1-3 μg/L)[51,82] and can induce intersex condition in fathead minnow testes (40 μg/L).[83] In many fish species, environmentally relevant concentrations of antidepressants (less than 1 μg/L) are reported to disrupt stress responses (venlafaxine),[84] reproductive and predator avoidance behaviors (fluoxetine),[47] brain monoamine levels (venlafaxine),[85] and diurnal activity patterns (fluoxetine/sertraline/venlafaxine mixtures).[86] Finally, the dynamic evolution of pharmaceutical mixtures[1] and complex interactive effects between chemicals[87] are difficult to model in a lab, and modulating factors like temperature[88] and pH[89,90] make field studies indispensable to the task of characterizing the biological impacts of effluent exposure. Considering these challenges, RNA sequencing is an appropriate and powerful tool for characterizing the biological effects of effluent on aquatic organisms exposed to field and field-like conditions.

Larval zebrafish (*Danio rerio*) are an excellent model for identifying transcriptome-based biological effects of effluent exposure. Because the zebrafish genome is fully sequenced and biological pathways are largely conserved across vertebrates,[91] identified impacts that are likely relevant to other aquatic organisms as well. Tracking gene expression at multiple time points during embryo and early larval development provides key insight as (1) development is a highly coordinated process dependent upon completion of successive stages,[92,93] and (2) stages differ in vulnerability to environmental perturbations that disrupt development.[94,95] Our research objective was to relate the transcriptomic response of zebrafish embryos exposed to water samples from an effluent-dominated stream to its evolving chemical composition as described in Zhi et al. (2020).[1] An additional goal was to identify biomarkers of effluent exposure that

broaden the range of biological impacts that could be monitored in surface water containing emerging contaminants from wastewater. Zebrafish embryos at 3 and 6 days post-fertilization (dpf) were used to characterize the transcriptomic impacts of WWTP effluent across the reaches of an effluent-dominated stream 100 meters above and below the effluent outfall. These two developmental stages represent periods before and after reliance on yolk ends and thus capture distinct vulnerabilities to environmental insult. Water samples used for exposures in this study were taken in two seasons (winter and spring) and selected due to their contrasting pharmaceutical profiles. We hypothesized that effluent exposure would reveal biological effects beyond current endocrine system related biomarkers, that gene expression would vary with chemical exposure over two seasons, and that disrupted biological pathways would differ by stage of development.

2.2 Materials and Methods

2.2.1 Study Sites and Water Sampling

Muddy Creek is a small effluent-dominated stream in Coralville, Iowa (latitude 41°42'00", longitude 91°33'46") that receives approximately 5,300 m^3 of effluent per day from the North Liberty WWTP[96] and discharges to the Iowa River. The stream's 22.5 km^2 drainage area encompasses a mix of suburban (60%) and agricultural land uses (24.5%).[1] Three previously established USGS sampling sites were used: (1) 0.1 km above the WWTP outfall (US1), (2) the effluent outfall (effluent), and (3) 0.1 km below the outfall (DS1) (Figures A.1 and A.2). Monthly grab samples using the single vertical at centroid-of-flow method[97] were taken in triplicate from each site over 12 baseflow sampling events between September 2017 and August 2018. Replicate samples were used for measurement of 113 pharmaceuticals using a

previously published USGS method,[98] a bioluminescent yeast estrogenicity assay,[99] and zebrafish embryo exposures.[62] Water samples were shipped on ice to the University of Wisconsin-Milwaukee where they were stored at -80ºC prior to use in zebrafish embryo assays and to the USGS Organic Geochemistry Research Lab (Lawrence, KS) for solid phase extraction[100] prior to estrogenicity analysis at the Eastern Ecological Science Center (Kearneysville, WV). Further characterization of the field sites, detailed methods for water sampling, and analysis of the monthly chemical data are available in Zhi et al. (2020).[1]

2.2.2 Animals

Zebrafish embryos were obtained from group spawning events of a wild type 5D zebrafish lab culture (University of Wisconsin-Milwaukee). Adult zebrafish of mixed sexes were housed in a flow-through aquatic system (Aquaneering, San Diego, CA) with recirculating dechlorinated municipal water and fed TetraMin flake twice daily. The system was maintained at 27ºC in a 16:8-hr light/dark cycle. All procedures were conducted in accordance with animal use and care protocols approved by the Institutional Animal Care and Use Committee of the University of Wisconsin-Milwaukee.

2.2.3 Embryo exposures

Fertilized embryos were screened for uniformity in developmental stage progression. Simultaneous 3- and 6-day exposures were performed separately using five replicate petri dishes containing groups of 20 embryos (6 hours post-fertilization) immersed in 30 mL of sample water from each site. Parafilm-sealed petri dishes were incubated at 27°C under a 16:8-hour light/dark schedule. Upon completion, surviving larval fish from each replicate dish were pooled into 1.5 mL tubes and snap frozen in liquid nitrogen for RNA extraction. Samples

exposed to the January and May 2018 US1, effluent, and DS1 sites were selected for RNA sequencing in this study. The selection of January and May sampling events was based on prior published work[1] at this site in which these months captured seasonal pharmaceutical use patterns with higher concentrations of antibiotics in January and antihistamines in May (Figure A.3). The site above the outfall (US1) was used as an in-stream baseline for assessing the relative impact of wastewater effluent exposure.

2.2.4 RNA Sequencing

RNA Extraction, Library Prep, and Sequencing. Total RNA was isolated using standard protocol for Direct-zol RNA MiniPrep (Zymo Research, R2051). Whole embryos were homogenized in TRIzol with a pestle in a microfuge tube, and RNA was purified on Zymo-Spin IIC columns. Sample purity was assessed with a NanoDrop spectrophotometer (Thermo Fisher Scientific, Waltham, MA) with acceptable wavelength ratios of 1.8-2.0 for 260/280nm and 2.0-2.2 for 260/230 nm. RNA integrity (RIN) was measured on an Agilent Bioanalyzer 2100 (Agilent, Santa Clara, CA), and samples with a RIN>7 were used. RNA was quantified on a Qubit 2.0 fluorometer (Invitrogen, Thermo Fisher Scientific, Waltham, MA). Two samples (January US1 3 dpf and May US1 6 dpf) had RIN scores below 7 and were not used for RNA sequencing. Libraries were prepared using Illumina TruSeq Stranded mRNA sample preparation kit (Illumina, RS-122-2102) and IDT for Illumina – TruSeq RNA UD Indexes (Illumina, 20022371) following standard protocol, using 200ng of total RNA. Libraries were sequenced on an Illumina NovaSeq6000 (paired-end 150 bp reads).

Processing of RNAseq Data. The total genomic yield surpassed 2.104 billion paired-end reads with a median per-sample yield of 51 million fragments and a population standard

deviation of 14 million fragments. Sequence data was quality-assessed using FastQC v0.11.5,[101] and sequencing adapters were clipped using Cutadapt v1.18. The resulting quality-controlled data was pseudoaligned and sample-quantified against the GRCz11 Ensembl release of the zebrafish reference transcriptome using Kallisto v0.45.0.[102,103]

DaMiRseq was used to filter and normalize raw count data.[104] Transcripts were removed if they had fewer than 10 counts across 70% of samples or were hypervariant (coefficient of variance threshold of 3). Raw counts were normalized to library size using variance stabilizing transformation (vst), which reduces the dependence of the mean on variance. DESeq2 was used to perform analysis of differential expression between the upstream baseline (US1) and the effluent and DS1 samples.[105] Resulting tables of differentially expressed transcripts (DETs) were re-annotated with Ensembl reference information and relationally joined with Kallisto sample quantification counts using custom tooling. Transcripts differentially expressed at the effluent and DS1 sites (vs. US1) were considered significant at a Benjamini-Hochberg (B-H) adjusted p-value<0.01 and $|\log_2$ fold change$|>1$. To characterize developmental differences at the upstream reference site, DESeq2 was also used to perform analysis of differential expression between the 3 and 6 dpf exposures to US1 samples from the same month. Transcripts were considered to have significantly higher expression at 3 dpf (vs. 6 dpf) and 6 dpf (vs. 3 dpf) at a B-H adjusted p-value<0.01 and $|\log_2$ fold change$|>1$. RNA-seq data are available in the National Center for Biotechnology Information's Gene Expression Omnibus under accession number GSE179335.

2.2.5 PLS-DA and Functional Enrichment.

MixOmics[106] was used for partial least squares-discriminant analysis (PLS-DA) to determine the relative influence of month, exposure length, and site on the overall transcriptome. PLS-DA was performed over all exposures to compare the influence of month and exposure length and performed separately over the 3 and 6 dpf exposures to compare the influence of month and site.

Overrepresentation analysis was conducted on DETs from each comparison using the Kyoto Encyclopedia of Genes and Genomes (KEGG) pathway database[107] and gene ontology (GO) annotations from the Gene Ontology Consortium. GO terms and KEGG pathways overrepresented among significant DETs (vs. US1) were identified using clusterProfiler[108] which employed hypergeometric enrichment tests with a B-H adjusted p-value<0.05 to control for multiple testing and an FDR<0.1. GO terms and KEGG pathways overrepresented among significant US1 3 dpf DETs (vs. 6 dpf) and 6 dpf DETs (vs. 3 dpf) were identified through hypergeometric enrichment tests in g:Profiler using a custom g:SCS significance threshold to control for multiple comparisons and a corrected p-value cutoff of 0.05.[109]

2.2.5 Bioluminescent Yeast Estrogenicity

Total estrogenicity of sample extracts[100] was determined using the bioluminescent yeast estrogen screen (BLYES) as previously described,[99,110] but with minor modifications detailed in Appendix A. The detection limit for this assay was 0.18 ng/L $E_2Eq_{(BLYES)}$.

2.3 Results and Discussion

2.3.1 Transcriptome profiles correspond to effluent chemistry differences across exposure month and differ by developmental stage.

Signatures of WWTP effluent were present in both months at each developmental stage, evident in the full transcriptome and in the proportion of DETs (vs. US1) shared between the effluent and DS1 sites, whose similar chemical profiles are the result of the minimal dilution of the effluent at DS1 (82% in both months).[1] Developmental stage was a strong determinant of the transcriptome profile among all samples (Figure 2.1a). Similarity between the effluent and DS1 sites was evident in PLSDA performed separately on the 3 and 6 dpf exposures where the effluent and DS1 sites of each month were more similar to each other than to the US1 site (Figure 2.1b and c). The influence of effluent exposure was also evident in the proportion of DETs shared between the effluent and DS1 sites within a month and developmental stage. In the January 3 and 6 dpf exposures, 40-42% of DETs were shared between the effluent and DS1 sites. In the May exposures, 76-82% of DETs were shared between sites (Figure 2.1e). All DETs shared between sites within the same month and developmental stage had consistent fold change directions (positive or negative). The overlap between the effluent and DS1 transcriptomes likely reflects the high proportion of effluent to DS1 streamflow in both months: 89% in January and 80% in May (Table A2).[111] Total concentrations of detected chemicals at the effluent and DS1 sites were 15851 and 13013 ng/L in January and 16844 and 13743 ng/L in

May, respectively (Figure A.3). Minimal dilution of the effluent (82% both months) was the only identifiable source of attenuation at DS1.[1]

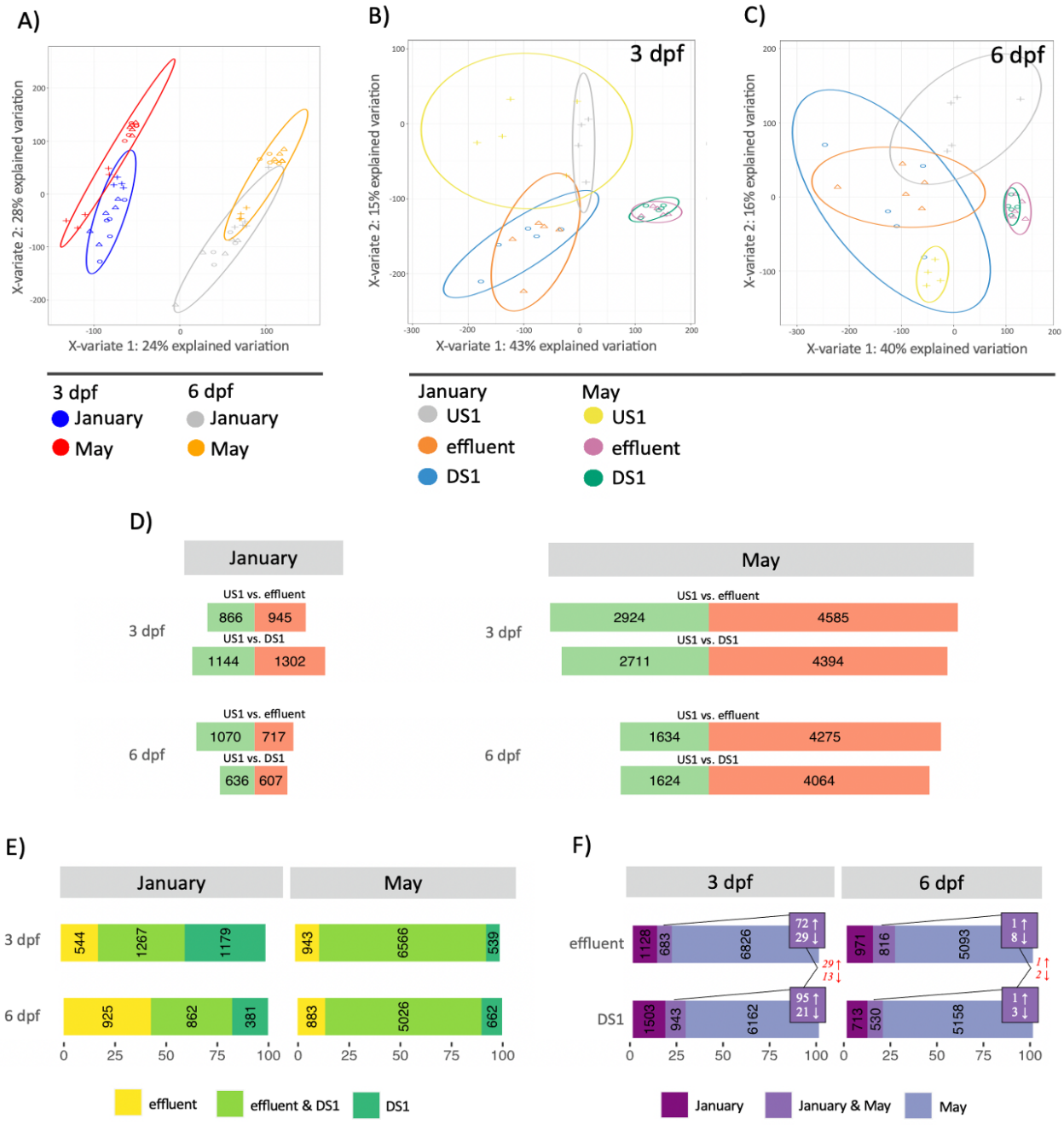

Figure 2.1. *Partial least squares discriminant analysis (PLS-DA) of January and May samples exposed to water from the effluent, DS1, and US1 sites at 3 dpf and 6 dpf. Ovals represent 95% confidence intervals. Sites: + = US1, △= effluent, and ○ = DS1. (A) PLS-DA using samples grouped by month of exposure and developmental stage: Jan 3 dpf (n=14), Jan 6 dpf (n=15), May 3 dpf, (n=15), May 6 dpf (n=14). (B) PLS-DA of 3 dpf samples classified by month*

and site: Jan 3 dpf US1 (n=4), Jan 3 dpf effluent (n=5), Jan 3 dpf DS1 (n=5), May 3 dpf US1 (n=5), May 3 dpf effluent (n=5), May 3 dpf DS1 (n=5). (C) PLS-DA of 6 dpf samples classified by month and site: Jan 6 dpf US1 (n=5), Jan 6 dpf effluent (n=5), Jan 6 dpf DS1 (n=5), May 6 dpf US1 (n=4), May 6 dpf effluent (n=5), May 6 dpf DS1 (n=5). (D) The total number of upregulated (red) and downregulated (green) transcripts with significant differential expression (DETs) from the US1 baseline are represented for each month, developmental stage, and site. DETs were defined as protein-coding transcripts with $|log_2$ fold change$|$ >1 and adjusted p-value <0.01. (E) Number and percent of DETs shared between and unique to the effluent and DS1 sites in each month and developmental stage. (F) Number and percent of DETs shared between and unique to January and May at both developmental stages and sites. Callout boxes indicate the number of shared DETs up- and downregulated in both months (white) and additionally at both the effluent and DS1 sites (red).

The comparatively few DETs (vs. US1) shared between months at the same site and developmental stage highlights the influence of seasonal differences in stream chemistry. Only 8 to 12 % of DETs were shared across month, and those with consistent fold change directions represented at most 1% of DETs (Figure 2.1f). Effluent concentrations of antidepressants (4152 ng/L) and antihistamines (3838 ng/L) were 30 and 36% higher in May compared to January, and H2 antagonists (917 ng/L) and antivirals (841 ng/L) were three times higher. In January, effluent concentrations of antibiotics (992 ng/L) and the corrosion inhibitor methyl-1H-benzotriazole (713 ng/L) were three times higher than in May and beta-blockers at 980 ng/L was 28% higher (Figure A.3, Table A.3).

Among directionally consistent DETs shared between months, 51 were common to both the effluent and DS1 sites in the 3 dpf exposures, and 3 were common to both sites in the 6 dpf exposures. These transcripts appear robust to seasonal variation in Muddy Creek stream chemistry, capturing impacts related to metabolism and autophagy, and could serve as early markers of WWTP effluent exposure (Figure 2.2). Among the 39 upregulated 3 dpf DETs shared at the effluent and DS1 sites were multiple transcripts involved in metabolic processes that generate cellular energy including suclg2, gnpda2, slc2a2, g6pca.2, tmem86b, aldh1l1, abhd14b, cers3a, and abcb11b (Figure 2.2). Growth inhibition and disruption of metabolic pathways are

commonly observed responses to pharmaceutical exposures, although contrary to these results, gene expression is often suppressed.[112,113] For example, downregulation of two genes involved in the citric acid (TCA) cycle, succinate-CoA ligase (suclg2) and glucose-6-phosphatase a (g6pca.2), has been reported in response to neuro-pharmaceutical and antibiotic exposures. The tricyclic antidepressant, mianserin, downregulated g6pca.2 and energy metabolism KEGG pathways[113] in 3 dpf larval zebrafish. Similarly, suclg2 was downregulated in adult Chinese rare minnow (*Gobiocypris rarus*) (1 µg/L carbamazepine)[114] and in 3 dpf zebrafish larvae (antibiotic mixtures of 0.1-100 µg/L), where it was established as a highly influential hub gene.[115]

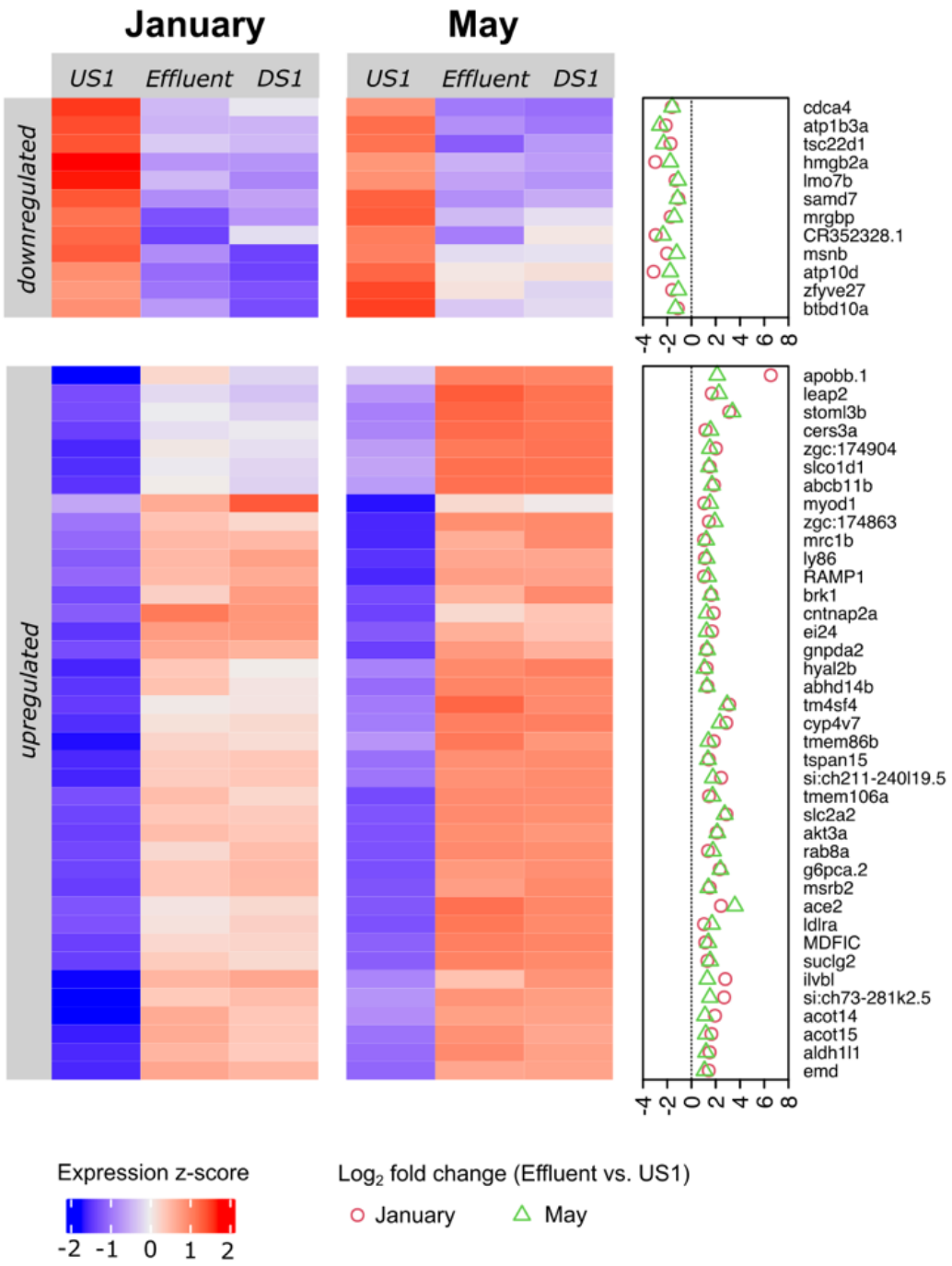

Figure 2.2. *Expression of the 51 protein-coding DETs (adjusted p-value <0.01 and $|log_2$ fold change$|>1$) common to both January and May 3 dpf exposures. DETs were up- or downregulated at both effluent and DS1 (vs. US1). Expression is represented as the z-score of vst counts by transcript.*

2.3.2 Common transcripts suggest important new wastewater exposure biomarkers.

Transcripts related to autophagy were also among the 39 upregulated DETs common to all 3 dpf exposures. The careful regulation of autophagy enables the rapid recycling of cellular components required for the many changes in cellular architecture fundamental to embryogenesis.[116] Regulation of autophagy is also relevant to xenobiotic exposure scenarios in which protein damage occurs or disruptions to cellular energy production require recycled amino acids as a replacement energy source for the TCA cycle.[117] Autophagy related genes upregulated at the January and May effluent and DS1 sites included mannose receptor C (mrc1b) and etoposide induced 2.4 (ei24). Mannose receptors are involved in phagocytosis and endocytic pathways, and mrc1b specifically enables the migration of microglia to the optic tectum during the development of the brain lymphatic system in zebrafish embryos.[118,119] Ei24 is a transmembrane protein in the endoplasmic reticulum that enables crosstalk between the ubiquitin-proteosome system and autophagy, both of which carry out protein recycling, the former by ushering ubiquitin-tagged proteins to the proteosome and the latter through transport of large proteins to lysosomes.[117] Disruptions to normal cellular functions have been described in response to downregulation of these genes,[117,119] so the significance of their upregulation may merely be that an increased need for amino acid recycling requires upregulation of autophagy promoters.

Collagen XIV alpha 1b (col14a1b) was downregulated in the 6 dpf exposures in both months at the effluent and DS1 sites. It was the only 6 dpf DET of a principal isoform with consistent fold change direction month and site. Collagen XIV proteins regulate collagen fibril

formation at all life stages, but col14a1b is only expressed during embryogenesis, likely involved in the formation of embryonic basement membranes and undifferentiated epithelia.[120]

2.3.3 Significant differences in expression signatures across months reflect chemical mixtures.

Differences in expression signatures between US1 and the effluent and DS1 sites were more pronounced in May vs. January, with 2.9 to 4.6 times more DETs (vs. US1) at each site and developmental stage, a greater number of which contributed to enriched functional terms and pathways (Figure 2.1d). Enriched KEGG pathways and biological process Gene Ontology (GO:BP) terms involving the musculoskeletal system, heart, cell adhesion, metabolism, and embryo and larval development were downregulated in January and upregulated in May (Figure 2.3). Nearly all enriched GO:BP terms in 3 and 6 dpf May exposures were upregulated (180 to 238) and few were downregulated (0 to 11) (Table S5). In contrast, the only enriched GO:BP terms in January resulted from downregulated DETs. The reverse mirroring of up and downregulated terms in January and May suggests the possibility of divergent impacts from chemical mixtures between months as well as the possibility of a shift in US1 water chemistry.

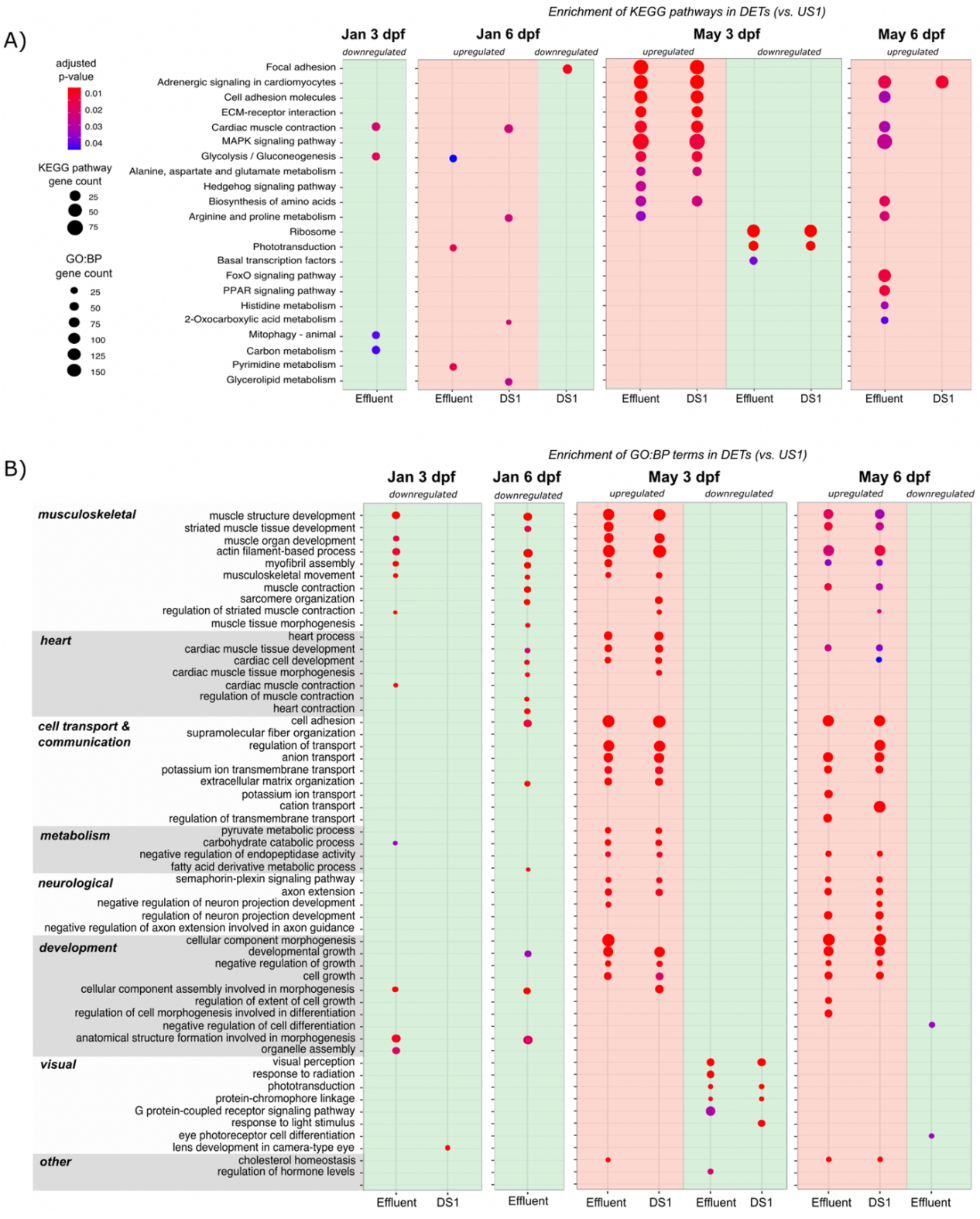

***Figure 2.3**. Statistically significant (adjusted p-value <0.05) overrepresentation of biological pathways and processes of differentially expressed transcripts (DETs, $|log_2$ fold change$|$ >1 and adjusted p-value <0.01) up- and downregulated at effluent and DS1 (vs. US1, the upstream reference) in zebrafish embryo exposures (Jan 3 dpf, Jan*

3 dpf, May 6 dpf). Overrepresentation analysis of Kyoto Encyclopedia of Genes and Genomes[64] (KEGG) pathways and Gene Ontology (GO:BP) was performed in clusterProfiler (R v4.0.1). (A) Overrepresented KEGG pathways from each set of DETs (vs. US1). (B) Selected overrepresented GO:BP terms from each set of DETs (vs. US1).

Although no major biological pathways or processes were unique to the January exposures, several were unique to May. Among upregulated DETs, unique KEGG pathways and biological processes included adrenergic signaling in cardiomyocytes, cell adhesion, ECM receptor interaction, neurological development functions, amino acid biosynthesis and metabolism, and the MAPK, FoxO, and PPAR signaling pathways (Figure 2.3). Regulation of hormone levels, phototransduction and other visual processes were downregulated in May, primarily at 3 dpf, although phototransduction was also upregulated in the January 6 dpf exposures.

The MAPK and adrenergic signaling in cardiomyocytes pathways were upregulated at both developmental stages in May and could be related to several pharmaceuticals present in Muddy Creek effluent including metformin (antidiabetic), beta-blockers, and SSRI/SSNRIs. Metformin regulates glucose levels through inhibition of ATP production within the mitochondria which activates the energy sensing AMP kinase (AMPK) pathway and leads to glucose uptake and fat oxidation in the liver.[49] Metformin also impacts other energy dependent pathways, including the mitogen activated protein kinase (MAPK) signaling pathways, which regulate cell proliferation, apoptosis, glycolysis,[121] and adrenergic signaling pathways responsible for regulation of metabolic “fight or flight” responses to stress. The enrichment of the MAPK, heart contractions/adrenergic signaling in cardiomyocytes, and glycolysis/gluconeogenesis pathways in the May 3 dpf exposures is suggestive of metformin as

a candidate explanatory factor. Two out of those three pathways were enriched at 3 and 6 dpf in January and 6 dpf in May.

In the May 3 dpf exposure, 54 transcripts were deregulated across the adrenergic signaling in cardiomyocytes pathway, including ion membrane transporters, the actin-myosin crossbridge, and a β2-adrenergic receptor (adrb2b) involved in regulation of heart rate (Figure A.4b). Adrenergic signaling receptors are involved in a wide variety of biological processes including heart contractions, lipolysis (breakdown of triglycerides), blood flow, and regulation of metabolism,[122] which could involve interaction with the FoxO and MAPK pathways, both disrupted in the May 6 dpf exposures. Although few studies have examined sublethal impacts of exposure to beta-blockers on fish, propranolol at 80 ng/L is reported to reduce larval zebrafish heart rate[123] and atenolol at 0.01 nM (2 ng/L) can block epinephrine-stimulated glucose production in trout hepatocytes.[124] Total concentrations of the three beta blockers measured at the Muddy Creek effluent site (metoprolol, atenolol, and propanolol) exceed these levels by orders of magnitude (i.e., 980 ng/L in January and 701 ng/L detected in May) (Figure A.3). Although enrichment of the adrenergic signaling pathway was unique to the May exposures, the enrichment of the cardiac muscle contraction pathway in the January exposures involved many of the same transcripts (Figure A.5). The dysregulation of cardiac processes across month and developmental stage is consistent with the presence beta-blockers.

The antidepressant, venlafaxine, also has documented impacts that span many interconnected pathways and biological processes and was one of the top pharmaceuticals detected in Muddy Creek with effluent concentrations at 1240 ng/L (January) and 1550 ng/L (May) (Figure A.3). Venlafaxine is known to disrupt neurological development,[125] MAPK

signaling,[126] metabolism,[84] stress response, locomotor activity,[127] and adrenergic signaling.[124,125] Although the exact mechanism of action on the MAPK pathway is unclear, the direct impact of venlafaxine may result from upregulation of brain derived neuroeffector (BDNF), which initiates a phosphorylation cascade that reaches the MAPK pathway.[126] Impacts to larval fish have been documented at low concentrations; an 80-hour exposure of larval zebrafish to just 80 ng/L of venlafaxine was sufficient to increase embryonic malformations, including loss of pigmentation.[128] Pigmentation abnormalities in larval zebrafish have been associated with delayed development and reduced fitness in other studies, which has been suggested as a possible link to beta-adrenergic signaling given the presence of adrenergic receptors on pigment-producing melanophores.[129] The lack of similar biological pathway and process enrichments in January, however, suggests that venlafaxine is not driving enrichment patterns of DETs between the months examined during this study.

Visual system impacts occurred primarily in the May 3 dpf exposures through enrichment of the phototransduction KEGG pathway and several other visual GO:BP terms among downregulated DETs (Figure 2.3a and 2.3b). Transcripts were downregulated across the phototransduction cascade and included light-sensitive pigments, transducins involved in G-protein signaling, Ca^{2+} and Na^{+} voltage-gated channel proteins, and rhodopsin kinases that deactivate phototransduction in dark conditions (Figure A.4a). In total 71 unique genes were enriched among vision-related biological processes at the effluent site and 61 at DS1.

Impaired eye development in fish necessarily impacts neurological functioning, behavior and metabolic processes, and thus may later impair growth, reproduction, and survival.[80] Many chemicals found in wastewater effluent, including progestins,[130,131] antidepressants,[132,133]

flame-retardants,[134] and pesticides,[135,136] have been associated with visual system disruptions including altered gene expression in the phototransduction cascade. Progestins such as dydrogesterone[130] and norethindrone[131] have been shown to disrupt circadian rhythm, eye development, and the phototransduction cascade during zebrafish development. Antidepressants are known to alter visual motor response in larval fish,[133] and high doses of paroxetine and fluoxetine (100 µg/L) also disrupted phototransduction.[132] At 1 µg/L, the organophosphorus flame retardant triphenyl phosphate has been shown to disrupt phototactic behavior in larval zebrafish and downregulate key photopigment opsin genes, including several on the phototransduction cascade that were downregulated at the effluent and DS1 sites in the May 3 dpf exposures (rho, opn1mw1, opn1mw2).[134] The pyrethroid pesticide cypermethrin impairs eye development in fish embryos[135] and disrupts gene expression across the developing visual system, including the phototransduction cascade (downregulated).[136,137] The fatty acid binding protein 11b (fabp11b), downregulated by cypermethrin,[136] plays an important role in fatty acid metabolism in the developing eye of zebrafish embryos, and was also significantly downregulated ($p<0.01$) in the May 3 dpf exposure with $\log_2$ fold changes of -2.4 and -2.5 at effluent and DS1, respectively.

2.3.4 Upstream estrogenicity signal in May identified by transcripts.

Notable estrogenicity was observed at all sites during monthly collections. This included an estrogenic signal with unknown origins detected by the BLYES assay in May at US1 (Figure 2.4a). The greatest estrogenic measurement of 3.7 ng/L $E_2Eq_{(BLYES)}$ occurred at the US1 site in May, the highest at any of the Muddy Creek field sites over the 12-month study period. This measurement was more than double the estrogenicity of US1 in January at 1.52 $E_2Eq_{(BLYES)}$ ng/L,

which had the lowest measured estrogenicity among stream sample exposures used for RNA sequencing. Estrogenicity was most variable at US1, which had the highest and lowest E_2Eq values of all sites over the 12-month sampling period (1.03 E_2Eq ng/L in November 2017 and 3.7 ng/L in May 2018) (Figure 2.4a). In contrast, estrogenicity measurements below US1 ranged from 1.54 to 1.88 $E_2Eq_{(BLYES)}$ ng/L at the effluent and from 1.55 to 2.37 $E_2Eq_{(BLYES)}$ ng/L at DS1 (Figure 2.4a). The January and May US1 samples thus represent contrasting estrogenic stream gradients with US1 estrogenicity lowest of the three sites in January and highest in May.

Current predicted no effect concentrations (PNOECs) range from 0.1 to 0.73 ng/L $E_2Eq_{(BLYES)}$[138,139] thus identifying the baseline estrogenicity of Muddy Creek as high and of biological significance. The impact of estrogenicity on the zebrafish transcriptome was suggested in comparisons of the 3 and 6 dpf exposures at US1. Functional enrichment of transcripts with significantly higher expression at 6 dpf (vs. 3 dpf) resulted in few typical developmental processes in May but many in January (Figure 2.4c). There were several pharmaceutical detections at US1 in both months,[1] however, not at levels that could explain a strong estrogenicity signal or 6 dpf developmental impacts. In May, more chemicals were detected at US1 and concentrations tended to increase relative to January, but none of the detections in either month were at levels known to be bioactive (Figure A.3). An alternative explanation of the high estrogenicity signal at US1 could be the presence of undetected analytes. Strategic non-targeted chemical analysis could help resolve cases in which distinct bioeffects occur but are not explained by the chemicals detected in a targeted analysis, which would be particularly useful for field reference sites.[140]

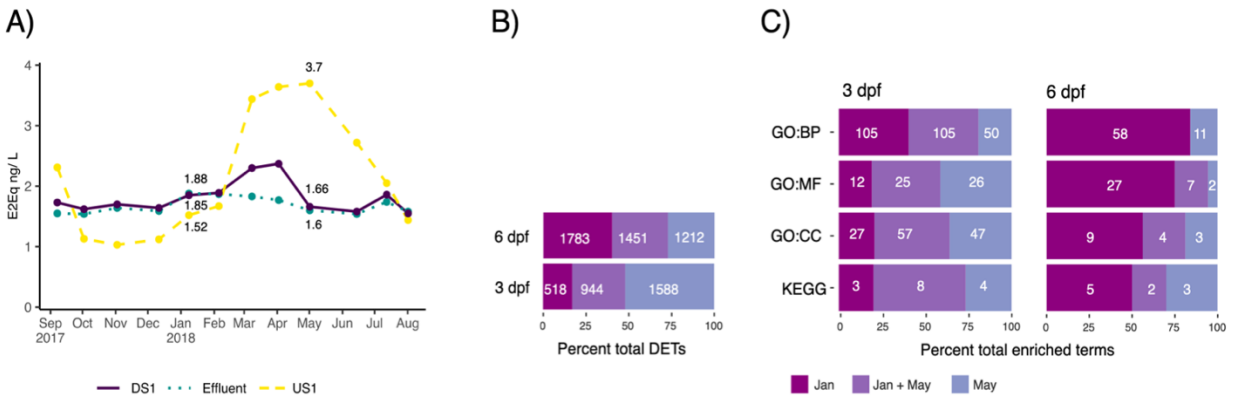

Figure 2.4. A) Calculated estrogen equivalents (E_2Eq in nanograms per liter) relative to 17 β-estradiol of extracts from monthly 1-liter grab samples collected at baseflow, September 2017-August 2018. (B) Percent of total differentially expressed transcripts (DETs) with higher upstream reference (US1) expression at 3 dpf (vs. 6 dpf) and 6 dpf (vs. 3 dpf) unique to and shared between January and May (log_2 fold change >1 between developmental stages and B-H adjusted p-value <0.01). Colors represent the quantity unique to or shared between months. (C) Overrepresentation of biological process (GO:BP), molecular function (GO:MF), and cellular component (GO:CC) Gene Ontology terms and KEGG terms (adjusted p-value <0.05) among DETs with significantly higher expression at 3 or 6 dpf at US1 in January and May.

2.3.5 Stage of development is a significant determinant of transcriptomic response to upstream estrogenicity signal in May.

Differential gene expression and PLS-DA suggest that exposure to the estrogenicity signal at US1 may impact 3 and 6 dpf larvae differently and in ways that are likely due to developmental changes in early fish development. The transition from a rapidly growing embryo to a free-feeding larva leaves tell-tale signatures in the transcriptome that should be evident in comparisons of 3 and 6 dpf.[93,141] To determine whether these signatures of normal development occurred in the January and May exposures at the US1 reference site, we identified overrepresented KEGG pathways and GO terms among transcripts differentially expressed at 3 dpf (vs. 6 dpf) and 6 dpf (vs. 3 dpf) as indicators of developmental progression. At the US1 baseline in both months, there was a consistent overrepresentation of GO terms and KEGG pathways among genes associated with development at 3 dpf.[141] These

overrepresented terms encompassed many biological processes related to this period of rapid cell proliferation and differentiation. Of the 105 biological process GO terms enriched in both January and May 3 dpf transcripts, 80 related to DNA replication and the cell cycle (Figure 2.4c).

Estrogenicity appeared to impact the 6 dpf transcriptome and alter developmental progression in the 6 dpf May exposures. KEGG pathways and GO term enrichments indicative of normal development at 6 dpf (vs. 3 dpf) were present in January, but not in May, which may reflect the sensitivity of this developmental stage to estrogenic exposures (Figure 2.4c). Although more DETs with higher expression at 6 dpf (compared to 3 dpf) were shared between months, there were relatively few shared enrichments (Figure 2.4b); however, several shared molecular functions (GO:MF) related to protein metabolism, an expected contrast between the fully functioning gut of 6 dpf larvae and the yolk-dependence of 3 dpf embryos.[93,141] Enrichments unique to January encompassed a wide variety of processes known to be more relevant to the 6 dpf life stage (vs. 3 dpf) and related to the immune system, response to the environment, circadian rhythm, visual system, bile synthesis, ammonium transport, lipid transport, all of which are required for hunting and free-feeding. Digestion and metabolism, the most prevalent category, made up nearly half of all enriched terms (25/58).

In contrast, the few enrichments unique to May transcripts with higher expression at 6 dpf (vs. 3 dpf) were narrow in scope and related to amino acid catabolism and biosynthesis, glycerolipid metabolism, and membrane transporters. Overall, May lacked enrichment of genes linked to typical developmental pathways. Pathways related to the visual system and muscle development were absent and there were notably few related to digestion and metabolism, which represented less than 50 genes total. Although this analysis suggests the possibility that

that normal development at 6 dpf was disrupted, there are many other factors unaccounted for that could contribute to the contrast between January and May comparisons. An additional consideration is that synchronicity across individuals during development lessens as development progresses into the larval stage.[94] Thus, the 3 dpf developmental stage may serve as a more reliable model for relating the bioeffects of effluent exposure to chemical composition.

2.3.6 Environmental implications.

A goal of our research was to identify common transcriptome markers of effluent exposure in larval zebrafish as well as markers specific to developmental stage and seasonal variation in pharmaceutical mixtures. Ultimately, we see that variation in chemical signatures across months is recapitulated in gene expression, and that even with estrogenic input observed in the US1 reference site, the transcriptome can still reveal key relationships between pathways and processes relevant to understanding environmental effects of chemical exposures. There were several dozen significant DETs from the 3-day exposures that had consistent fold change directions in both months, including transcripts with key roles in embryo and larval fish development such as mrc1b and ei24 and many related to energy production and metabolism. These transcripts do not represent therapeutic or other known targets of any particular chemical detected, and rather likely represent the off-target impacts that many pharmaceuticals have on metabolic functioning and fish development and therefore could provide new biomarkers for monitoring the impact of effluent. In addition, the disruption of normal developmental pathways in the 6 dpf larval fish underscores the need for biomarkers

specific to developmental stage and indicates that specific developmental pathways may serve as biomarkers of endocrine disruption.

Chapter 3: *In vitro* predictions vs. *in vivo* reality: Molecular impacts of exposure to WWTP effluent in zebrafish embryos are partially predicted from aggregated ToxCast data

3.1 Introduction

Over the past several decades, the ability to detect environmental contaminants at very low concentrations (ng-ug/L) has vastly outpaced ability to interpret their biological significance.[14] While *in vivo* toxicological studies provide the most robust effects data for environmental contaminants, the need for relevant bioeffects data is far too vast and immediate for the traditional whole-animal approach to toxicology.[142] The problem of prioritizing chemical contaminants found at low concentrations is compounded in aquatic environments where complex mixtures exist and can evolve rapidly over time[1,143] with potential impacts to many biological pathways. In the case of wastewater effluent, which serves as a consistent source of pharmaceuticals, pesticides and other compounds with designed bioactivity, sublethal endpoints that capture changes in growth and behavior are needed as effects of this nature have potential to decrease resilience and impact reproductive success.[78,84]

Pharmaceutical mixtures in wastewater effluent have been shown to harm organisms and aquatic ecosystems,[144] and variation and complexity of exposure conditions make tools that assess bioeffects and predict exposure risk critical to the task of prioritizing contaminant mixtures that may pose harm to aquatic organisms. The discovery of potent endocrine disrupting effects in environmental contaminants in wildlife near the turn of the century galvanized interest in assessing the environmental safety of the tens of thousands of chemicals

known to be in circulation.[42,58] Evaluating the safety of so many chemicals required a shift to high throughput screening (HTS) methods as traditional animal toxicity testing would not have been feasible at such a scale due to the time and resources required. The ToxCast and Tox21 programs (hereafter referred to as ToxCast) were established to meet this need through the use of highly standardized *in vitro* HTS assays in which endpoints and dose-response curves are comparable between assays and chemicals.[64,145] ToxCast assays evaluate the bioactivity of individual chemicals over a wide range of assays designed to detect effects at the cellular and molecular level across over 300 signaling pathways.[146,147] To date, over 9,000 chemicals have been tested in at least some of the 1473 assays across 15 different platforms.[148] These platforms are primarily cell-based in assay design, with one biochemical-based platform and one whole-organism (zebrafish) platform. Assay endpoints include non-specific effects (e.g., cytotoxicity, oxidative stress, cell morphology changes) and specific pathway-based effects measuring things like nuclear receptor activity (e.g., androgen receptor, aryl hydrocarbon receptor). The interpretive value of this data has increased with the expanding universe of adverse outcome pathways (AOPs), which seek to build linear models linking specific molecular initiating events resulting from chemical exposures to responses at progressively higher levels of biological organization and then to an adverse outcome at the organismal level.[149]

ToxCast data has been successfully used to prioritize chemicals and bioeffects concerning human and wildlife exposure in many contexts.[66,100,150] Nevertheless, several factors limit the interpretive strength of ToxCast predictions in aquatic ecotoxicology. Some of these limitations include a lack of species representation (nearly all cell-based assays are mammalian) and the fact that pharmaceuticals have less assay coverage than needed given the specificity of

their design. Additionally, while ToxCast data is rich in molecular effects data, standardized phenotype data are still needed to connect those effects to key events and adverse effects in associated AOPs. Although ToxCast endpoints encompass nearly 400 unique gene targets and 148 AOPs, disruptions within a biological pathway are not uniform and assays can miss consequential biological responses. Given these limitations, *in vivo* exposures with aquatic species are needed to compare to ToxCast predictions and to identify biological effects that should be prioritized in the ongoing project of expanding biological pathway coverage in new ToxCast assays. Transcriptomics and other non-targeted 'omics data provide opportunity to identify activity across all biological pathways and confirm activity within genes and pathways of interest.

The goal of this project was to use aggregated ToxCast assay data to identify the potential biological impacts of detected chemicals, both individually and in mixtures, as chemical composition evolves spatially over a 5 km stretch of an effluent-dominated stream and seasonally across seven monthly sampling events. Impacts predicted by ToxCast were compared to gene expression patterns previously identified in an RNA sequencing experiment of larval zebrafish exposed to environmental water samples taken from sites along an effluent dominated creek in Iowa (January and May 2018). Additional targeted gene expression in exposure to samples from seven monthly sampling events between January and August 2018 was also used in conjunction with ToxCast predictions to identify potential chemicals and mixtures over three seasons that may pose harm to larval fish.

3.2 Materials and Methods

3.2.1 Study Sites and Water Sampling

Muddy Creek, an effluent-dominated stream in Coralville, Iowa (latitude 41°42'00", longitude 91°33'46") was the field site for this study as described in Chapter 2. Additional description of the field site is available in a prior publication as are complete water sampling and chemical analysis methods.[1] All chemical data used in this study has been publicly released and is available online.[111] In brief, Muddy Creek has a low annual baseflow and a 22.5 km^2 drainage area composed of mixed suburban (60%) and agricultural (24.5%) land uses.[1] The stream receives 0.061 m^3/s from the North Liberty WWTP,[96] which accounts for 80-90% of streamflow below the effluent outfall. Streamflow ranged from 0.034 to 0.19 m^3/s (median 0.061 m^3/s) on the actual sampling time points used in this study (January-August 2018) at the U.S. Geological Survey (USGS) gaging station (station ID 05454090; DS2). Monthly grab samples used for chemical analysis and zebrafish embryo exposures were taken using the single vertical at centroid-of-flow method[97] during baseflow conditions between January 2018 and August 2018 from four USGS sampling sites: (1) 0.1 km above the WWTP outfall (US1), (2) the effluent outfall (effluent), (3) 0.1 km below the outfall (DS1), and (4) 5.1 km downstream from the outfall at a USGS gaging station (DS2) (Figure A1).

3.2.2 Chemical data

The chemical data used in this study consists of previously reported data collected and analyzed by USGS in which all sampling procedures and analytical methods are fully described in prior publications.[1,111] Samples were collected at the four USGS sampling sites described above and analyzed for 113 pharmaceuticals and CECs at the USGS National Water Quality

Laboratory (NWQL, Denver, CO). Chemical concentrations reported as estimated are values between the limit of quantitation and long-term method detection limit and were included as detections in the analyses described.

3.2.3 Zebrafish embryo exposures

Fertilized embryos from wild type 5D zebrafish (University of Wisconsin-Milwaukee) were exposed to water samples from each of the four Muddy Creek sampling sites and a dechlorinated tap water control for 6-day exposures to stream water samples. Animal care protocol and embryo exposure procedures are fully described in Chapter 2. Briefly, groups of 20 fertilized embryos were screened for developmental uniformity at 6 hours post-fertilization and placed in petri dishes with 30 mL of sample water from each stream site. Petri dishes were incubated at 27°C under a 16:8-hour light/dark schedule for 6 days. Surviving larvae from each dish were pooled into 1.5 mL tubes and frozen in liquid nitrogen for subsequent RNA extraction. All samples from the monthly exposures between January and August 2018 were used in gene expression assays for the study except for March 2018, which was excluded due to size constraints. The upstream site 100 meters above the outfall (US1) was used as an in-stream baseline for assessing the relative impact of wastewater effluent exposure.

Total RNA was use isolated using the standard protocol for Direct-zol RNA MiniPrep (Zymo Research, R2051). Whole embryos were homogenized in TRIzol with a pestle in a microfuge tube, and RNA was purified on Zymo-Spin IIC columns. Sample purity was assessed with a NanoDrop spectrophotometer (Thermo Fisher Scientific, Waltham, MA) with acceptable wavelength ratios of 1.8-2.0 for 260/280nm and 2.0-2.2 for 260/230 nm and quantified on a Qubit 2.0 fluorometer (ThermoFisher Scientific, Waltham, MA).

3.2.3 Gene expression

nCounter. Nanostring nCounter Technology (Seattle, Washington) was used to directly quantify transcript abundance for 46 genes associated with exposure to pharmaceuticals and other wastewater contaminants in samples from seven monthly 6 dpf exposures (January-August 2018, excluding March 2018). The nCounter platform provides transcript quantification comparable to quantitative real-time polymerase chain reaction (qPCR) in sensitivity and specificity with the advantage of being able to multiplex up to 800 gene targets per sample. The nCounter analysis platform directly evaluates transcript abundance through imaging color-coded probes designed to capture specific mRNA targets such that no conversion to cDNA is required.[151] Probes were selected based on the RNAseq data presented in Chapter 2 and other literature[152,153] and represent genes associated with endocrine disruption from exposure to CECs,[152] disruptions to cellular energy metabolism, and circadian rhythm. CodeSet details for the 50 gene targets (46 genes of interest and 4 housekeepers) are provided in Table 3.1. The nCounter assay was conducted per manufacturer protocol using 50 ng RNA per sample and 24-hour hybridizations. nSolver Analysis Software 4.0 was used for quality control of the transcript abundance data. Eight negative control probes were included by the manufacturer to capture non-specific binding. As per manufacturer guidance, the negative control probe with the highest counts was removed from each sample if it registered more than twice the number of counts as any other negative control probe within a sample. The limit of detection (LOD) was determined separately in each exposure month and site as the geometric mean of the negative control probes plus two standard deviations. The LOD ranged from 21.5 to 35.7, and genes with

counts below the LOD in any sample for a given comparison between a stream site and the upstream reference (US1) were excluded from further analysis.

The R package NanoStringDiff[154] (v 1.20.0) was used to normalize counts to housekeeping genes, negative control probes, and positive control probes, which account for pipetting errors and other lane differences, and for differential expression analysis. Housekeeping genes included acidic ribosomal phosphoproteins (arp), eukaryotic translation elongation factor 1 alpha 1, like 1 (eef1a1l1), hypoxanthine phosphoribosyltransferase 1 (hprt1), and actin beta 1(actb1), which were selected based on literature[152,155] and assessed for stability using NormFinder.[156] The stability values of housekeeping genes ranged from 0.05 to 0.08, which indicates low variation between sample subgroups. Because nCounter transcript abundance data is count-based, a normal distribution cannot be assumed for low-expression genes with counts close to zero. Thus, statistical methods used for other count-based transcript abundance data (e.g., RNAseq) are most appropriate. Differential expression between stream site and the reference (US1) was calculated in NanoStringDiff[154] which uses a negative binomial-based model and an empirical Bayes shrinkage method to estimate a dispersion parameter for each gene. A gene was considered to have significant differential expression between stream site and the US1 reference if the magnitude of its $\log_2$ fold change exceeded 0.75 with a Benjamini-Hochberg (B-H) adjusted p-value below 0.05.

RNA sequencing data. RNA sequencing data from the 6 dpf larval zebrafish exposures at the US1, effluent, and DS1 sites in January and May were used as described in Chapter 2. Differentially expressed transcripts (DETs) in comparisons of the effluent and DS1 sites to the upstream reference (US1) were considered significant at a $\log_2$ fold change threshold of 1 (B-H

adjusted p-value < 0.01). Statistical significance and biological relevance of functional annotation groups represented among DETs was established through overrepresentation analysis (B-H adjusted p-value<0.05).

Table 3.1*. Genes and target sequences used in the custom Nanostring CodeSet. Melting temperatures for the reporter probes (Tm RP) and capture (Tm CP) probes are indicated in degrees Fahrenheit. Housekeeping genes are noted with an asterisk.*

Accession Number	Gene	Tm CP	Tm RP	Target Sequence
NM_131846.2	ache	80	81	TTAATCTGTTGTAAGCATAAGAGTGCAGATCAAAGAAAAGGGAAAACTGATGACCATAACCCTTAATAGTCTCTTTTCAGAACGGCAATGGCTGCCAAAG
NM_131031.2	actb1*	83	84	AGGAAGTGCTTCTAAACAGAACTGTTGCCACCTTAAAATGGCCATGCAATGAGATTCAAACGAACGACCAACCTAAACCTCTCGAACAAGATGACATCAG
AF134852.1	arp*	85	81	CACCGGGCTCGGTCCTGAGAAGACCTCTTTCTTCCAGGCTTTGGGAATCACCACCAAGATCTCCAGAGGAACCATTGAAATCTTGAGTGACGTTCAGCTT
NM_001024816.2	ahr1b	85	81	ACAAAACTGAGAACTGGATCCATACACCATTGTCTCAAGTGCCTACAACAGAATCTGAGACAGCTAACTTTAACCAGCATGATACTACTTTGGTGAACTC
NM_131128.1	apoa1a	85	82	GAGCAGCACCTCTCAGGGCTTAATCATGAAATTCGTGGCTCTTGCACTGACTCTTCTCTTGGCCTTGGGTTCCCAGGCCAATTTGTTCCAGGCTGATGCC
NM_001083123.1	ar	83	80	TTCCTCTGTATGAAGGCCCTCCTCCTGTTTAGCGTCATTCCAGTGGAGGGGCTGAAGAGTCAGAAGTATTTTGATGAGCTGCGTCTGACGTACATAAACG
NM_199611.3	arg2	86	84	AGAGATGTGGATCCAGGCGAGCATGTATTCCTAAAGACCCTGGGAATTCAGTACTTCTCCATGCGGGACATTGACAGAATGGGCATTCAGAGAGTAATGG
NM_001271393.1	camk2b1	83	81	AAATACGGATAAATAAGGCCTCAGCGAGTCGTCTGTGAAACGCCATGCTTTCCGTCGCACCTTCCCAGTGTCAATAACGTTACACTGAATCACCGTCCTC
NM_001114708.2	camk2d1	81	84	GTTCAACGCCAGGAGGAAGCTTAAAGGTGCTATTCTTACTACCATGCTTGCCACACGGAACTTCTCAAGCAAAAATCCATACAAGAAACCTGATGGTGTC
NM_130912.2	cat	81	83	GGGATTTTTGGAGCTTGCGTCCTGAATCGCTGCACCAGGTGTCTTTCCTGTTCAGTGATCGAGGGATTCCCGATGGCTACCGTCATATGAACGGATACGG
NM_131786.2	cry2	85	84	TACATGTATGGAAGGGTGGTGAGACTGAAGCCCTGGAAAGATTAAATAAACACTTGGATAGGAAGGCCTGGGTAGCAAATTTTGAGAGGCCTAGAATATC
NM_131788.1	cry5	89	79	AGGCCATGGGTCACCCTAAAAAACCTATTCCTGCTCCAACCAACGAGGACATGCGAGGTGTGTCCACTCCACTTTCTGATGATCATGAAGAAAAGTTTGG
NM_212806.3	cyp17a1	84	82	CGTGGATTTTGCAAAGGTTTACTCTGGAGATGCCCACTGGCCAGCCTCTGCCTGACCTCCAGGGCAAGTTTGGCGTGGTTCTTCAACCCAAGAAATTCAA
NM_131154.3	cyp19a1a	85	85	CTCTACGTTTTCACCCGGTCGTGGACTTCACCATGCGGCGGGCGCTGGATGATGATGTCATCGAGGGCTACAACGTGAAGAAAGGAACAAACATCATACT
NM_131642.2	cyp19a1b	80	81	AACCTAATCCTGAACATTGGACGCATGCATAAGACAGAGTTCTTCAAAAAACCCAACGAATTCAGCTTGGAGAACTTCGAGAACACTGTTCCCAGTCGTT
NM_131879.2	cyp1a	84	82	ACGAAAACTCCAACCTGCAAGTGTCCGATGAGAAGATCGTAGGAATCGTCAATGACCTATTCGGAGCCGGTTTCGACACTATCAGTACGGCTCTGTCCTG

Accession Number	Gene	Tm CP	Tm RP	Target Sequence
NM_213067.1	dusp1	78	80	CCAGACGTTTGCTTGTCTGTAAACAAACAGCGAAATACCTCATGTGTCTGTAC TGTTGTCAGTCCGGTAAGAGTCCTCTTCCCTTAAGCACTACTAACAG
NM_131263.1	eef1a1l1*	84	81	GAAGGCTGCCAAGACCAAGTGAATTTCCCTCAATCACACCGTTCCAAAGGTT GCGGCGTGTTCTTCCCAACCTCTTGGAATTTCTCTAAACCTGGGCACT
NM_200016.1	eif3d	82	79	ATGTGCTGCACACGCTCTGTCAACTCCTGGGATATTATCGTTCAGCGTGTGGG CAACAAGCTCTTTTTCGACAAGAGAGACAACTCTGATTTTGATCTGC
NM_152959.1	esr1	89	88	GAGATGCTGGACGCTCAGCGGTTCCAGTCTTCAGGGAAGGTGCAGCGAGTG TGGTCTCAGAGCGAGAAAAACCCTCCATCTACACCCACAACCAGCAGCA
NM_180966.2	esr2a	82	84	GTCACACAAACACAGTACTTAAGGATGATCTGTAGTTTCGGGAGGATGGACA ACCAAAACACCCACATAAAAGCAAGGAGTAGGATTTCACAAGACGAAA
NM_174862.3	esr2b	81	89	CCCTGAACAATTGGTTAGCTGTATTCTAGAGGCGGAGCCACCTCAAATTTACC TGAGAGAGCCGGTGAAAAAGCCATACACTGAGGCTAGCATGATGATG
NM_205569.1	fosab	85	89	GCTCAAAGAAAAAGAGAGGTTAGAGTTCATCCTCGCCGCACACAAACCCATC TGCAAGATCCCGGCCGACGCCAGCTTCCCAGAGCCGTCCTCCTCTCCC
NM_131585.1	fth1a	85	89	ACCCTCACATGTGCGATTTCATTGAGACACACTACTTGGACGAGCAGGTCAAA TCCATCAAAGAACTGGGCGACCATGTGACCAACCTGCGCCGCATGGG
NM_001077326.1	gabra1	89	89	ACTCGAGGGGCGGCGCAGTCCGTGGTCGTGGCTGACGATGGTTCCCGTCTCA ACCAGTATGACTTGATGGGACAGAGCGTAGACTCGGGCGTGGTGCAGT
NM_131869.2	gnat2	81	82	CCACGGACACAAAGAACGTCGAGATTGTGTTTAACGCCGTGACAGACATTAT CATCAAAGAAAACCTTAAGGACTGCGGTCTGTTCTAAACACCATCCAC
NM_199967.1	gngt1	84	80	GCCCATGGACACCTGTTAAAAACGTAATACTTGCTGGAATTCGCTGCCCAAAA AAGGACATTCTCAAACACGGATAGACGTTGGTTAACTCTAAATGGCT
NM_001204332.1	gngt2b	89	86	CTCCTAGCAGGACACAACACACTTCTCTGACTGCCGCAGGGCCCGACAATCCA CAGTCAGGATGGCTCGGGACATGTCAGATAAAGAAATCCTGAAGATG
NM_182887.2	gnrh3	84	85	CAATGGAGCAGCTTTCACCAATACACATAGTGAATGAGGTGGATGCTGAAGG TTTGCCTCTGAAAGGACAAAGATTTCCAGACAGACGGGGAAGAGTGTA
NM_001007281.2	gpx1a	81	85	AAATACGTCCGTCCTGGAAATGGCTTCGAGCCCAAATTCCAAATTCTGGAGA AGCTGGAAGTGAATGGTGAAAACGCCCACCCTCTGTTTGCGTTCCTGA
NM_001327762.1	gstt1a	80	82	TGGATTCTGCCTTGGAGGATCTCAACATGTCTTTGAAGATCTTTGAGGACAAA TTTCTGCAGAGCAGGCCCTTCATAATAGGGGATAAAATATCTCTGGC
NM_001310042.1	hif1ab	82	80	CCCAGTGGAACCAGACATCAGTTCTGAATTTAAACTCGACCTGGTTGAGAAA CTGTTTGCTATTGATACCGAAGCAAAGACACCTTTTTCCACCCAGCCC
NM_212986.2	hprt1*	85	80	CAGGTTAGTGGTCCTCCACTCAGGGTCTCTGGTGAGGTGTGTGCTGTTAATG CACCTTACATTTACATTCACTTATACCTCCACAGGCACCCAACAAACA
NM_205584.2	hsd17b1	85	80	CCTCCATGGACGGCTCTCAGTACATCAGAGCAATGAGCAAACTCATCTTCTCT TCTCCCGGTACAGATGCACAGAAATGATGCCAACACAGAGTTTCATT
NM_212797.1	hsd3b2	83	86	TCCTTTATATACACCAGCAGCATTGAGGTAGCGTGTCCCAATCGCAGCGGTG AACCCATCATCAACGGCCACGAGGACACGCCTTACTCCTCTTATCCTA
NM_001098732.1	hspb15	85	82	TGCAAGAAAATACAAGCTTCCGGCTGACTTAGACCTAAAACAGATCAGCTCC ATGCTGTCTCCAGATGGTGTTCTCTCAGTTGAAGCTCCATTAACGGGC
NM_001098257.2	igfbp1b	86	84	CTCATCCAGCAGGGTCCGTGTCACACTGAGCTTCTCGCGTCTCTGGACGTCAT CACAGAGTCTCAGCAGGCGTTGGGAGAGAAGTTCACCAGTTTCTACC

Accession Number	Gene	Tm CP	Tm RP	Target Sequence
NM_131075.1	mt	92	81	TGCGCCAAGACTGGAGCTTGCAACTGTGGTGCCACCTGCAAGTGCACCAATT GCCAGTGTACAACCTGCAAGAAGAGTTGCTGTTCTTGTTGCCCGTCTG
NM_001020711.3	nr3c1	82	83	TCAGCAACCAGTTACCAAAATTCAAAGATGGGAGTGTTAAACCGCTGCTCTTT CACCAGAAATGAATCTCCTCCCAACAGCAGGACACGATGCCTTAAAT
NM_214751.1	pck1	89	89	AGGACGGTGAACCGTGTGCTCACCCGAACTCCCGCTTCTGTACGCCGGCCGC TCAGTGTCCCATCATCGACCCGCAGTGGGAGTCTCCTGAAGGCGTCCC
NM_213192.1	pck2	84	85	TGGTTCCGGAAAGATCAGAAGACTGGCTCCTTTCTGTGGCCAGGATTTGGAG AGAACGCCCGTGTCCTTGAGTGGATCTTCAAACGATGTGGCCGTACCA
NM_212439.2	per1b	81	80	TTTGGCTCCCACGAAGAGGTTGTGGTCTGTTTGCAAGCTCGATTTGGGCGGA GATATGGAATACTTCGCTTTAGCCCACTCTGGATTTGACCTCAAGACG
NM_001161333.1	pparaa	80	83	GCTCCTCTGCTCCATCATAATGTCATATTCGCAGGCTGGAGTTGTAGATATGG GAACGTGGCTAACGAAGTGTAACTTTTAGAGTGGTCTGCGTCATACC
NM_131467.1	pparg	85	81	GAGACAAAGCTTCGGGGTTTCATTACGGCGTTCACGCCTGCGAGGGATGCAA GGGTTTTTTCCGCAGGACGATTCGCCTGAAGCTGGTGTACGATCACTG
NM_131294.1	sod1	80	83	GGTGTTGCAAAAATTGAAATCGAGGATGCAATGCTAACTTTGTCAGGCCAAC ATTCTATTATTGGGAGGACCATGGTGATTCATGAGAAGGAGGATGACT
NM_131663.1	star	84	84	CAAACTGAGATTGAGAGTATCAACGGGGAGAAGGTCATGAGTAAAGTCCTG CCTGGCATTGGAAAGGTTTTTAAGTTGGAAGTGACCCTGGAACAGCAGA
NM_198914.2	sult2st1	86	75	ATGGGACTGAACACCTCATCTGATCTCTCCTGAGCTGCATACATTCACTGTAG CCTTTGGTGCTCGATTAGTATACAGATGTTTTATCCACTCCAGCATA
NM_131396.1	thraa	86	89	ATTGTGAAGACGTTACACAATCGACCTGAGCCCACCGTGTCAGAGTGGGAAC TCATTCGTATGGTGACGGAGGCTCATCGGCACACCAATGCCCAGGGCC
NM_131340.1	thrb	80	83	CATTGACAAAGTTACCCGAAACCAGTGCCAAGAATGTCGCTTCAAGAAATGC ATCGCTGTTGGCATGGCTACAGACTTGGTATTGGATGACAGTAAACGT
NM_001044897.3	vtg1	82	86	AAGTTACTGGCAAGTTTTCTTGGGGTGCGGAGTGCAAACAGTATGCAGTCTT TGCTAAAGCTGAAGCTGGTGTCCTGGGTGAATTCCCTGCTGCACGTCT

3.2.3 ToxCast bioeffects screening

The 109 pharmaceuticals and degradates measured in Muddy Creek represent a small fraction of the over 4,500 active pharmaceutical ingredients in current use.[157] Globally, over 600 pharmaceuticals and transformation products have been detected in wastewater effluents.[158] The designed bioactivity of pharmaceuticals poses a particular threat to aquatic communities in combination with other exisiting threats to aquatic communities such as habitat loss and other anthropogenic watershed disturbances.[159–162] The stability of pharamceuticals in

the environment and their consistent presence all but guarantees sublethal effects among non-target organisms in wastewater effluent impacted streams and raises the question of whether molecular interactions and sublethal impacts resulting from pharmaceutical mixtures may eventually lead to adverse effects at an organismal or population level. As the ToxCast assay library has expanded, an increasing number of endpoints are designed to target specific biological pathways known to be impacted by contaminant exposures. ToxCast assays screen chemicals over a series of concentrations and are highly standardized in design and execution such that direct comparisons across chemicals and assays are possible. A chemical is considered "active" in a particular assay if the dose-response curve best fits a hill or gain-loss model over a constant model.

Concentrations of pharmaceuticals and other contaminants analyzed in Muddy Creek water samples were compared to bioactivity data in version 3.2 of the ToxCast database[163] using the open-source R package toxEval (v.1.2.0)[164] guided by previously published parameters.[165,166] The biological importance of detected chemicals is established through the use of exposure-activity ratio (EAR) values, which relate the measured concentration of a chemical in a sample to the concentration at which a threshold of bioactivity response is reached in a given ToxCast assay (Equation 1). A ratio greater than one indicates that the measured concentration of a chemical exceeded the threshold at which biological effects were detected in a particular assay. The threshold used to establish assay activity was activity concentration at cutoff (ACC), which is the concentration at which a dose response curve rises above background level.[167]

$$Exposure\ Activity\ Ratio\ (EAR) = \frac{measured\ conc.\ of\ the\ chemical\ (\mu M)}{ACC\ of\ the\ chemical{-}assay\ endpoint\ (\mu M)} \qquad (1)$$

The ACC is an assay-specific threshold determined from a multiplier of median absolute deviation of activity across all chemicals tested within the assay. Metrics like half-maximal concentration (AC50) can also be used to generate EAR values; however, the advantage of ACC is that it normalizes variation in chemical potency as the activity cutoff point is determined relative to all chemicals tested in a given assay.[168]

Assay endpoints with common biological targets or within the same AOP are presumed to have additive effects[169] and thus EAR values can be summed to represent integrated risk across multiple chemicals. EAR values were grouped and summed in different ways to address specific questions about the aggregated effects (Equation 2). To assess the relative biological importance of the different chemicals measured in Muddy Creek, individual assay-chemical EAR values were grouped and summed by chemical. To predict likelihood of molecular effects within specific biological pathways from exposure to all chemicals in a sampling event, EAR values were grouped and summed by the gene or biological targets of assay as has been done previously.[170–174] ToxCast EAR values used in this way are analogous to and have demonstrated consistenency with traditional *in vivo* toxicity quotients (TQ) generated from existing water-quality benchmarks.[166] A chemical prioritization study of contaminants in Great Lakes tributaries demonstrated consistency between a TQ of 0.01 and EAR of 0.001 when used as a threshold for establishing probable effects.[166] Thus, an EAR of 0.001 was used as an effects threshold in this study.

$$EAR_{group} = \sum EAR_{[all\ assay\ endpoints\ relevant\ to\ the\ group]} \quad (2)$$

As pharmaceuticals are often tested in ToxCast as chemical salts formulations but quantified in the environment in their non-ionic forms, input CASRNs were adjusted to reflect

salt formulations if a non-ionic form was unavailable or had less assay coverage. Of the 67 pharmaceuticals detected over the sampling period, 49 had assay data available as either a free compound (15) or salt (34), of which 20 only had data available in salt form and 14 had greater assay coverage. Table B.1 lists pharmaceuticals formulations used in the ToxCast analysis that differed from those measured analytically in stream water samples. As described in Blackwell 2017, non-ionic and salt forms were considered equipotent for the purposes of EAR generation and the molecular weights used to calculate ACC values (µM) reflect measured compounds.[167]

Of the 1473 assays in the ToxCast database, 449 were available for the chemicals measured in the study. Many of the quality assurance considerations described in prior studies[165,167,175] to eliminate non-specific and irrelevant endpoints and unreliable dose-response curves were also used in this study. Quality control flags are used within the ToxCast database to identify unreliable dose-response curves and false-positive results. Assay-chemical pairs were excluded from consideration if any one of the following quality control flags was assigned: “Borderline active”, “Only highest conc above baseline, active”, “Gain AC50 < lowest conc & loss AC50 < mean conc”, and “Biochemical assay with < 50% efficacy”. Assays reporting in the “loss” direction from the Attagene platform and “gain” direction from the NovaScreen platform were also removed from consideration as these assays were not designed or optimized for those signal directions. All remaining assay-endpoint curves contributing to EAR values>0.001 were manually inspected to ensure that only reliable dose-response curves were considered ACC value determination. All exclusions are summarized in Table B.2.

A final curated selection of 276 assays were considered for determining EAR values for the 49 detected chemicals with ToxCast assay coverage, which resulted in 955 unique chemical-

assay combinations. Assays used for EAR determination monitored some of the following bioeffects and targets: cytotoxicity (75), steroidal and non-steroidal nuclear receptors (40), rhodopsin-like receptors (38), DNA binding (27), ctyochrome activity (16), ion channel activity (7) and steroid hormone acticivity (5). The median number used to screen each chemical was eight and ranged from one assay for 11 chemicals to 78 assays used to screen the anithistamine loratadine.

3.3 Results and Discussion

3.3.1 ToxCast predicts bioeffects that capture a narrow set of pharmaceuticals with some seasonal and spatial variation within the stream.

Although nearly half of the 49 chemicals with ToxCast assay coverage generated EAR values that exceeded the 0.001 threshold for biological relevance, a smaller set of chemicals was responsible for the most relevant bioeffects predicted by ToxCast assays (Table B.3). When individual chemical-assay EAR values were summed by chemical (EAR_{chem}), 24 of the 49 chemicals with ToxCast assay coverage generated EAR_{chem} values above 0.001, and 18 chemicals generated individual chemical-assay EAR values above 0.001 (Table B.3). Assays contributing to EAR_{chem} values above 0.001 evaluated biological targets relevant to some specific biological pathways, such as those containing steroidal nuclear receptors or G protein-coupled receptors, and others with non-specific effects like DNA repair and cytotoxicity (Table B.3).

Chemicals responsible for predicted bioeffects most relevant to fish included carbamazepine, diphenhydramine, and metformin, which all had EAR_{chem} values that exceeded 0.01 at the effluent and DS1 sites in every month examined (Figure 3.1). In all months except for April, carbamazepine EAR values exceeded 0.1 at the effluent and DS1 sites. The maximum

EAR_{chem} values (ranging from 0.042 to 0.25) at the effluent, DS1 and DS2 sites in all months excpet April and May were generated by carbamazepine. Carbamazepine is an anticonvulsant known to be persistent in the environment and did not differ substantially between month or between stream sites (Effluent, DS1, and DS2). On the other hand, diphenhydramine, a first-generation antihistamine did exhibit variation by stream site and month with the highest concentrations observed at the effluent and DS1 sites during sampling events in April and May, months that mark spring allergy season in Iowa. Diphenhydramine frequently went undetected at the DS2 site (5 km below the WWTP effluent outfall) but consistently detected in the approximate range of 50-200 ng/L at the effluent and DS1 sites (Figure B.4). Chlorpheniramine, omeprazole, and thiabendazole also had bioeffects predicted with EAR_{chem} values above 0.01 at the effluent site in at least four of the seven months analyzed.

Many of the chemicals detected at highest concentrations in the months analyzed were not among those with high EAR_{chem} values. Notably missing were relevant endpoints for the ten antidepressants and degradates surveyed in Muddy Creek, some of which occurred at levels known to cause behavioral changes in fish including venlafaxine[125,176] and bupropion.[177] Venlafaxine did have two EAR_{chem} hits above 0.001 at the effluent sites in January and May, but they were the result of non-specific endpoints (cytotoxicity as measured by the "Tox21 RT HEPG2 GLO" assay series) (Figure 3.1). Several pharmaceuticals and degradates (fexofenadine, guanylurea, gabapentin, sulfamethoxazole, and tramadol) were consistently detected at concentrations above 100 ng/L at the effluent, DS1, and DS2 sites in the months examined but have not yet been screened in any ToxCast assays (Figure B.3)

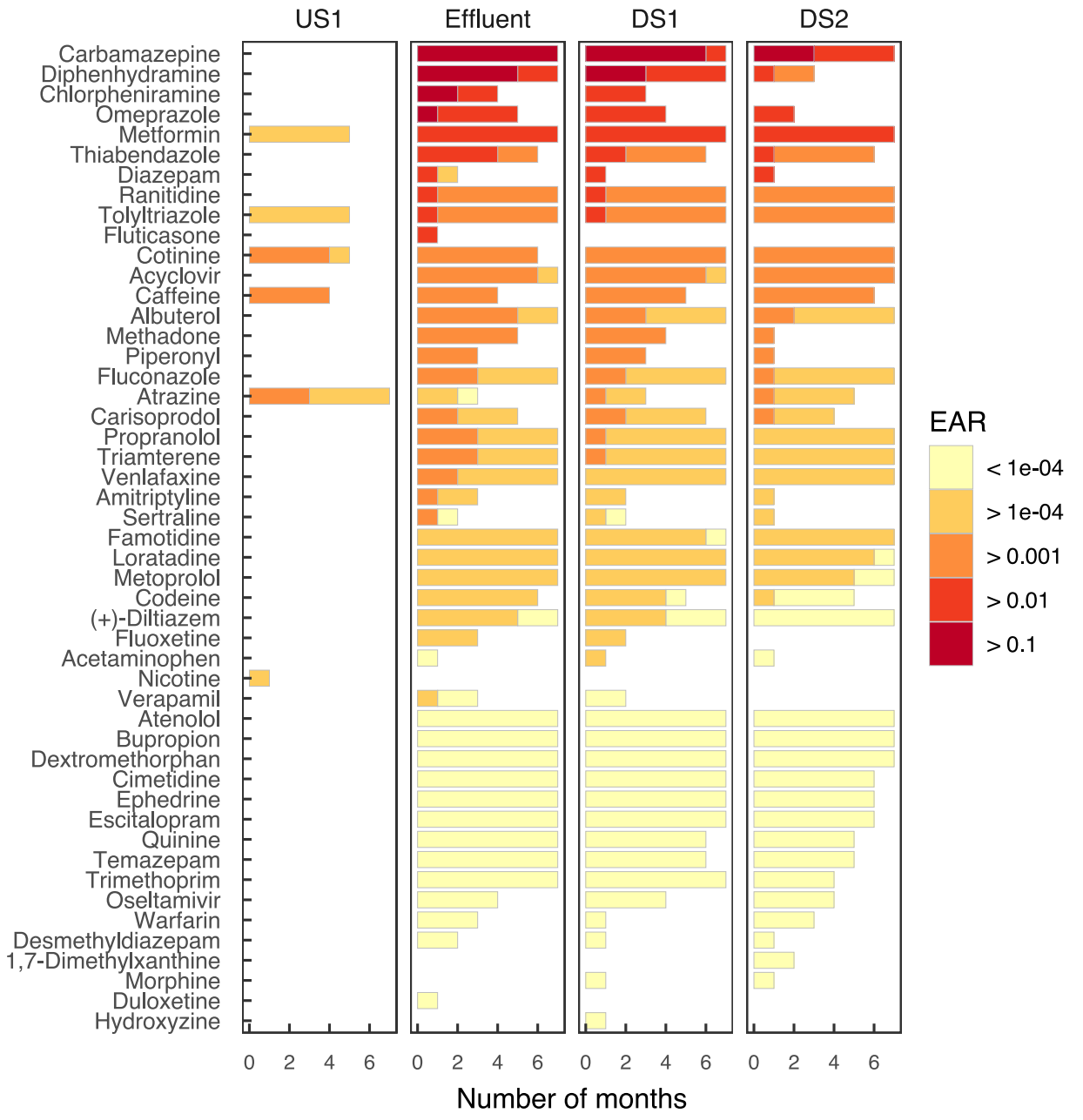

Figure 3.1. *Exposure activity ratio (EAR) values for each chemical-assay endpoint are summed by chemical to produce the EAR_{chem} values shown below for the 49 pharmaceuticals and other CECs detected at each stream site in monthly sampling events (January 2018 – August 2018, excluding March). Individual exposure-activity ratios are calculated as the quotient of the measured concentration of each chemical in a sampling event divided by activity concentration at cutoff (ACC) for a specific assay.*

Assessing EAR values grouped and summed by common gene and biological targets instead of by chemical provides a way to compare predicted biological pathway effects to those

observed experimentally through gene expression. Over the seven months examined, 20 assay gene targets that had at least two instances of EAR_{gene} values above 0.001 (Table 3.2, Figure 3.1). The androgen receptor (AR) was the target of the top EAR_{gene}, which was aggregated from EAR values of four chemicals with bioactivity in four distinct AR agonism assays. However, in all instances, carbamazepine contributed to the bulk of EAR_{gene} value for AR. Diphenhydramine was the only chemical that contributed to EAR_{gene} values for the H_1 histamine receptor gene (HRH1) despite the presence of other chemicals with the same mechanisms of action. Chlorpheniramine, another a first-generation antihistamine designed to target the H_1 histamine receptors, has not been screened against any histamine assays in ToxCast.

Table 3.2. *ToxCast* assay gene targets and chemical mixtures that generated EAR values greater than 0.001 when grouped and summed by gene target are shown below. Shaded months indicate the presence of at least one site with ΣEAR_{gene} >0.001. Maximum ΣEAR_{gene} values noted in the month in which the maximum EAR value occurred. *Fluticasone only contributed to ΣEAR_{gene} mixtures for AR and NR3C1 in May.

Gene	Chemicals	Jan	Feb	Apr	May	Jun	Jul	Aug
AR	Carbamazepine, Ranitidine, Metformin, Fluticasone*	0.29						
HRH1	Diphenhydramine				0.21			
FOS|JUN	Caffeine					0.038		
NR3C1	Metformin, Fluticasone*				0.024			
CYP1A1	Thiabendazole	0.010						
SOX1	Caffeine	0.0059						
CYP1A2	Thiabendazole	0.0056						
OPRM1	Methadone							0.0052
CHRM3	Diphenhydramine			0.0030				
CHRM5	Diphenhydramine			0.0026				
TSHR	Albuterol		0.0025					
SLC6A4	Methadone							0.0022
PPP2CA	Thiabendazole	0.0020						
CHRM1	Diphenhydramine			0.0019				
CHRM2	Diphenhydramine			0.0016				
CYP2C19	Diphenhydramine				0.0015			
CHRM4	Diphenhydramine			0.0014				
PDE4A	Atrazine					0.0014		
HTR2C	Diphenhydramine			0.0014				

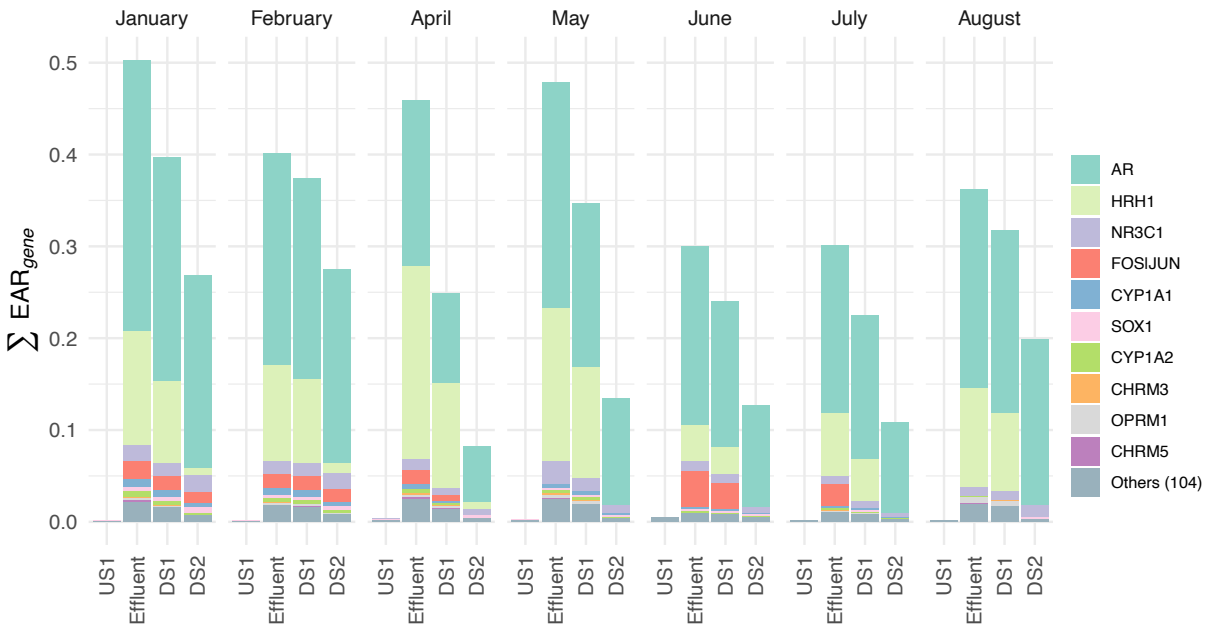

Figure 3.2. *Exposure activity ratios of chemical-assay endpoints summed by gene target (ΣEAR_{gene}) in each month and site.*

3.3.2 Contextualizing the high EAR values of carbamazepine and diphenhydramine.

The two primary chemical and gene targets prioritized in the ToxCast analysis already have well-documented ecotoxicological impacts, particularly with respect to fish. The adverse effects of carbamazepine on the male reproductive system that are well known in mammals[178–181] have also been reported in fish. In *Danio rerio*, chronic (6-week) carbamazepine exposure at 0.5 µg/L decreased reproductive success and 11-ketotestosterone (KT) plasma levels in both male and females, and increased mortality among directly exposed embryos.[176,182] Paternal exposure to carbamazepine 10 µg/L led to transgenerational impairments in reproductive behaviors and success.[183] Carbamazepine functions as voltage-gated sodium channel blocker is prescribed to treat seizures, neuropathic pain, and bipolar II.[184] Although the mechanism through which carbamazepine disrupts 11-ketotestosterone production and lowers

reproductive capacity is unclear, and it is possible that reducing the excitability of neurons (by maintaining voltage gated sodium channels in their inactive state) may also decrease the neuronal stimulation needed for steroid hormone synthesis and normal reproductive organ function.[185] In *Danio rerio*, chronic (6-week) exposures to carbamazepine at 0.5 µg/L decreased reproductive success and 11-ketotestosterone (KT) plasma levels in both males and females and increased mortality among directly exposed embryos.[176,182] Paternal exposure to carbamazepine at 10 µg/L led to transgenerational impairments in fecundity and behaviors related to reproductive success.[183,186] Exposure to 1 µg/L upregulated AR transcription in female medaka (*Oryzias latipes*).[187] A 28-day exposure to carbamazepine in gilthead sea bream (*Sparus aurata*) generated significant enrichment of androgen and estrogen metabolism pathways.[188]

Diphenhydramine is a first generation H_1 antihistamine with several mechanisms of action relevant to ecotoxicity. In competing with histamine to bind to H_1 receptors in smooth muscle cells, it prevents the vascular dilation that causes swelling and redness associated with allergic reactions.[189] More recently, recently diphenhydramine has been shown to reduce allergic response not just by competitively blocking HRH1 but also by inhibiting production of histamine in the first place by downregulating the rate limiting enzyme that synthesizes histamine, histidine decarboxylase (HDC).[190] Diphenhydramine crosses the blood-brain barrier allowing it to target the 5H-T (serotonin) reuptake transporter (SERT),[191] which is the source of its sedative effects, and the muscarinic acetylcholinesterase receptor, which it competitively antagonizes.

The LC50 of diphenhydramine is high in fish (692 mg/L for 3 dpf zebrafish and 262 for 6 dpf),[189] and as a result antihistamines are often considered to pose low risk to aquatic vertebrates. However, sublethal impacts on behavior have been documented at much lower concentrations of diphenhydramine, possibly owing to its inhibition of serotonin reuptake.[191] For example, an LOEC of 5.6 μg/L was established for reduced feeding rate in fathead minnows (*Promelas pimephales*).[192] More recently, the histaminergic system has drawn attention for the role it plays in modulating aggression and other behaviors important in establishing social hierarchies in zebrafish.[193,194] Histidine decarboxylase (hdc) was shown to be upregulated in dominant zebrafish, along with histamine receptors hrh1 and hrh2.[195] Elevated hdc expression was maintained in adult offspring of dominant (male and female) zebrafish pairings in a transgenerational study that identified inherited dominant and subordinate behaviors.[194] In addition to the production of histamine for allergic responses, hdc also plays a role during embryonic brain development where histamine regulates the number of hypocretin/orexin neurons that are hypothesized to eventually regulate the number of mast cells producing histamine in adults.[196] The expression of hdc in larval zebrafish thus may contribute to the plasticity of the histaminergic system in the brain later in adulthood. Finally, the histamine/H_1 receptor axis is now also recently known to play an essential role during cardiac development in larval zebrafish in promoting cardiomyocyte differentiation through activation of the ERK 1/2-STAT3 pathway.[197]

3.3.2 I*n vivo* data aligns with some ToxCast bioeffect predictions.

In vivo exposures capture some molecular and pathway-based impacts predicted by ToxCast assay data, such as impacts to the histaminergic system and some biomarkers of

cardiovascular impacts. Although most protein targets in ToxCast are likely conserved across all vertebrate species,[198] ToxCast assays were primarily designed to target mammalian endpoints.[146] Thus, many exposure bioeffects relevant to zebrafish development are not screened in existing ToxCast assays, including the visual system, metabolic, and musculoskeletal impacts observed in the January and May embryo exposures (Chapter 2).

Diphenhydramine generated EAR_{gene} values for the HRH1 gene target of 0.17 and 0.12 at the effluent and DS1 sites in May and 0.12 and 0.09 at the effluent and DS1 sites in January. While the HRH1 gene was not detected in RNA sequencing of zebrafish larvae in Chapter 2, histidine metabolism was statistically overrepresented at the effluent site in the 6 dpf May exposure. Notably, there was a -4 log_2 fold change ($p<0.01$) in hdc expression at both the effluent and DS1 sites in May (at both 3 and 6 dpf) but no significant differential expression of the gene in January (Figure 3.3). Diphenhydramine was the only antihistamine detected with the ability to downregulate hdc expression.[190] Diphenhydramine concentrations at the effluent and DS1 sites were 113 and 81 ng/L in January and 150 and 109 ng/L in May (Figure B.4).

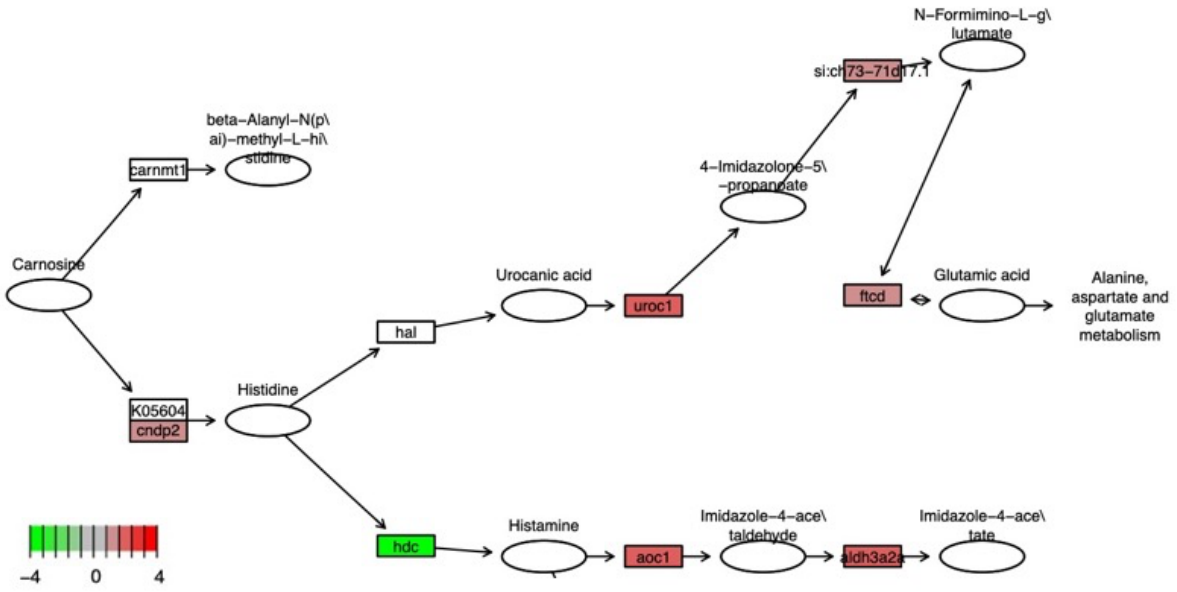

Figure 3.3. *Gene expression from RNA-sequencing of 6 dpf larval zebrafish exposed to water from the May effluent site. Log2 fold changes relative to the US1 site are shown on the KEGG pathway for histidine metabolism (dre00340).*[107] *Ovals indicate metabolites and rectangles indicate genes. Pathway rendered by Pathview.*[199]

Of all assay gene targets with EAR values>0.001 in January and May, eight had significant differential expression in RNA sequencing of larval zebrafish exposures: AR, SLC6A4A, OPRM1, PPP2CA, CYP1A, NR3C1, CHRM4A, CHRM2A, and PDE4A. The two targets with the greatest EAR values when summed by gene target were the androgen receptor (AR) and the glucocorticoid receptor (NR3C1), both of which are on the gonadotropin releasing hormone receptor pathways (Panther Pathway, P06664). The three chemicals identified in ToxCast assays contributing to these EARs were ranitidine, metformin, and fluticasone; however, fluticasone was only quantified above detection limit in May (0.32 ng/L at effluent). NR3C1 was not differentially expressed in the two exposure months used for RNA sequencing, but AR was significantly upregulated in the 3 dpf May comparisons between US1 and effluent (log_2 fold change 1.28, adjusted p-value<0.01) and between US1 and DS1 (log_2 fold change 1.39, p<0.01).

However, the androgen receptor was not detected in January exposures there was little evidence of systematic impacts to hormone and reproductive pathways in either month.

The phosphatase 2a catalytic unit (PPP2CA) and the cholinergic receptor muscarinic 2 (CHRM2) are both involved in cardiovascular processes. The antifungal agent, thiabendazole, generated significant bioactivity in an assay targeting PPP2CA, a gene involved in several biological pathways including the KEGG pathway, "Adrenergic signaling in cardiomyocytes," with EAR values of 0.002 and 0.001 at the effluent site in January and May respectively. Although "Adrenergic signaling in cardiomyocytes" was only overrepresented among differentially expressed transcripts in the May exposures (Figure 2.3), the zebrafish ortholog ppp2ca was significantly dysregulated at the effluent site in the 6 dpf exposures of both months (log_2 fold changes of 5.0 in May and -4.7 in January, p-value<0.05). In an assay targeting CHRM2, diphenhydramine generated EAR values of 0.001 at the effluent site in both January and May. In zebrafish, chrm2a plays a role in the development of the cardiac conduction system and regulation of heart rate. Chrm2a was significantly upregulated at the effluent and DS1 sites in the May 3 and 6 dpf exposures with log_2 fold changes ranging from 3.6 to 4.6 (p-value<0.01) and was significantly downregulated at DS1 in the January 3 dpf exposure (log_2 fold change -2.6, p-value<0.05).

Targeted gene expression was used to quantify expression of select genes differentially expressed in RNA sequencing and other common wastewater biomarkers in zebrafish across seven monthly exposures between January-August 2018 (excluding March). Transcript abundance measurements from the NanoString platform were also used to validate differential expression in RNA sequencing from Chapter 2. Eight genes differentially expressed at the

Effluent and DS1 sites in May and January were also significant in RNA sequencing and fold changes between the two platforms were comparable ($R^2 = 0.82$) (Figure A.6). Of the 46 genes targeted by the NanoString CodeSet, 21 were differentially expressed in comparisons of the effluent, DS1, or DS2 sites to the upstream reference (US1) ($|\log_2$ fold change$|>0.75$, $p<0.05$) (Figure 3.4). Genes with significant differential expression targeted pathways related to steroid hormones, brain and eye development, lipid and glucose metabolism, circadian rhythm, and xenobiotic response. Genes related to circadian rhythm (per1b, cry2, cry5) were differentially expressed at DS1 and DS2 in January, May, and June. Genes with neurological and visual system functions were upregulated at DS2 in January (gngt2b, gngt1, gabra1) and downregulated at the effluent site in May (gnat2, gngt2b). Pck1 plays a role in glucose metabolism and was downregulated in April (DS2) and June (all sites) but upregulated in May (DS1, DS2).

Genes with functions related to steroid hormones and reproductive processes were upregulated at DS2 in January (cyp19a1b, cyp17a, hsd17b1, hsd3b2, and vtg), upregulated at DS2 in February (cyp17a), and upregulated at the effluent and DS1 sites in April (vtg1, cyp17a). The lack of differential expression in these reproduction related genes at the effluent site is notable. One technical factor was that several of these genes were expressed at levels close to the limit of detection at the effluent site and thus could not be reliably quantified.

Figure 5.4. *Log_2 fold changes (vs. US1 reference) of all genes with significant (B-H adjusted p-value<0.01) upregulation (red) and downregulation (green) relative to the US1 reference site.*

3.4 Environmental implications.

The prioritization of pharmaceuticals and other CECs that exist in complex chemical mixtures in wastewater effluent-dominated surface water is a challenge. Traditional ecotoxicological endpoints such as mortality and gross deformities may drastically underestimate exposure risks in fish as they do not capture the neurological impacts and other sublethal impacts of pharmaceutical exposure that may alter feeding and reproductive behavior.[200] The EAR approach to leveraging environmental chemical data against the chemical-assay dose-response curves in the ToxCast database can identify and aggregate potential molecular bioeffects to generate predictions about sublethal impacts that may be relevant to aquatic species.

Sublethal molecular and biological pathway impacts predicted by ToxCast assay data identified carbamazepine and diphenhydramine individually as likely to cause molecular impacts with respect to androgen and H_1 histamine receptors. The overrepresentation of the histidine metabolism KEGG pathway and downregulation of hdc in May was consistent with ToxCast predictions. While the histaminergic system in zebrafish allows for substantial brain plasticity, the potential impacts of suppressed hdc expression during early development on aggression and social behavior in adulthood should be further explored. Mixtures of chemicals with AR activity (carbamazepine, metformin, ranitidine, and fluticasone) were predicted to effect reproductive pathways, but gene and pathway-based biomarkers of endocrine disruption were not evident in global and targeted gene expression of zebrafish larvae. However, many of these genes are expressed at very low levels during larval development. While it is possible that biologically relevant changes in gene expression occurred below the detection limit in both RNA sequencing and NanoString, it is also possible that the impact of some endocrine disruptors may depend on stage of development and could impact pathways outside those associated directly with reproduction.

Enormous complexity is involved in assessing the risk of biological effects from exposure to complex chemical mixtures in wastewater effluent. Contaminants found in wastewater effluent, including pharmaceuticals, pesticides, and other chemicals with designed bioactivity, can alter gene expression and disrupt cellular functions at very low exposure concentrations, but the associated risk of those impacts ultimately depends on whether they lead to adverse effects within individuals. The AOP framework has proven invaluable to the task of integrating knowledge from the ToxCast database with ‘omics and phenotype data to establish the

relevance of early biochemical responses to chemical exposures.[201] However, the utility of ToxCast bioeffects predictions in aquatic ecotoxicology is inherently limited by the coverage of biological pathways and biological functions within the ToxCast library. While the conservation of biological pathways relevant to both human health and other vertebrates is substantial, effluent-dominated streams continuously expose fish to contaminant mixtures, which may result in exposure scenarios less relevant to human health such as continuous exposure during early development via membranes and digestive system and eventually through gills. The ToxCast library would be improved by the addition of assay endpoints specific to fish (such as vitellogenin induction), and the addition of essay endpoints with high specificity to mechanisms of action in common pharmaceutical and CECs. Greater coverage of pharmaceuticals within existing assays is also necessary. Currently, the only endpoints specific to fish in the ToxCast database are from *in vivo* HTS assays from the Tanguay lab that assess developmental morphology in zebrafish embryos.[202] However, recently, HTS assays with behavioral endpoints in embryonic and larval zebrafish have demonstrated higher sensitivity compared to morphological endpoints.[95,203] Incorporating these and other behavioral assays into ToxCast would likely capture lower effect levels relevant to the neurological effects of exposure to pharmaceuticals and CECs.

Chapter 4: Conclusions and Future Research

The goal of this thesis was to identify potential gene and pathway-based biomarkers of exposure to an effluent-dominated stream in zebrafish larvae as they relate to changes in the chemical composition of the stream over space (above and below the effluent outfall) and time (seven monthly sampling events). The 3 and 6 dpf exposures of larval zebrafish to January and May water samples (Chapter 2) revealed transcriptomic signatures that differed by developmental stage and by chemical composition of sampling sites and months. Although biological processes related to heart development were overrepresented in both months, the effect was more pronounced in May, particularly with respect to the 3 dpf exposures. In the May 6 dpf exposures, histidine metabolism was overrepresented, suggesting the influence of antihistamines which were detected at higher concentrations in May compared to January. Visual and neurological development processes were also overrepresented in May and not January, which may relate to the higher total concentration of antidepressants in May.

In Chapter 3, ToxCast *in vitro* assay data was leveraged against chemical data from the same seven monthly water samples used for zebrafish exposures. Both ToxCast and global gene expression identified impacts within the histaminergic system that were unique to, or more pronounced in May compared to January. Impacts to cardiac functioning were also suggested in both analyses. Biological Processes and KEGG pathways related to the cardiovascular system were overrepresented among DETs in both exposure months, and two ToxCast assay gene targets involved in cardiac functioning (PPP2CA and CHRM2) that generated EAR values above the 0.001 were significantly dysregulated in both January and May zebrafish embryo exposures.

Many of the pharmaceuticals found at the highest concentrations in each month (fexofenadine, venlafaxine, gabapentin, sulfamethoxazole, metoprolol, acyclovir, lidocaine, and tramadol), did not contribute substantially to bioeffects predictions. Rather a select few chemicals targeting steroid pathways (carbamazepine and metformin) and the H_1 histamine receptor (diphenhydramine) were responsible for the most prominent bioeffects.

The use of the US1 site as a baseline reference for establishing gene expression changes related to detected contaminants normalized differential gene expression against the background water chemistry of the stream. However, In Chapter 2, the high estrogenicity measured at US1 in May and but not at US1 in January suggests the possibility of consequential chemical inputs not detected in the USGS chemical analysis. Despite the high estrogenicity at US1 in May, commonly used biomarkers of endocrine disruption were not detected in either NanoString or RNA-sequencing. Neither was there evidence of systematic overrepresentation of reproductive pathways among differentially expressed transcripts in RNA-sequencing.

This thesis was motivated by the need to expand the range of biological impacts currently monitored in aquatic ecosystems contaminated with complex mixtures of bioactive chemicals from wastewater effluent. While traditional ecotoxicological endpoints for fish provide important information about growth, reproduction, and acute toxicity, molecular sublethal impacts related to specific biological pathways can provide more sensitive and granular endpoints. Both HTS *in vitro* assay data and global and targeted gene expression were used to identify potential impacts of exposure on zebrafish larvae. The resulting associations between chemical composition, ToxCast predicted bioeffects, and changes in gene expression

from zebrafish embryo exposures are exploratory in nature and suggest several directions for future studies.

(1) Lab-based exposures are needed to the test the associations observed in this thesis between chemicals prioritized by ToxCast assay data and the bioeffects observed in larval zebrafish exposures. Specific relationships to investigate include the effects of diphenhydramine on histidine metabolism and the effects of thiabendazole and diphenhydramine on cardiovascular development.

(2) Many pharmaceuticals detected at high concentrations in WWTP effluent have either not been screened by many ToxCast assays or haven't been screened at all. Pharmaceuticals and degradates that are consistently detected in effluent-dominated surface water at high concentrations (e.g., fexofenadine, metformin, and venlafaxine) should be prioritized for testing within ToxCast regardless of whether their pharmacokinetic properties low risk to aquatic organisms. The constant presence of such pharmaceuticals may expose species throughout development and adulthood. In these cases, transcriptomics and other 'omics strategies could be used to identify potential off-target biological impacts at multiple life stages.

(3) Investigation is needed to characterize the ways endocrine disruption manifests during embryonic and larval zebrafish development. Many pharmaceuticals indirectly target endocrine system pathways and have the potential to alter reproductive functioning in

adult fish. However, little is known about how exposure to pharmaceuticals that indirectly target the endocrine system alter other pathways during development.

(4) To improve ability to predict bioeffects from CEC mixture composition in aquatic environments, analyses are needed that correlate water chemistry parameters and chemical composition to transcriptomic and other 'omics data.

While ToxCast and other "systems toxicology" approaches to predictive toxicity offer much needed tools for assessing mixture toxicity of emerging contaminants, these tools can only predict the effects they were designed to evaluate and are only as reliable the data that supports them. As is the case with data from all targeted analyses in environmental chemistry and toxicology, the bioeffects predictions generated from ToxCast assays represent "the tip of the iceberg" with respect to what aquatic organisms likely experience. The lack of specificity to aquatic organisms within ToxCast assays and the low assay coverage for top pharmaceutical contaminants makes the integration of *in vivo* bioeffects data with *in vitro* predictions even more important.

References

1. Zhi, H. *et al.* Occurrence and Spatiotemporal Dynamics of Pharmaceuticals in a Temperate-Region Wastewater Effluent-Dominated Stream: Variable Inputs and Differential Attenuation Yield Evolving Complex Exposure Mixtures. *Environ. Sci. Technol.* 54, 12967–12978 (2020).
2. Bradley, P. M. *et al.* Multi-region assessment of pharmaceutical exposures and predicted effects in USA wadeable urban-gradient streams. *PLoS One* 15, e0228214 (2020).
3. Kolpin, D. W., Skopec, M., Meyer, M. T., Furlong, E. T. & Zaugg, S. D. Urban contribution of pharmaceuticals and other organic wastewater contaminants to streams during differing flow conditions. *Sci. Total Environ.* 328, 119–130 (2004).
4. González-Alonso, S. *et al.* Occurrence of pharmaceutical, recreational and psychotropic drug residues in surface water on the northern Antarctic Peninsula region. *Environ. Pollut.* 229, 241–254 (2017).
5. Blair, B. D., Crago, J. P., Hedman, C. J. & Klaper, R. D. Pharmaceuticals and personal care products found in the Great Lakes above concentrations of environmental concern. *Chemosphere* 93, 2116–2123 (2013).
6. Bexfield, L. M., Toccalino, P. L., Belitz, K., Foreman, W. T. & Furlong, E. T. Hormones and Pharmaceuticals in Groundwater Used As a Source of Drinking Water Across the United States. *Environ. Sci. Technol.* 53, 2950–2960 (2019).
7. Lapworth, D. J., Baran, N., Stuart, M. E. & Ward, R. S. Emerging organic contaminants in groundwater: A review of sources, fate and occurrence. *Environ. Pollut.* 163, 287–303 (2012).
8. Golovko, O. *et al.* Occurrence and removal of chemicals of emerging concern in wastewater treatment plants and their impact on receiving water systems. *Sci. Total Environ.* 754, 142122 (2021).
9. Blair, B. D. *et al.* Evaluation of a model for the removal of pharmaceuticals, personal care products, and hormones from wastewater. *Sci. Total Environ.* 444, 515–521 (2013).
10. Rosi-Marshall, E. J. & Royer, T. V. Pharmaceutical Compounds and Ecosystem Function: An Emerging Research Challenge for Aquatic Ecologists. *Ecosystems* 15, 867–880 (2012).
11. Schoenfuss, H. L. *et al.* Complex mixtures, complex responses: Assessing pharmaceutical mixtures using field and laboratory approaches. *Environ. Toxicol. Chem.* 35, 953–965 (2016).
12. Drzymała, J. & Kalka, J. Ecotoxic interactions between pharmaceuticals in mixtures: Diclofenac and sulfamethoxazole. *Chemosphere* 259, (2020).
13. Altenburger, R., Walter, H. & Grote, M. What contributes to the combined effect of a complex mixture? *Environ. Sci. Technol.* 38, 6353–6362 (2004).
14. Diamond, J. M. *et al.* Prioritizing contaminants of emerging concern for ecological

screening assessments. *Environ. Toxicol. Chem.* 30, 2385–2394 (2011).

15. OECD. Pharmaceutical Residues in Freshwater. *OECD Stud. Water* (2019).
16. Sörengård, M. *et al.* Mass loads, source apportionment, and risk estimation of organic micropollutants from hospital and municipal wastewater in recipient catchments. *Chemosphere* 234, 931–941 (2019).
17. Onesios, K. M., Yu, J. T. & Bouwer, E. J. Biodegradation and removal of pharmaceuticals and personal care products in treatment systems: a review. *Biodegradation* 20, 441–466 (2009).
18. Göbel, A., Thomsen, A., McArdell, C. S., Joss, A. & Giger, W. Occurrence and Sorption Behavior of Sulfonamides, Macrolides, and Trimethoprim in Activated Sludge Treatment. *Environ. Sci. \& Technol.* 39, 3981–3989 (2005).
19. Kasprzyk-Hordern, B., Dinsdale, R. M. & Guwy, A. J. The removal of pharmaceuticals, personal care products, endocrine disruptors and illicit drugs during wastewater treatment and its impact on the quality of receiving waters. *Water Res.* 43, 363–380 (2009).
20. Krzeminski, P. *et al.* Performance of secondary wastewater treatment methods for the removal of contaminants of emerging concern implicated in crop uptake and antibiotic resistance spread: A review. *Sci. Total Environ.* 648, 1052–1081 (2019).
21. Khetan, S. K. & Collins, T. J. Human pharmaceuticals in the aquatic environment: A challenge to green chemisty. *Chem. Rev.* 107, 2319–2364 (2007).
22. Mackay, D., Hughes, D. M., Romano, M. L. & Bonnell, M. The role of persistence in chemical evaluations. *Integr. Environ. Assess. Manag.* 10, 588–594 (2014).
23. Kolpin, D. W. *et al.* Pharmaceuticals, hormones, and other organic wastewater contaminants in U.S. streams, 1999-2000: A national reconnaissance. *Environ. Sci. Technol.* (2002). doi:10.1021/es011055j
24. Focazio, M. J. *et al.* A national reconnaissance for pharmaceuticals and other organic wastewater contaminants in the United States — II) Untreated drinking water sources. *Sci. Total Environ.* 402, 201–216 (2008).
25. Pratt, L. A., Brody, D. J. & Gu, Q. Antidepressant Use Among Persons Aged 12 and Over:United States,2011-2014. *NCHS Data Brief* 1–8 (2017).
26. Rice, J. & Westerhoff, P. High levels of endocrine pollutants in US streams during low flow due to insufficient wastewater dilution. *Nat. Geosci.* 10, 587–591 (2017).
27. Brooks, B. W. Fish on Prozac (and Zoloft): Ten years later. *Aquat. Toxicol.* 151, 61–67 (2014).
28. Klein, E. Y. *et al.* Assessment of WHO antibiotic consumption and access targets in 76 countries, 2000–15: an analysis of pharmaceutical sales data. *Lancet Infect. Dis.* 21, 107–115 (2021).
29. Van Boeckel, T. P. *et al.* Global antibiotic consumption 2000 to 2010: An analysis of

national pharmaceutical sales data. *Lancet Infect. Dis.* 14, 742–750 (2014).

30. National Center for Health Statistics. *Health, United States, 2013: With Special Feature on Prescription Drugs*. *DHHS Publication No. 2014* 60, (2014).

31. Ternes, T. A. *et al.* Removal of pharmaceuticals during drinking water treatment. *Environ. Sci. Technol.* 36, 3855–3863 (2002).

32. Rice, J. & Westerhoff, P. Spatial and Temporal Variation in De Facto Wastewater Reuse in Drinking Water Systems across the U.S.A. *Environ. Sci. Technol.* 49, 982–989 (2015).

33. Rice, J., Wutich, A. & Westerhoff, P. Assessment of De Facto Wastewater Reuse across the U.S.: Trends between 1980 and 2008. *Environ. Sci. Technol.* 47, 11099–11105 (2013).

34. Nguyen, T. T. & Westerhoff, P. K. Drinking water vulnerability in less-populated communities in Texas to wastewater-derived contaminants. *npj Clean Water* 2, 1–9 (2019).

35. Meehan, K., Ormerod, K. J. & Moore, S. A. Remaking Waste as Water: The Governance of Recycled Effluent for Potable Water Supply. *Water Altern.* 6, 67–85 (2013).

36. Schäfer, R. B., Kühn, B., Malaj, E., König, A. & Gergs, R. Contribution of organic toxicants to multiple stress in river ecosystems. *Freshw. Biol.* 61, 2116–2128 (2016).

37. Schultz, M. M. *et al.* Antidepressant Pharmaceuticals in Two U.S. Effluent-Impacted Streams: Occurrence and Fate in Water and Sediment, and Selective Uptake in Fish Neural Tissue. *Environ. Sci. Technol.* 44, 1918–1925 (2010).

38. Vajda, A. M. *et al.* Demasculinization of male fish by wastewater treatment plant effluent. *Aquat. Toxicol.* 103, 213–221 (2011).

39. Blazer, V. S. *et al.* Retrospective analysis of estrogenic endocrine disruption and land-use influences in the Chesapeake Bay watershed. *Chemosphere* 266, 129009 (2021).

40. Hinck, J. E., Blazer, V. S., Schmitt, C. J., Papoulias, D. M. & Tillitt, D. E. Widespread occurrence of intersex in black basses (Micropterus spp.) from U.S. rivers, 1995–2004. *Aquat. Toxicol.* 95, 60–70 (2009).

41. Overturf, M. D., Anderson, J. C., Pandelides, Z., Beyger, L. & Holdway, D. A. Pharmaceuticals and personal care products: A critical review of the impacts on fish reproduction. *Crit. Rev. Toxicol.* 45, 469–491 (2015).

42. Schug, T. T. *et al.* Minireview: Endocrine Disruptors: Past Lessons and Future Directions. *Mol. Endocrinol.* 30, 833–47 (2016).

43. van der Ven, K. *et al.* Effects of the antidepressant mianserin in zebrafish: Molecular markers of endocrine disruption. *Chemosphere* 65, 1836–1845 (2006).

44. Kreke, N. & Dietrich, D. R. Physiological endpoints for potential SSRI interactions in fish. *Crit. Rev. Toxicol.* 38, 215–247 (2008).

45. Hansen, C. H., Larsen, L. W., Sørensen, A. M., Halling-Sørensen, B. & Styrishave, B. The six most widely used selective serotonin reuptake inhibitors decrease androgens and

increase estrogens in the H295R cell line. *Toxicol. In Vitro* 41, 1–11 (2017).

46. Schultz, M. M. *et al.* Selective uptake and biological consequences of environmentally relevant antidepressant pharmaceutical exposures on male fathead minnows. *Aquat. Toxicol.* 104, 38–47 (2011).

47. Weinberger, J. & Klaper, R. Environmental concentrations of the selective serotonin reuptake inhibitor fluoxetine impact specific behaviors involved in reproduction, feeding and predator avoidance in the fish Pimephales promelas (fathead minnow). *Aquat. Toxicol.* 151, 77–83 (2014).

48. Ansai, S., Hosokawa, H., Maegawa, S. & Kinoshita, M. Chronic fluoxetine treatment induces anxiolytic responses and altered social behaviors in medaka, Oryzias latipes. *Behav. Brain Res.* 303, 126–136 (2016).

49. Rena, G., Hardie, D. G. & Pearson, E. R. The mechanisms of action of metformin. *Diabetologia* 60, 1577–1585 (2017).

50. Niemuth, N. J. *et al.* Metformin exposure at environmentally relevant concentrations causes potential endocrine disruption in adult male fish. *Environ. Toxicol. Chem.* 34, 291–296 (2015).

51. Ussery, E. *et al.* Effects of environmentally relevant metformin exposure on Japanese medaka (Oryzias latipes). *Aquat. Toxicol.* 205, 58–65 (2018).

52. MacLaren, R. D., Wisniewski, K. & MacLaren, C. Environmental concentrations of metformin exposure affect aggressive behavior in the Siamese fighting fish, Betta splendens. *PLoS One* 13, e0197259 (2018).

53. Kidd, K. A. *et al.* Collapse of a fish population after exposure to a synthetic estrogen. *Proc. Natl. Acad. Sci. U. S. A.* 104, 8897–901 (2007).

54. Best, J. D. & Alderton, W. K. Zebrafish: An in vivo model for the study of neurological diseases. *Neuropsychiatr. Dis. Treat.* 4, 567–576 (2008).

55. Owen, S. F. *et al.* Comparative physiology, pharmacology and toxicology of β-blockers: Mammals versus fish. *Aquat. Toxicol.* 82, 145–162 (2007).

56. Gamperl, A. K., Wilkinson, M. & Boutilier, R. G. Beta-adrenoreceptors in the trout (Oncorhynchus mykiss) heart: characterization, quantification, and effects of repeated catecholamine exposure. *Gen. Comp. Endocrinol.* 95, 259–272 (1994).

57. Haider, S. & Baqri, S. S. beta-adrenoceptor antagonists reinitiate meiotic maturation in Clarias batrachus oocytes. *Comp. Biochem. Physiol. A. Mol. Integr. Physiol.* 126, 517–525 (2000).

58. Fent, K., Weston, A. A. & Caminada, D. Ecotoxicology of human pharmaceuticals. *Aquat. Toxicol.* 76, 122–159 (2006).

59. Ibabe, A., Grabenbauer, M., Baumgart, E., Fahimi, H. D. & Cajaraville, M. P. Expression of peroxisome proliferator-activated receptors in zebrafish (Danio rerio). *Histochem. Cell Biol.* 118, 231–239 (2002).

60. Simmons, D. B. D. *et al.* Omics for aquatic ecotoxicology: Control of extraneous variability to enhance the analysis of environmental effects. *Environ. Toxicol. Chem.* 34, 1693–1704 (2015).

61. Schirmer, K., Fischer, B. B., Madureira, D. J. & Pillai, S. Transcriptomics in ecotoxicology. *Anal. Bioanal. Chem.* 397, 917–923 (2010).

62. Yang, L. *et al.* Transcriptional profiling reveals barcode-like toxicogenomic responses in the zebrafish embryo. *Genome Biol.* 8, 1–17 (2007).

63. Hausen, J. *et al.* Fishing for contaminants: identification of three mechanism specific transcriptome signatures using Danio rerio embryos. *Environ. Sci. Pollut. Res.* 25, 4023–4036 (2018).

64. Dix, D. J. *et al.* The ToxCast Program for Prioritizing Toxicity Testing of Environmental Chemicals. *Toxicol. Sci.* 95, 5–12 (2007).

65. Li, S. *et al.* An integrated approach for identifying priority contaminant in the Great Lakes Basin – Investigations in the Lower Green Bay/Fox River and Milwaukee Estuary areas of concern. *Sci. Total Environ.* 579, 825–837 (2017).

66. Rose, L. D. *et al.* Use of high-throughput screening results to prioritize chemicals for potential adverse biological effects within a West Virginia watershed. *Sci. Total Environ.* 677, 362–372 (2019).

67. De Baat, M. L. *et al.* Smarter Sediment Screening: Effect-Based Quality Assessment, Chemical Profiling, and Risk Identification. *Environ. Sci. Technol.* 53, 14479–14488 (2019).

68. Bolong, N., Ismail, A. F., Salim, M. R. & Matsuura, T. A review of the effects of emerging contaminants in wastewater and options for their removal. *Desalination* 239, 229–246 (2009).

69. Meyer, J. L. *et al.* The Contribution of Headwater Streams to Biodiversity in River Networks1. *JAWRA J. Am. Water Resour. Assoc.* 43, 86–103 (2007).

70. Nilsen, E. *et al.* Critical review: Grand challenges in assessing the adverse effects of contaminants of emerging concern on aquatic food webs. *Environ. Toxicol. Chem.* 38, 46–60 (2019).

71. Wirbisky, S. E. *et al.* Embryonic atrazine exposure elicits alterations in genes associated with neuroendocrine function in adult male zebrafish. *Toxicol. Sci.* 153, 149–164 (2016).

72. Hicken, C. E. *et al.* Sublethal exposure to crude oil during embryonic development alters cardiac morphology and reduces aerobic capacity in adult fish. *Proc. Natl. Acad. Sci. U. S. A.* 108, 7086–7090 (2011).

73. Corcoran, J., Winter, M. J. & Tyler, C. R. Pharmaceuticals in the aquatic environment: A critical review of the evidence for health effects in fish. *Crit. Rev. Toxicol.* 40, 287–304 (2010).

74. Schmitz, M. *et al.* Environmentally-relevant mixture of pharmaceutical drugs stimulates sex-steroid hormone production and modulates the expression of candidate genes in the

ovary of juvenile female rainbow trout. *Aquat. Toxicol.* 205, 89–99 (2018).

75. Huang, S. S. Y. *et al.* A multi-omic approach to elucidate low-dose effects of xenobiotics in zebrafish (Danio rerio) larvae. *Aquat. Toxicol.* 182, 102–112 (2017).

76. Parolini, M., Ghilardi, A., De Felice, B. & Del Giacco, L. Environmental concentration of fluoxetine disturbs larvae behavior and increases the defense response at molecular level in zebrafish (Danio rerio). *Environ. Sci. Pollut. Res.* 26, 34943–34952 (2019).

77. Martinez, R. *et al.* Developmental fluoxetine exposure in zebrafish reduces offspring basal cortisol concentration via life stage-dependent maternal transmission. *PLoS One* 14, 1–28 (2019).

78. Vera-Chang, M. N., Moon, T. W. & Trudeau, V. L. Ancestral fluoxetine exposure sensitizes zebrafish to venlafaxine-induced reductions in cortisol and spawning. *Endocrinology* 160, 2137–2142 (2019).

79. Ford, A. T. & Fong, P. P. The effects of antidepressants appear to be rapid and at environmentally relevant concentrations. *Environ. Toxicol. Chem.* 35, 794–798 (2016).

80. Chen, L. Visual system: An understudied target of aquatic toxicology. *Aquat. Toxicol.* 225, 105542 (2020).

81. Strähle, U. & Grabher, C. The zebrafish embryo as a model for assessing off-target drug effects. *DMM Dis. Model. Mech.* 3, 689–692 (2010).

82. Jacob, S. *et al.* Does the antidiabetic drug metformin affect embryo development and the health of brown trout (Salmo trutta f. fario)? *Environ. Sci. Eur.* 30, 48 (2018).

83. Niemuth, N. J. & Klaper, R. D. Emerging wastewater contaminant metformin causes intersex and reduced fecundity in fish. *Chemosphere* 135, 38–45 (2015).

84. Best, C., Melnyk-Lamont, N., Gesto, M. & Vijayan, M. M. Environmental levels of the antidepressant venlafaxine impact the metabolic capacity of rainbow trout. *Aquat. Toxicol.* 155, 190–198 (2014).

85. Melnyk-Lamont, N., Best, C., Gesto, M. & Vijayan, M. M. The antidepressant venlafaxine disrupts brain monoamine levels and neuroendocrine responses to stress in rainbow trout. *Environ. Sci. Technol.* 48, 13434–13442 (2014).

86. Melvin, S. D., Buck, D. R. & Fabbro, L. D. Diurnal activity patterns as a sensitive behavioural outcome in fish: effect of short-term exposure to treated sewage and a sub-lethal PPCP mixture. *J. Appl. Toxicol.* 36, 1173–1182 (2016).

87. Backhaus, T. Medicines, shaken and stirred: A critical review on the ecotoxicology of pharmaceutical mixtures. *Philos. Trans. R. Soc. B Biol. Sci.* 369, (2014).

88. Osterauer, R. & Köhler, H. R. Temperature-dependent effects of the pesticides thiacloprid and diazinon on the embryonic development of zebrafish (Danio rerio). *Aquat. Toxicol.* 86, 485–494 (2008).

89. Bittner, L., Teixido, E., Seiwert, B., Escher, B. I. & Klüver, N. Influence of pH on the uptake and toxicity of B-blockers in embryos of zebrafish, Danio rerio. *Aquat. Toxicol.* 201, 129–

137 (2018).

90. Bittner, L., Teixidó, E., Keddi, I., Escher, B. I. & Klüver, N. pH-Dependent Uptake and Sublethal Effects of Antihistamines in Zebrafish (Danio rerio) Embryos. *Environ. Toxicol. Chem.* 38, 1012–1022 (2019).

91. Garcia, G. R., Noyes, P. D. & Tanguay, R. Advancements in zebrafish applications for 21stcenturytoxicology. *Pharmacol. Ther.* 161, 11–21 (2016).

92. Kimmel, C., Ballard, W., Kimmel, S., Ullmann, B. & Schilling, T. Stages of embryonic development of the zebrafish. *Dev. Dyn.* 203, 253–310 (1995).

93. White, R. J. *et al.* A high-resolution mRNA expression time course of embryonic development in zebrafish. *bioRxiv* 1–32 (2017). doi:10.1101/107631

94. Truong, L. & Tanguay, R. L. Evaluation of embryotoxicity using the zebrafish model. *Methods Mol. Biol.* 1641, 325–333 (2017).

95. Reif, D. M. *et al.* High-throughput characterization of chemical-associated embryonic behavioral changes predicts teratogenic outcomes. *Arch. Toxicol.* 90, 1459–1470 (2016).

96. FOX Engineering Associates Inc. *Wastewater Treatment Plant Facility Plan Update North Liberty , Iowa.* (2014).

97. U.S. Geological Survey. National Field Manual for the Collection of Water-Quality Data. in *Chapter A4. Collection of Water Samples, Version 2; Techniques of Water-Resources Investigations 09-A4* (2006). doi:10.3133/twri09A4

98. Furlong, E. T. *et al.* Determination of human-use pharmaceuticals in filtered water by direct aqueous injection: high-performance liquid chromatography/tandem mass spectrometry. (2014). doi:10.3133/tm5B10

99. Ciparis, S., Iwanowicz, L. R. & Voshell, J. R. Effects of watershed densities of animal feeding operations on nutrient concentrations and estrogenic activity in agricultural streams. *Sci. Total Environ.* 414, 268–276 (2012).

100. Romanok, K. M. *et al. Methods used for the collection and analysis of chemical and biological data for the Tapwater Exposure Study, United States, 2016–17*. *Open-File Report* (2018). doi:10.3133/ofr20181098

101. Andrews, S. *et al.* FastQC: A Quality Control Tool for High Throughput Sequence DataNo Title. (2010).

102. Martin, M. Cutadapt removes adapter sequences from high-throughput sequencing reads. *EMBnet.journal* 17, 10–12 (2011).

103. Bray, N. L., Pimentel, H., Melsted, P. & Pachter, L. Near-optimal probabilistic RNA-seq quantification. *Nat. Biotechnol.* 34, 525–527 (2016).

104. Chiesa, M., Colombo, G. & Piacentini, L. DaMiRseq-an R/Bioconductor package for data mining of RNA-seq data: normalization, feature selection and classification. *Bioinformatics* 34, 1416–1418 (2018).

105. Love, M. I., Huber, W. & Anders, S. Moderated estimation of fold change and dispersion for RNA-seq data with DESeq2. *Genome Biol.* 15, 550 (2014).

106. Rohart, F., Gautier, B., Singh, A. & Lê Cao, K. A. mixOmics: an R package for 'omics feature selection and multiple data integration. *bioRxiv* 1–19 (2017). doi:10.1101/108597

107. Kanehisa, M. & Goto, S. KEGG: Kyoto Encyclopedia of Genes and Genomes. *Nucleic Acids Res.* 28, 27–30 (2000).

108. Yu, G., Wang, L.-G., Han, Y. & Qing-Yu, H. clusterProfiler: an R Package for Comparing Biological Themes Among Gene Clusters. *Omi. A J. Integr. Biol.* 16(5), 284–287 (2012).

109. Raudvere, U. *et al.* G:Profiler: A web server for functional enrichment analysis and conversions of gene lists (2019 update). *Nucleic Acids Res.* 47, W191–W198 (2019).

110. Sanseverino, J. *et al.* Use of Saccharomyces cerevisiae BLYES expressing bacterial bioluminescence for rapid, sensitive detection of estrogenic compounds. *Appl. Environ. Microbiol.* 71, 4455–4460 (2005).

111. Meppelink, S. M. *et al.* Water-quality data for a pharmaceutical study at Muddy Creek in North Liberty and Coralville, Iowa, 2017-2018. (2020).

112. Yang, M. *et al.* Growth inhibition and coordinated physiological regulation of zebrafish (Danio rerio) embryos upon sublethal exposure to antidepressant amitriptyline. *Aquat. Toxicol.* 151, 68–76 (2014).

113. Wu, M. *et al.* Global transcriptomic analysis of zebrafish in response to embryonic exposure to three antidepressants, amitriptyline, fluoxetine and mianserin. *Aquat. Toxicol.* 192, 274–283 (2017).

114. Yan, S. *et al.* Environmentally relevant concentrations of carbamazepine induce liver histopathological changes and a gender-specific response in hepatic proteome of Chinese rare minnows (Gobiocypris rarus). *Environ. Pollut.* 243, 480–491 (2018).

115. Qiu, W. *et al.* Single and joint toxic effects of four antibiotics on some metabolic pathways of zebrafish (Danio rerio) larvae. *Sci. Total Environ.* 716, 137062 (2020).

116. Wada, Y., Sun-Wada, G. H., Kawamura, N. & Aoyama, M. Role of autophagy in embryogenesis. *Curr. Opin. Genet. Dev.* 27, 60–66 (2014).

117. Nam, T., Han, J. H., Devkota, S. & Lee, H. W. Emerging paradigm of crosstalk between autophagy and the ubiquitin-proteasome system. *Mol. Cells* 40, 897–905 (2017).

118. Jung, H. M. *et al.* Development of the larval lymphatic system in zebrafish. *Dev.* 144, 2070–2081 (2017).

119. Kuil, L. E. *et al.* Reverse genetic screen reveals that Il34 facilitates yolk sac macrophage distribution and seeding of the brain. *DMM Dis. Model. Mech.* 12, 1–12 (2019).

120. Nauroy, P. *et al.* Gene profile of zebrafish fin regeneration offers clues to kinetics, organization and biomechanics of basement membrane. *Matrix Biol.* 75–76, 82–101 (2019).

121. Yi, Y., Zhang, W., Yi, J. & Xiao, Z. X. Role of p53 family proteins in metformin anti-cancer activities. *J. Cancer* 10, 2434–2442 (2019).

122. Massarsky, A., Trudeau, V. L. & Moon, T. W. β-blockers as endocrine disruptors: The potential effects of human β-blockers on aquatic organisms. *J. Exp. Zool. Part A Ecol. Genet. Physiol.* 315 A, 251–265 (2011).

123. Finn, J. *et al.* Effects of propranolol on heart rate and development in Japanese medaka (Oryzias latipes) and zebrafish (Danio rerio). *Aquat. Toxicol.* 122–123, 214–221 (2012).

124. Ings, J. S., George, N., Peter, M. C. S., Servos, M. R. & Vijayan, M. M. Venlafaxine and atenolol disrupt epinephrine-stimulated glucose production in rainbow trout hepatocytes. *Aquat. Toxicol.* 106–107, 48–55 (2012).

125. Thompson, W. A., Arnold, V. I. & Vijayan, M. M. Venlafaxine in Embryos Stimulates Neurogenesis and Disrupts Larval Behavior in Zebrafish. *Environ. Sci. Technol.* 51, 12889–12897 (2017).

126. Shen, P. *et al.* Venlafaxine exerts antidepressant effects possibly by activating MAPK–ERK1/2 and P13K–AKT pathways in the hippocampus. *Behav. Brain Res.* 335, 63–70 (2017).

127. Melvin, S. D. Effect of antidepressants on circadian rhythms in fish: Insights and implications regarding the design of behavioural toxicity tests. *Aquat. Toxicol.* 182, 20–30 (2017).

128. Rodrigues, P., Cunha, V., Oliva-Teles, L., Ferreira, M. & Guimarães, L. Norfluoxetine and venlafaxine in zebrafish larvae: Single and combined toxicity of two pharmaceutical products relevant for risk assessment. *J. Hazard. Mater.* 400, 123171 (2020).

129. Xu, J. & Xie, F. α- and β-Adrenoceptors of zebrafish in melanosome movement: A comparative study between embryo and adult melanophores. *Biochem. Biophys. Res. Commun.* 405, 250–255 (2011).

130. Shi, W. J. *et al.* Dydrogesterone affects the transcription of genes in visual cycle and circadian rhythm network in the eye of zebrafish. *Ecotoxicol. Environ. Saf.* 183, (2019).

131. Bridges, K. N. *et al.* Alterations to the vision-associated transcriptome of zebrafish (Danio rerio) following developmental norethindrone exposure. *Environ. Toxicol. Pharmacol.* 69, 137–142 (2019).

132. Huang, I. J., Dheilly, N. M., Sirotkin, H. I. & McElroy, A. E. Comparative transcriptomics implicate mitochondrial and neurodevelopmental impairments in larval zebrafish (Danio rerio) exposed to two selective serotonin reuptake inhibitors (SSRIs). *Ecotoxicol. Environ. Saf.* 203, 110934 (2020).

133. Huang, I. J., Sirotkin, H. I. & McElroy, A. E. Varying the exposure period and duration of neuroactive pharmaceuticals and their metabolites modulates effects on the visual motor response in zebrafish (Danio rerio) larvae. *Neurotoxicol. Teratol.* 72, 39–48 (2019).

134. Shi, Q. *et al.* Optical toxicity of triphenyl phosphate in zebrafish larvae. *Aquat. Toxicol.*

210, 139–147 (2019).

135. Dawar, F. U., Zuberi, A., Azizullah, A. & Khan Khattak, M. N. Effects of cypermethrin on survival, morphological and biochemical aspects of rohu (Labeo rohita) during early development. *Chemosphere* 144, 697–705 (2016).

136. Ranjani, T. S. *et al.* Phenotypic and trascriptomic changes in zebrafish (Danio rerio) embryos/larvae following cypermethrin exposure. *Chemosphere* 249, 126148 (2020).

137. Zhang, J. *et al.* The single and joint toxicity effects of chlorpyrifos and beta-cypermethrin in zebrafish (Danio rerio) early life stages. *J. Hazard. Mater.* 334, 121–131 (2017).

138. Laurenson, J. P., Bloom, R. A., Page, S. & Sadrieh, N. Ethinyl estradiol and other human pharmaceutical estrogens in the aquatic environment: A review of recent risk assessment data. *AAPS J.* 16, 299–310 (2014).

139. Wu, F. *et al.* Predicted no-effect concentration and risk assessment for 17-[beta]-estradiol in waters of china. *Rev. Environ. Contam. Toxicol.* 228, 31–56 (2014).

140. Kumar, N., Zhao, H. N., Awoyemi, O., Kolodziej, E. P. & Crago, J. Toxicity Testing of Effluent-Dominated Stream Using Predictive Molecular-Level Toxicity Signatures Based on High-Resolution Mass Spectrometry: A Case Study of the Lubbock Canyon Lake System. *Environ. Sci. Technol.* (2021). doi:10.1021/acs.est.0c05546

141. Yang, H. *et al.* Deep mRNA Sequencing Analysis to Capture the Transcriptome Landscape of Zebrafish Embryos and Larvae. *PLoS One* 8, (2013).

142. Ankley, G. T. *et al.* Pathway-Based Approaches for Assessing Biological Hazards of Complex Mixtures of Contaminants: A Case Study in the Maumee River. *Environ. Toxicol. Chem.* 00, 1–25 (2020).

143. Webb, D. T. *et al.* Emerging investigator series: municipal wastewater as a year-round point source of neonicotinoid insecticides that persist in an effluent-dominated stream. *Environ. Sci. Process. Impacts* 23, 678–688 (2021).

144. Brodin, T. *et al.* Ecological effects of pharmaceuticals in aquatic systems—impacts through behavioural alterations. *Philos. Trans. R. Soc. B Biol. Sci.* 369, (2014).

145. Judson, R. *et al.* The toxicity data landscape for environmental chemicals. *Environmental Health Perspectives* 117, 685–695 (2009).

146. Kavlock, R. *et al.* Update on EPA's ToxCast program: Providing high throughput decision support tools for chemical risk management. *Chem. Res. Toxicol.* 25, 1287–1302 (2012).

147. Tice, R. R., Austin, C. P., Kavlock, R. J. & Bucher, J. R. Improving the human hazard characterization of chemicals: A Tox21 update. *Environmental Health Perspectives* 121, 756–765 (2013).

148. Richard, A. M. *et al.* ToxCast Chemical Landscape: Paving the Road to 21st Century Toxicology. *Chem. Res. Toxicol.* 29, 1225–1251 (2016).

149. Villeneuve, D. L. *et al.* Adverse outcome pathway (AOP) development I: Strategies and principles. *Toxicol. Sci.* 142, 312–320 (2014).

150. Elliott, S. M. *et al.* Contaminants in bald eagles of the upper Midwestern U.S.: A framework for prioritizing future research based on in-vitro bioassays. *Environ. Pollut.* 244, 861–870 (2019).

151. Geiss, G. K. *et al.* Direct multiplexed measurement of gene expression with color-coded probe pairs. *Nat. Biotechnol.* 26, 317–325 (2008).

152. Hahn, C. M., Iwanowicz, L. R., Cornman, R. S., Mazik, P. M. & Blazer, V. S. Transcriptome discovery in non-model wild fish species for the development of quantitative transcript abundance assays. *Comp. Biochem. Physiol. - Part D Genomics Proteomics* 20, 27–40 (2016).

153. Niemuth, N. J. & Klaper, R. D. Low-dose metformin exposure causes changes in expression of endocrine disruption-associated genes. *Aquat. Toxicol.* 195, 33–40 (2018).

154. Wang, H. *et al.* NanoStringDiff: A novel statistical method for differential expression analysis based on NanoString nCounter data. *Nucleic Acids Res.* 44, e151 (2016).

155. Filby, A. L. & Tyler, C. R. Appropriate 'housekeeping' genes for use in expression profiling the effects of environmental estrogens in fish. *BMC Mol. Biol.* 8, 10 (2007).

156. Andersen, C. L., Jensen, J. L. & Ørntoft, T. F. Normalization of real-time quantitative reverse transcription-PCR data: A model-based variance estimation approach to identify genes suited for normalization, applied to bladder and colon cancer data sets. *Cancer Res.* 64, 5245–5250 (2004).

157. Ursu, O. *et al.* DrugCentral 2018: An update. *Nucleic Acids Res.* 47, D963–D970 (2019).

158. Eike, D., Marcus, R. & Dirk, J. The database 'Pharmaceuticals in the Environment' - Update and new analysis. *Umweltbundesamt* 103 (2019).

159. Scott, M. C. Winners and losers among stream fishes in relation to land use legacies and urban development in the southeastern US. *Biol. Conserv.* 127, 301–309 (2006).

160. Van Donk, E., Peacor, S. D., Grosser, K. & De Senerppont Domis, L. N. Pharmaceuticals May Disrupt Natural Chemical Information Flows and Species Interactions in Aquatic Systems: Ideas and Perspectives on a Hidden Global Change. *How to Recruit Volunt. Donors Third World?* 238, 22–28 (2015).

161. Brodin, T., Fick, J., Jonsson, M. & Klaminder, J. Dilute concentrations of a psychiatric drug alter behavior of fish from natural populations. *Science (80-.).* 339, 814–815 (2013).

162. Kidd, K. A. *et al.* Direct and indirect responses of a freshwater food web to a potent synthetic oestrogen. *Philos. Trans. R. Soc. B Biol. Sci.* 369, (2014).

163. US EPA. ToxCast & Tox21 summary Files from invitrodb_v3.2. (2020). Available at: https://www.epa.gov/chemical-research/exploring-toxcast-data-downloadable-data. (Accessed: 1st April 2020)

164. De Cicco, L. A., Corsi, S. R., Villeneuve, D. L., Blackwell, B. R. & Ankley, G. T. toxEval: Evaluation of measured concentration data using the ToxCast high-throughput screening database or a user-defined set of concentration benchmarks. (2019).

doi:10.5066/P906UQ5I

165. Blackwell, B. R. *et al.* Potential Toxicity of Complex Mixtures in Surface Waters from a Nationwide Survey of United States Streams: Identifying in Vitro Bioactivities and Causative Chemicals. *Environ. Sci. Technol.* 53, 973–983 (2019).

166. Corsi, S. R. *et al.* Prioritizing chemicals of ecological concern in Great Lakes tributaries using high-throughput screening data and adverse outcome pathways. *Sci. Total Environ.* 686, 995–1009 (2019).

167. Blackwell, B. R. *et al.* An 'eAR' on Environmental Surveillance and Monitoring: A Case Study on the Use of Exposure-Activity Ratios (EARs) to Prioritize Sites, Chemicals, and Bioactivities of Concern in Great Lakes Waters. *Environ. Sci. Technol.* 51, 8713–8724 (2017).

168. Filer, D. L., Kothiya, P., Woodrow Setzer, R., Judson, R. S. & Martin, M. T. Tcpl: The ToxCast pipeline for high-throughput screening data. *Bioinformatics* 33, 618–620 (2017).

169. Nirmalakhandan, N., Arulgnanendran, V., Mohsin, M., Sun, B. & Cadena, F. Toxicity of mixtures of organic chemicals to microorganisms. *Water Res.* 28, 543–551 (1994).

170. Fay, K. A. *et al.* Differentiating pathway-specific from nonspecific effects in high-throughput toxicity data: A foundation for prioritizing adverse outcome pathway development. *Toxicol. Sci.* 163, 500–515 (2018).

171. Altenburger, R. *et al.* Mixture effects in samples of multiple contaminants – An inter-laboratory study with manifold bioassays. *Environ. Int.* 114, 95–106 (2018).

172. Cedergreen, N. *et al.* A review of independent action compared to concentration addition as reference models for mixtures of compounds with different molecular target sites. *Environ. Toxicol. Chem.* 27, 1621–1632 (2008).

173. Ermler, S., Scholze, M. & Kortenkamp, A. The suitability of concentration addition for predicting the effects of multi-component mixtures of up to 17 anti-androgens with varied structural features in an in vitro AR antagonist assay. *Toxicol. Appl. Pharmacol.* 257, 189–197 (2011).

174. Kortenkamp, A., Backhaus, T. & Faust, M. State of the art report on mixture toxicity. (2009).

175. Bradley, P. M. *et al.* Mixed-chemical exposure and predicted effects potential in wadeable southeastern USA streams. *Sci. Total Environ.* 655, 70–83 (2019).

176. Galus, M. *et al.* Chronic effects of exposure to a pharmaceutical mixture and municipal wastewater in zebrafish. *Aquat. Toxicol.* 132–133, 212–222 (2013).

177. Franco, M. B. *et al.* Exposure to dilute concentrations of bupropion affects zebrafish early life stages. *Chemosphere* 222, 175–183 (2019).

178. De Oliva, S. U. & Miraglia, S. M. Carbamazepine damage to rat spermatogenesis in different sexual developmental phases. *Int. J. Androl.* 32, 563–574 (2009).

179. Isojärvi, J. I. T. *et al.* Effect of epilepsy and antiepileptic drugs on male reproductive

health. *Neurology* 62, 247–253 (2004).

180. Reis, R. M., de Angelo, A. G., Sakamoto, A. C., Ferriani, R. A. & Lara, L. A. S. Altered sexual and reproductive functions in epileptic men taking carbamazepine. *J. Sex. Med.* 10, 493–499 (2013).

181. Chen, S.-S., Shen, M.-R., Chen, T.-J. & Lai, S.-L. Effects of Antiepileptic Drugs on Sperm Motility of Normal Controls and Epileptic Patients with Long-Term Therapy. *Epilepsia* 33, 149–153 (1992).

182. Fraz, S., Lee, A. H. & Wilson, J. Y. Gemfibrozil and carbamazepine decrease steroid production in zebrafish testes (Danio rerio). *Aquat. Toxicol.* 198, 1–9 (2018).

183. Fraz, S. *et al.* Paternal Exposure to Carbamazepine Impacts Zebrafish Offspring Reproduction over Multiple Generations. *Environ. Sci. Technol.* 53, 12734–12743 (2019).

184. Gambeta, E., Chichorro, J. G. & Zamponi, G. W. Trigeminal neuralgia: An overview from pathophysiology to pharmacological treatments. *Mol. Pain* 16, 1744806920901890 (2020).

185. Galus, M. *et al.* Chronic, low concentration exposure to pharmaceuticals impacts multiple organ systems in zebrafish. *Aquat. Toxicol.* 132–133, 200–211 (2013).

186. Galus, M. *et al.* Effects of chronic, parental pharmaceutical exposure on zebrafish (Danio rerio) offspring. *Aquat. Toxicol.* 151, 124–134 (2014).

187. Yan, S. *et al.* Environmentally Relevant Concentrations of Carbamazepine Caused Endocrine-Disrupting Effects on Nontarget Organisms, Chinese Rare Minnows (Gobiocypris rarus). *Environ. Sci. Technol.* 52, 886–894 (2018).

188. Hampel, M. *et al.* Transcriptome analysis of the brain of the sea bream (Sparus aurata) after exposure to human pharmaceuticals at realistic environmental concentrations. *Mar. Environ. Res.* 129, 36–45 (2017).

189. Kristofco, L. A., Du, B., Chambliss, C. K., Berninger, J. P. & Brooks, B. W. Comparative Pharmacology and Toxicology of Pharmaceuticals in the Environment: Diphenhydramine Protection of Diazinon Toxicity in Danio rerio but Not Daphnia magna. *AAPS J.* 17, 175–183 (2015).

190. Mizuguchi, H. *et al.* Antihistamines suppress upregulation of histidine decarboxylase gene expression with potencies different from their binding affinities for histamine H1 receptor in toluene 2,4-diisocyanate-sensitized rats. *J. Pharmacol. Sci.* 130, 212–218 (2016).

191. Wong, D. T., Perry, K. W. & Bymaster, F. P. The discovery of fluoxetine hydrochloride (Prozac). *Nat. Rev. Drug Discov.* 4, 950 (2005).

192. Berninger, J. P. *et al.* Effects of the antihistamine diphenhydramine on selected aquatic organisms. *Environ. Toxicol. Chem.* 30, 2065–2072 (2011).

193. Reichmann, F. *et al.* The zebrafish histamine H3 receptor modulates aggression, neural activity and forebrain functional connectivity. *Acta Physiol.* 230, 1–17 (2020).

194. Sundvik, M., Puttonen, H., Semenova, S. & Panula, P. The bullies are the leaders of the next generation: Inherited aminergic neurotransmitter system changes in socially dominant zebrafish, Danio rerio. *Behav. Brain Res.* 409, 113309 (2021).

195. Filby, A. L., Paull, G. C., Hickmore, T. F. A. & Tyler, C. R. Unravelling the neurophysiological basis of aggression in a fish model. *BMC Genomics* 11, (2010).

196. Panula, P., Sundvik, M. & Karlstedt, K. Developmental roles of brain histamine. *Trends Neurosci.* 37, 159–168 (2014).

197. Zhu, X. *et al.* Disruption of histamine/H1R signaling pathway represses cardiac differentiation and maturation of human induced pluripotent stem cells. *Stem Cell Res. Ther.* 11, 1–20 (2020).

198. Lalone, C. A. *et al.* Evidence for Cross Species Extrapolation of Mammalian-Based High-Throughput Screening Assay Results. *Environ. Sci. Technol.* 52, 13960–13971 (2018).

199. Luo, W. & Brouwer, C. Pathview: pathway based data integration and visualization. *Bioinformatics* 29, 1830–1831 (2015).

200. Ford, A. T. *et al.* The Role of Behavioral Ecotoxicology in Environmental Protection. *Environ. Sci. Technol.* 55, 5620–5628 (2021).

201. Ankley, G. T. *et al.* Adverse outcome pathways: A conceptual framework to support ecotoxicology research and risk assessment. *Environ. Toxicol. Chem.* 29, 730–741 (2010).

202. Truong, L. *et al.* Multidimensional in vivo hazard assessment using zebrafish. *Toxicol. Sci.* 137, 212–233 (2014).

203. Thunga, P., Truong, L., Tanguay, R. L. & Reif, D. M. Concurrent Evaluation of Mortality and Behavioral Responses: A Fast and Efficient Testing Approach for High-Throughput Chemical Hazard Identification. *Front. Toxicol.* 3, 1–8 (2021).

204. Luo, W. & Brouwer, C. Pathview: an R/Bioconductor package for pathway-based data integration and visualization. *Bioinformatics* 29, 1830–1831 (2013).

Appendix A

Table of Contents

METHODS

Bioluminescent Yeast Estrogenicity Screen (BLYES). 20 µL of sample extract was added in triplicate to the wells of white, solid-bottom 96-well microtiter plates and evaporated at room temperature in a Class II biological safety cabinet. Following evaporation, 200 µL of a 48-hour culture of strain BLYES adjusted to 0.4 (OD_{600}) in fresh yeast minimal media (YMM eu^{-}, ura^{-}) was added to each well. A 12-point standard curve of 17β-estradiol (E2; Sigma-Aldrich Co.) was included on each plate. A media control was included on all plates to establish background luminescence. Plates were covered and incubated in the dark at 30 °C for 4 hours. Luminescence was quantified using a SpectraMax M4 microplate reader (Molecular Devices) in luminescence mode (1,000 millisecond integration time), and estrogen equivalents (E_2Eq) of each sample were determined via interpolation to a 4-parameter curve within SoftMax Pro 6.2.2 (Molecular Devices). Relative net agonistic activity per liter of sample was then calculated on the basis of sample concentration. The detection limit for this assay was 0.18 ng/L $E_2Eq_{(BLYES)}$.

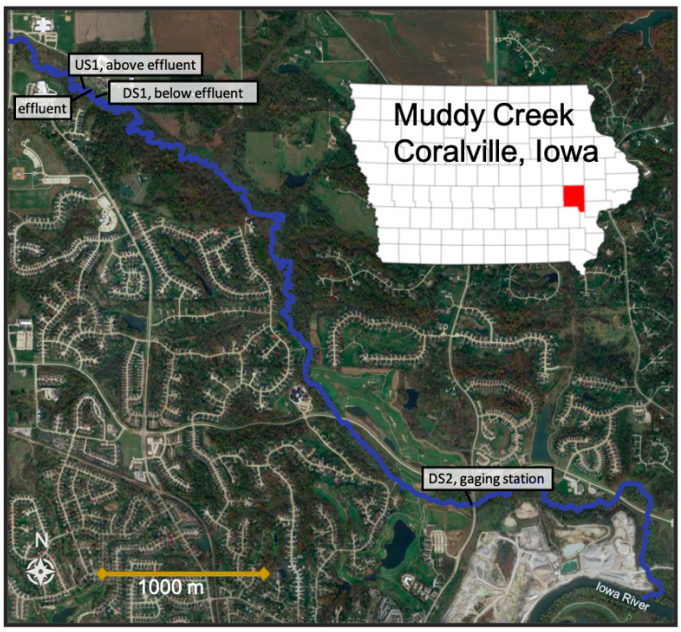

Figure A.1. Established USGS field sites along Muddy Creek in Coralville, IA, USA.

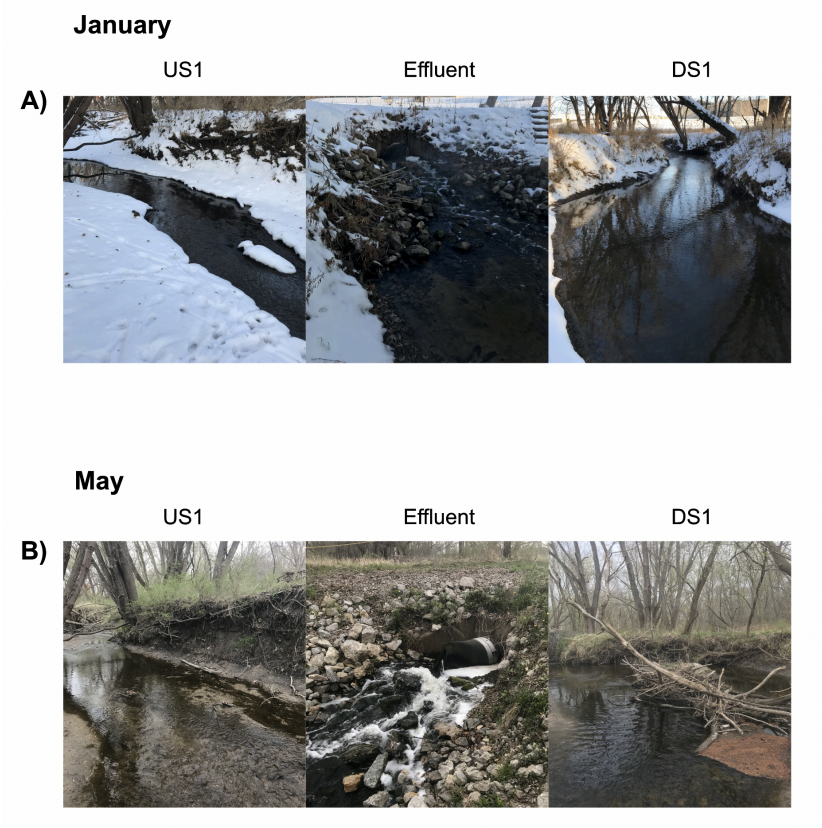

Figure A.2. Photos of each site taken by the authors on sampling days: January 8, 2018 and May 1, 2018.

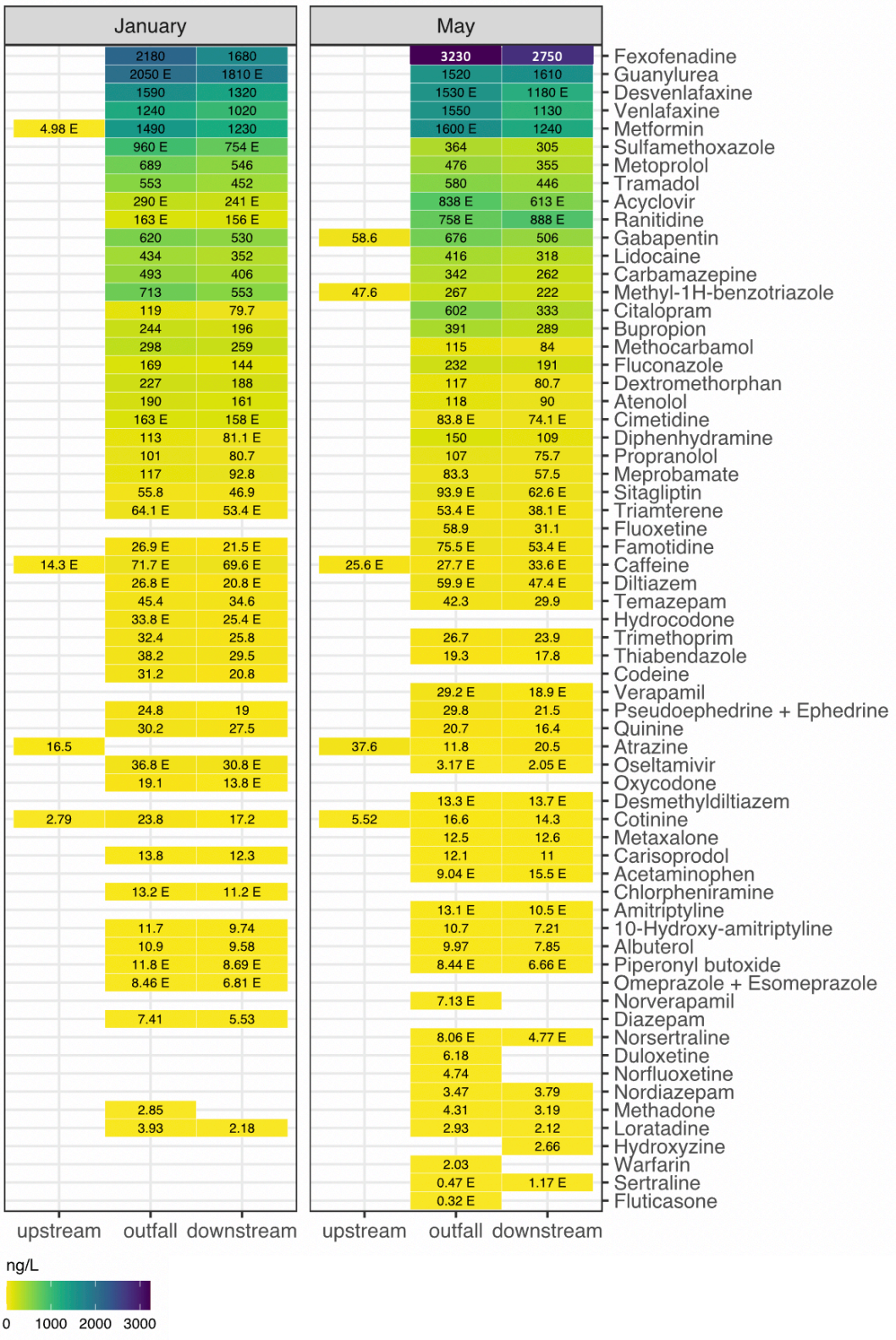

Figure A.3. Muddy Creek chemical detections (ng L^{-1}) in January and May 2018 at US1 (100 m above WWTP effluent outfall, 05454050), effluent (05454051), and DS1 (100 m below the effluent outfall, 05454052). "E" indicates estimated measurement.[111]

A) **Phototransduction KEGG pathway**
May 3 dpf (effluent vs. US1)

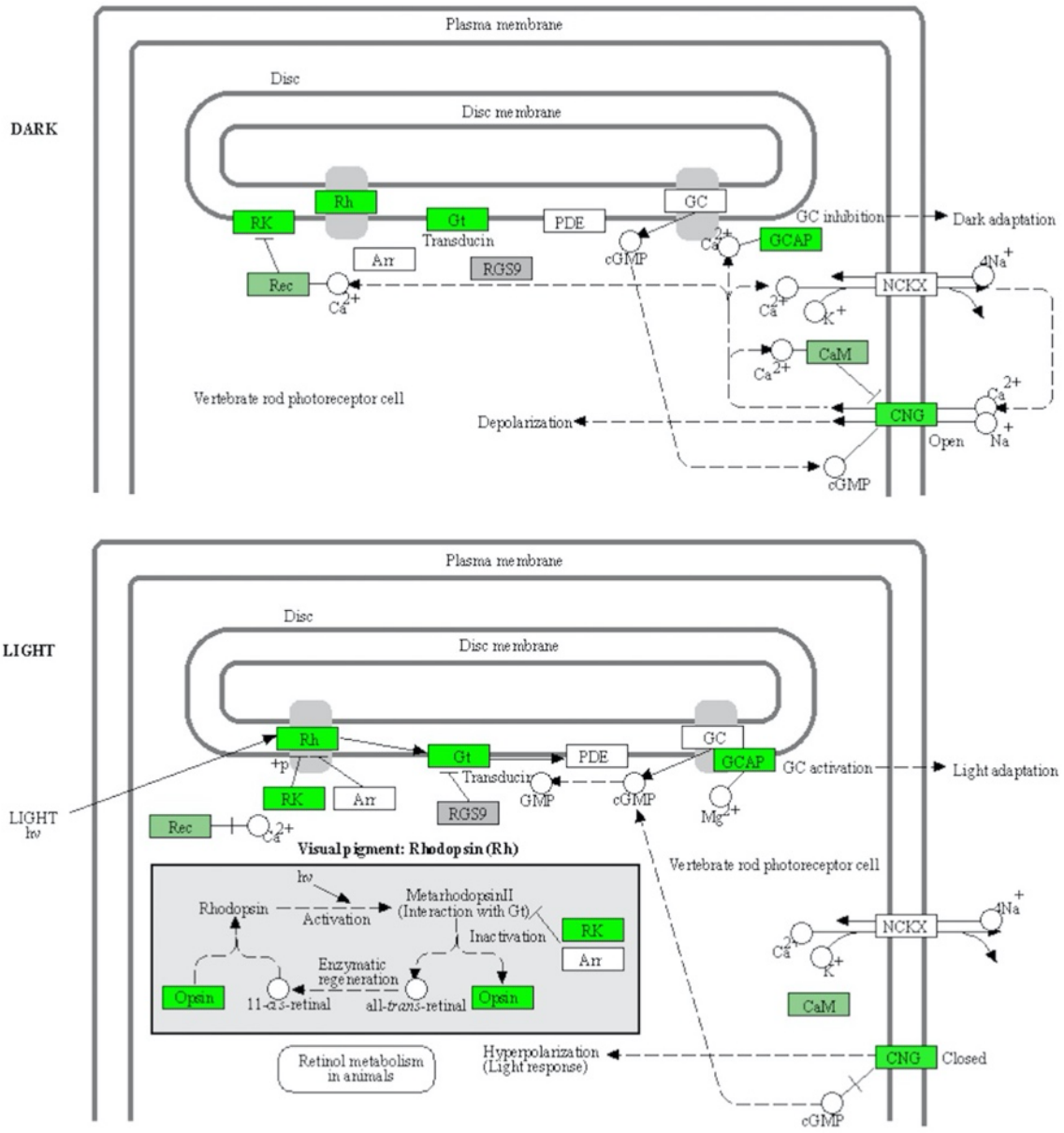

DETs on pathway

calm1a	gnat2	guca1c
calm1b	gnb1a	guca1g
calm2a	gngt1	opn1mw1
calm3a	grk1a	opn1mw2
calm3b	grk1b	rcvrn2
exorh	grk7b	rgs9b
gnat1	guca1b	rho

B) **Adrenergic signalling in cardiomyocytes KEGG pathway**
May 3 dpf (effluent vs. US1)

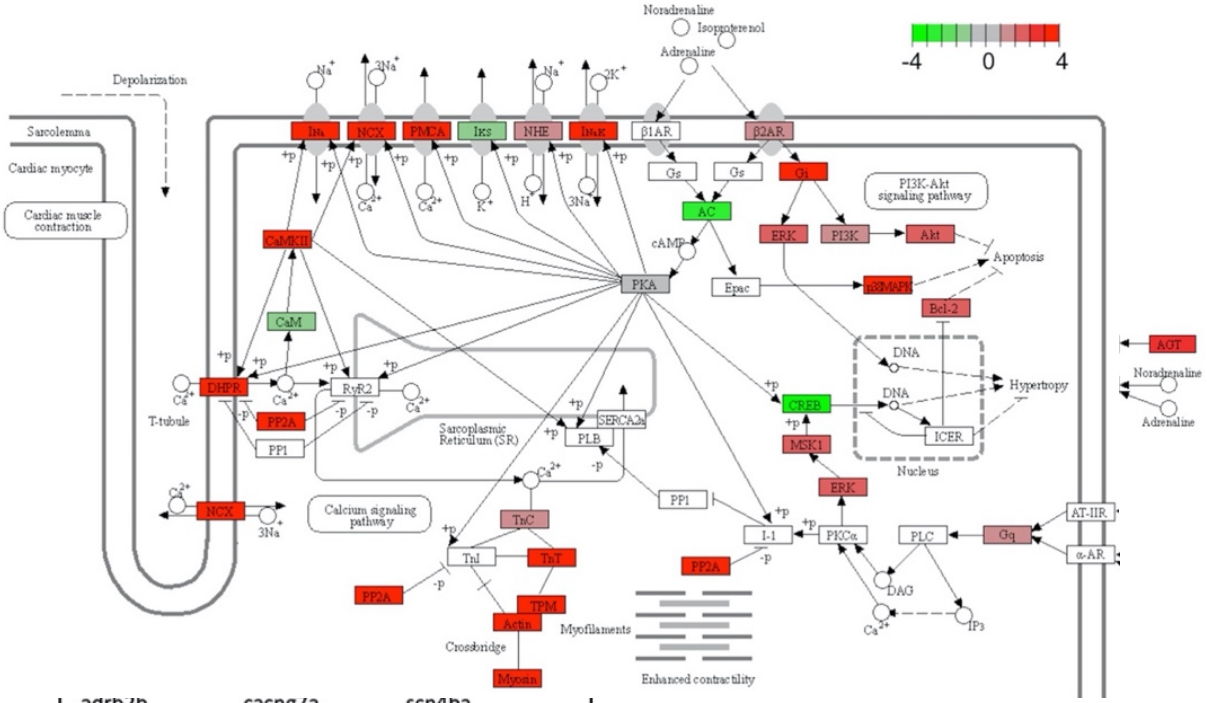

adrb2b	cacng7a	scn4ba
agt	camk2a	si:ch211-139a5.9
agtr2	camk2d1	si:ch211-225p5.8
akt3a	camk2g1	slc8a1b
atp1a2a	cmlc1	slc8a3
atp1b1b	creb3l2	slc8a4a
atp1b2a	gnai3	smyhc2
atp2b3a	gnaia	tnnc1b
atp2b3b	mapk1	tnnt2c
bcl2a	mapk13	tnnt2e
cacna1da	mapk14a	tpm1
cacna1sb	myh7l	tpm2
cacna2d2a	pik3r6a	tpm4b
cacna2d2b	plcb3	tpma
cacna2d3	ppp2ca	zgc:171775
cacng1a	ppp2r3a	zgc:86709
cacng4b	ppp2r3c	

Figure A.6. KEGG pathways[107] enriched (adjusted p-value <0.05) among transcripts differentially expressed (DETs) (adjusted p-value <0.01, $|\log_2$ fold change$|$ >1) between the effluent and US1 site in the May 3 dpf exposure: (A) Phototransduction and (B) Adrenergic signaling in cardiomyocytes KEGG pathway. KEGG pathway diagrams rendered via pathview v1.30.1 (R v4.0.1).[204] Color scale reflects DET $\log_2$ fold change.

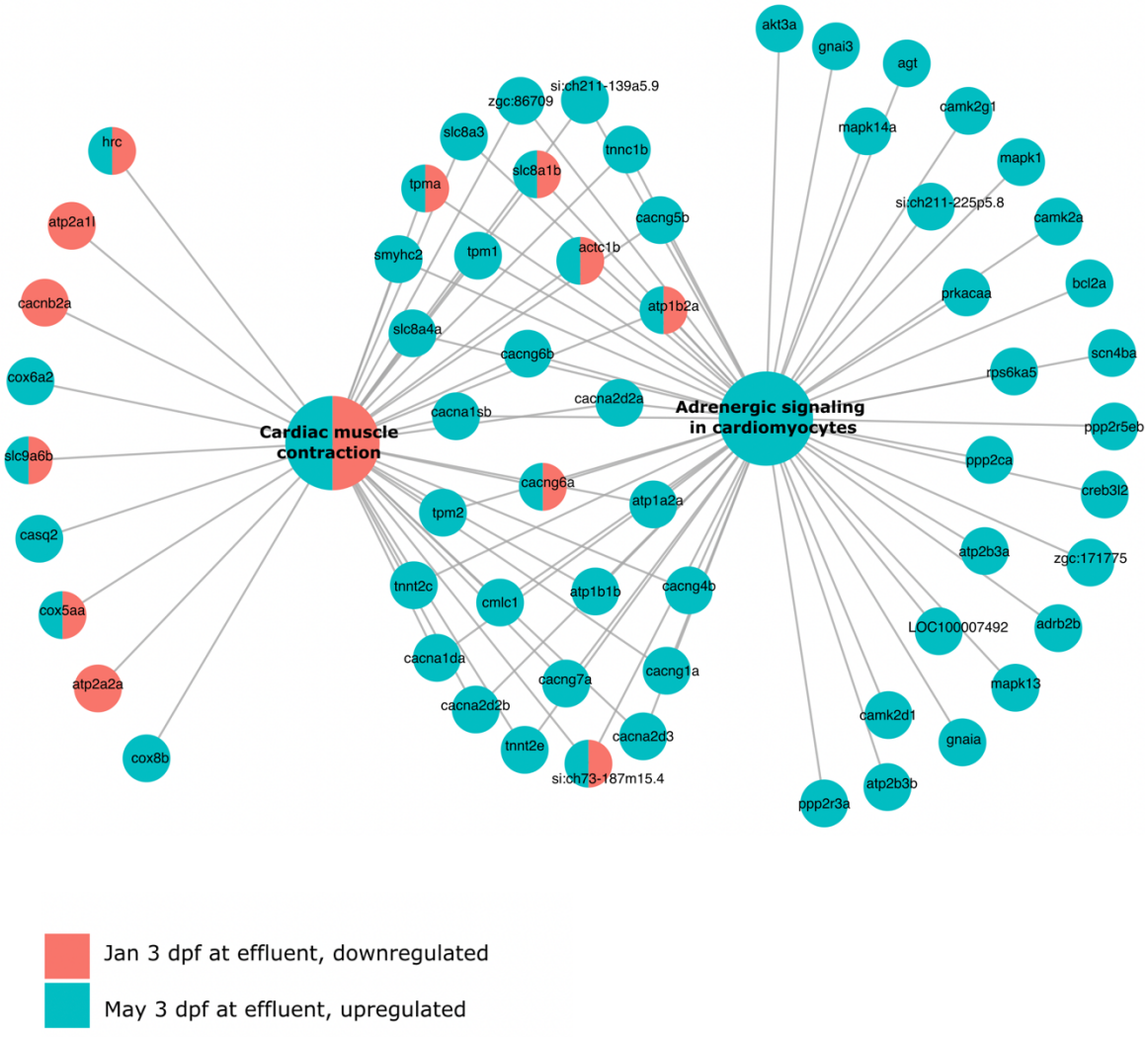

Figure A.5. DETs from January and May 3 dpf exposures on two enriched KEGG pathways: (1) Cardiac muscle contraction and (2) Adrenergic signaling in cardiomyocytes. Pathways were enriched (BH-adjusted p-value<0.05) among 3 dpf DETs at the effluent site (vs. US1) that were upregulated in January and downregulated in May.

NanoString	*RNAseq*	*gene*	*month*	*site*
0.8009611	2.610751	pck1	May	DS1
0.87886611	1.028346	fosab	Jan	DS1
1.63043612	1.318888	cyp1a	Jan	EFF
-2.1902871	-2.00028	fosab	May	DS1
-0.8334811	-0.46597	pparaa	May	DS1
-1.5214687	-1.61133	fosab	May	EFF
-0.9062394	-1.18363	gnat2	May	EFF
-0.9205855	-1.49584	gngt2b	May	EFF

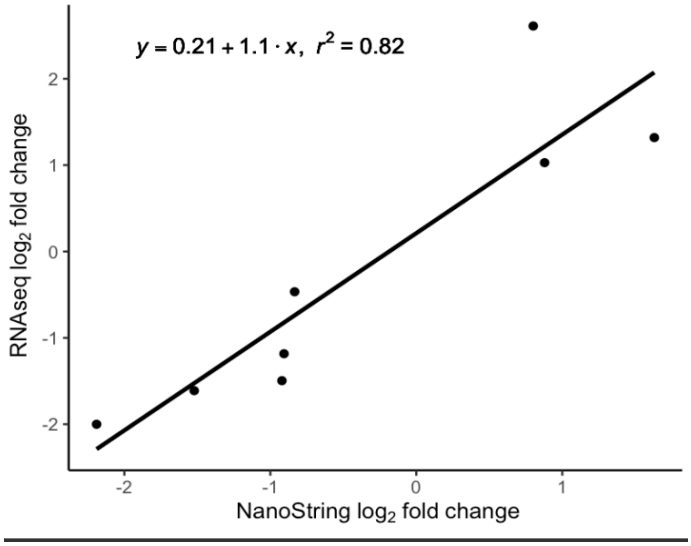

Figure A.6. Regression of $\log_2$ fold changes on the RNA sequencing and NanoString platforms. Genes validated are listed in the table above.

Table A1. Reporting limits from methods used in the 2017-2018 pharmaceutical study at Muddy Creek in North Liberty and Coralville, Iowa. Samples were analyzed at the National Water Quality Lab using LC-MS/MS as described by Furlong et. al. 2014.[98] Table adapted from Meppelink et al., 2020.[111]

Parameter name	Parameter code	CAS number	Reporting level		Source, use
1,7-Dimethylxanthine	67446	611-59-6	88	ng/L	Stimulant, metabolite of caffeine
10-Hydroxy-amitriptyline	67995	64520-05-4	8.3	ng/L	Degradate of amitriptyline
Abacavir	68022	136470-78-5	2	ng/L	Antiviral; reverse transcriptase inhibitor
Acetaminophen	67436	103-90-2	20	ng/L	Over-the-counter analgesic, antipyretic
Acyclovir	67484	59277-89-3	22	ng/L	Antiviral for treatment of herpes simplex
Albuterol	67437	18559-94-9	6.7	ng/L	Beta2-adrenergic receptor agonist for asthma treatment
Alprazolam	68250	28981-97-7	21	ng/L	Benzodiazepine used to treat anxiety disorders
Amitriptyline	67522	50-48-6	37	ng/L	Tricyclic antidepressant
Amphetamine	67461	300-62-9	4.4	ng/L	Psychostimulant
Antipyrine	67477	60-80-0	50	ng/L	Prescription analgesic, antipyretic
Atenolol	67502	29122-68-7	13	ng/L	Beta blocker used for treatment of hypertension
Atrazine	65065	1912-24-9	20	ng/L	Herbicide; used in this method to compare performance between compounds and between methods
Benztropine	67997	86-13-5	44	ng/L	Anticholinergic used in treatment of Parkinson's disease
Betamethasone	67485	378-44-9	114	ng/L	Synthetic glucocorticoid steroid used to treat inflammatory and autoimmune conditions
Bupropion	67439	34911-55-2	18	ng/L	Antidepressant and smoking cessation aid
Caffeine	67440	58-08-2	91	ng/L	Psychoactive stimulant in coffee, tea, and other preparations
Carbamazepine	67441	298-46-4	11	ng/L	Anticonvulsant and mood stabilizer used for epilepsy, bipolar disorder, trigeminal neuralgia
Carisoprodol	67498	78-44-4	20	ng/L	Muscle relaxant

Parameter name	Parameter code	CAS number	Reporting level		Source, use
Chlorpheniramine	67497	132-22-9	54	ng/L	Over-the-counter antihistamine for relief of allergy symptoms
Cimetidine	67442	51481-61-9	140	ng/L	Histamine H2-receptor antagonist that inhibits production of stomach acid
Citalopram	67505	59729-33-8	6.6	ng/L	Selective serotonin reuptake inhibitor (SSRI) used to treat major depression, anxiety disorders
Clonidine	67518	4205-90-7	61	ng/L	Antihypertensive
Codeine	67443	76-57-3	32	ng/L	Opiate used as analgesic, antitussive, and antidiarrheal
Cotinine	67444	486-56-6	6.4	ng/L	Metabolite of nicotine; tobacco constituent
Dehydronifedipine	67445	67035-22-7	20	ng/L	Metabolite of the antihypertensive nifedipine
Desmethyldiltiazem	67999	--	70	ng/L	Degradate of diltiazem
Desvenlafaxine	68251	93413-62-8	84	ng/L	Antidepressant serotonin-norepinephrine reuptake inhibitor, also major active metabolite of venlafaxine
Dextromethorphan	67468	125-71-3	8.2	ng/L	Cough suppressant in over-the-counter cold and cough medications
Diazepam (valium)	67499	439-14-5	4	ng/L	Benzodiazepine used to treat anxiety, insomnia, seizures
Diltiazem	67519	42399-41-7	10	ng/L	Calcium channel blocker used to treat hypertension, angina, some arrhythmias
Diphenhydramine	67447	147-24-0	48	ng/L	Antihistamine
Duloxetine	67448	116539-59-4	37	ng/L	Antidepressant; serotonin and norepinephrine reuptake inhibitor
Erythromycin	67449	114-07-8	80	ng/L	Macrolide antibiotic
Ezetimibe	67487	163222-33-1	205	ng/L	Cholesterol-reducing medication
Fadrozole	68012	102676-47-1	13	ng/L	Aromatase inhibitor used for treatment of breast cancer
Famotidine	68000	76824-35-6	34	ng/L	Histamine H2-receptor antagonist that inhibits production of stomach acid
Fenofibrate	67489	49562-28-9	6.4	ng/L	Fibrate drug used to reduce cholesterol levels
Fexofenadine	67510	83799-24-0	44	ng/L	Terfenadine degradate; an antihistamine used to treat allergies

Parameter name	Parameter code	CAS number	Reporting level		Source, use
Fluconazole	67478	86386-73-4	30	ng/L	Triazole antifungal
Fluoxetine	67450	54910-89-3	26	ng/L	Selective serotonin reuptake inhibitor (SSRI) used to treat major depression, anxiety disorders
Fluticasone propionate	67529	80474-14-2	30	ng/L	Synthetic corticosteroid used to treat asthma and eosinophilic esophagitis
Fluvoxamine	67521	54739-18-3	80	ng/L	Selective serotonin reuptake inhibitor (SSRI) antidepressant used to treat depression, anxiety disorders
Gabapentin	52817	60142-96-3	160	ng/L	Anticonvulsant and used to treat neuropathic pain
Glipizide	68001	29094-61-9	80	ng/L	Sulfonylurea antidiabetic drug
Glyburide	68002	10238-21-8	58	ng/L	Sulfonylurea antidiabetic drug
Guanylurea	52816	141-83-3	140	ng/L	Transformation product of Metformin
Hexamethylenetetramine	52815	100-97-0	110	ng/L	Used in the treatment of urinary tract infections
Hydrocodone	67506	125-29-1	40	ng/L	Semi-synthetic opioid, narcotic analgesic and antitussive
Hydrocortisone	67459	50-23-7	147	ng/L	Naturally-produced glucocorticoid hormone used for immunosuppressive and anti-inflammatory effects
Hydroxyzine	68005	68-88-2	7.4	ng/L	Antihistamine, sedative
Iminostilbene	67481	256-96-2	145	ng/L	Intermediate for manufacture of carbamazepine, tricyclic antidepressants, also degradate
Ketoconazole	68014	65277-42-1	113	ng/L	Antifungal
Lamivudine	68018	134678-17-4	16	ng/L	Reverse-transcriptase inhibitor used to treat Hepatitis-B
Lidocaine	67462	137-58-6	8	ng/L	Topical anesthetic
Loperamide	67515	53179-11-6	80	ng/L	Opioid antidiarrheal
Loratadine	67488	79794-75-5	7	ng/L	Antihistamine
Lorazepam	67470	846-49-1	202	ng/L	Benzodiazepine used for its anxiolytic, amnesic, sedative/hypnotic, anticonvulsant, and muscle relaxant effects
Meprobamate	67464	57-53-4	12	ng/L	Carbamate derivative used as an anxiolytic

Parameter name	Parameter code	CAS number	Reporting level		Source, use
Metaxalone	67504	1665-48-1	16	ng/L	Muscle relaxant
Metformin	67492	657-24-9	13	ng/L	Treatment of Type 2 diabetes
Methadone	67500	76-99-3	7.6	ng/L	Synthetic opioid used as an analgesic and to treat opioid addiction
Methocarbamol	67501	532-03-6	11	ng/L	Muscle relaxant
Methotrexate	67525	59-05-2	52	ng/L	Antimetabolite and antifolate drug used in treatment of cancer
Methyl-1H-benzotriazole	67514	29385-43-1	80	ng/L	Corrosion inhibitor; used in this method to compare performance between compounds and between methods
Metoprolol	67523	51384-51-1	10	ng/L	Used to treat cardiovascular disease, especially hypertension
Morphine	67458	57-27-2	80	ng/L	Opiate used as analgesic
Nadalol	68006	42200-33-9	20	ng/L	Beta blocker used to reduce high blood pressure, migraine headaches, chest pain
Nevirapine	68017	129618-40-2	46	ng/L	Antiretroviral used to treat HIV-1 infection
Nicotine	67493	54-11-5	58	ng/L	Alkaloid stimulant found in tobacco
Nizatidine	67479	76963-41-2	80	ng/L	Acid inhibitor used to treat ulcer and acid reflux disease
Nordiazepam	68252	1088-11-5	20	ng/L	Benzodiazepine drug used to treat anxiety; also active metabolite of diazepam and other benzodiazepine drugs
Norethindrone	67434	68-22-4	20	ng/L	Oral contraceptive component
Norfluoxetine	67451	56161-73-0	80	ng/L	Active metabolite of fluoxetine
Norsertraline	67532	87857-41-8	80	ng/L	Degradate of sertraline
Norverapamil	68007	67018-85-3	8.6	ng/L	Active metabolite of verapamil
Omeprazole + Esomprazole	67512	-	16	ng/L	Proton pump inhibitors used to treat dyspepsia and ulcers
Oseltamivir	67511	196618-13-0	15	ng/L	Antiviral
Oxazepam	67469	604-75-1	226	ng/L	Benzodiazepine used to treat anxiety, insomnia, and alcohol withdrawal

Parameter name	Parameter code	CAS number	Reporting level		Source, use
Oxycodone	67495	76-42-6	25	ng/L	Opiate used as analgesic and antidiarrheal; also compounded with acetaminophen or other anti-inflammatory drugs such as ibuprofen
Paroxetine	67527	61869-08-7	72	ng/L	Selective serotonin reuptake inhibitor (SSRI) antidepressant used to treat depression, obsessive-compulsive disorder, panic disorder, anxiety disorders
Penciclovir	68021	39809-25-1	80	ng/L	Antiviral for treatment of herpes infections
Pentoxifylline	67480	5/6/93	9.4	ng/L	Cardiovascular drug that improves blood flow
Phenazopyridine	68008	94-78-0	13	ng/L	Used to treat pain, irritation in urinary tract
Phendimetrazine	67496	634-03-7	20	ng/L	Stimulant used as an appetite suppressant
Phenytoin	67466	57-41-0	188	ng/L	Antiepileptic for seizures
Piperonyl butoxide	67435	51-03-6	60	ng/L	Pesticide synergist used in lice treatment medications; also used in this method to compare performance between compounds and between methods
Prednisolone	67483	50-24-8	150	ng/L	Corticosteroid drug used for the treatment of inflammatory and autoimmune conditions, also a metabolite of prednisone
Prednisone	67467	53-03-2	105	ng/L	Synthetic corticosteroid immunosuppressant drug
Promethazine	67524	60-87-7	114	ng/L	Antihistamine, antiemetic, sedative
Propoxyphene	68009	469-62-5	28	ng/L	Opioid analgesic used for mild pain
Propranolol	67516	525-66-6	26	ng/L	Beta blocker used for treatment of hypertension, tremors
Pseudoephedrine + Ephedrine	67460	-	6	ng/L	Appetite suppressant, decongestant, stimulant
Quinine	68011	130-95-0	80	ng/L	Antimalarial, bitter flavoring agent, mild antipyretic, and analgesic
Ractopamine	52814	97825-25-7	20	ng/L	Beta adrenoreceptor agonist growth promotant, used primarily in livestock
Raloxifene	67530	84449-90-1	80	ng/L	Selective estrogen receptor modulator prescribed for osteoporosis
Ranitidine	67452	66357-35-5	192	ng/L	Acid inhibitor used to treat ulcer and acid reflux disease
Sertraline	67528	79617-96-2	16	ng/L	SSRI antidepressant used to treat depression, obsessive-compulsive disorder, anxiety disorders
Sitagliptin	67531	486460-32-6	97	ng/L	Antihyperglycemic

Parameter name	Parameter code	CAS number	Reporting level		Source, use
Sulfadimethoxine	67503	122-11-2	30	ng/L	Sulfonamide antibiotic drug
Sulfamethizole	67476	144-82-1	104	ng/L	Sulfonamide antibiotic drug
Sulfamethoxazole	67454	723-46-6	20	ng/L	Sulfonamide antibiotic drug
Tamoxifen	68015	10540-29-1	270	ng/L	Estrogen receptor agonist used in the treatment of breast cancer
Temazepam	67471	846-50-4	18	ng/L	Hypnotic
Theophylline	67494	58-55-9	80	ng/L	Antiasthmatic, diuretic
Thiabendazole	67455	148-79-8	4	ng/L	Parasiticide, fungicide
Tiotropium	67508	186691-13-4	50	ng/L	Bronchodilator used for chronic obstructive pulmonary disease
Tramadol	67517	27203-92-5	7.4	ng/L	Opiate used as analgesic
Triamterene	67475	396-01-0	5.2	ng/L	Diuretic
Trimethoprim	67456	738-70-5	20	ng/L	Antibiotic used in treatment of urinary tract infections
Valacyclovir	67507	124832-26-4	163	ng/L	Antiviral for treatment of herpes infections
Venlafaxine	67534	93413-69-5	5.2	ng/L	Antidepressant; serotonin and norepinephrine reuptake inhibitor
Verapamil	67472	52-53-9	140	ng/L	Calcium channel blocker used in the treatment of hypertension, angina pectoris, cardiac arrhythmia
Warfarin	67457	81-81-2	6	ng/L	Anticoagulant, also used in rodenticides

Table A2. Field parameters for Muddy Creek, January and May 2018. Reprinted from Meppelink et al., 2020.

month	site	Discharge, instantaneous, cubic feet per second	Dissolved oxygen, milligrams per liter	pH, standard units	Specific conductance, microseimens per centimeter	Temperature, degrees Celsius	Turbidity, formazin nephelometric units (FNU)	Dissolved organic matter fluorescence (fDOM), micrograms per liter as quinine sulfate equivalents (QSE)
January	US1	0.38 *	9.2	7.4	1090	3.2	2.1	24.87
January	Effluent	3.22 *	9.1	7.6	3210	15.8	0.4	133.8
January	DS1	3.6 *	9.3	7.6	3000	14.3	1.5	124.6
January	DS2	1.22 *	11.6	7.8	2420	0	4.1	97.73
May	US1	0.71	7.7	7.6	889	13.9	14	40.34
May	Effluent	2.99	9.2	7.3	3040	14.9		153.8
May	DS1	3.7	9.1	7.5	2660	14.7	3.8	131.4
May	DS2	3.2	9	8	1890	13.8	4.5	89.59

* indicates value estimated by U.S. Geological Survey; the streamflow measurement for US1 for January was inadvertently deleted prior to formal documentation and was estimated by using available streamflow measurements from the December 2017 (US1 and DS1) to January 2018 (DS1) and by comparing photos from December 2017 and January 2018 at US1.

Table A3. Chemical classes of detected chemicals in January and May 2018.

Chemical classes		
CAS	**Chemical**	**Class**
27203-92-5	Tramadol	Analgesic-Antinflammatory
103-90-2	Acetaminophen	Analgesic-Antinflammatory
78-44-4	Carisoprodol	Analgesic-Antinflammatory
137-58-6	Lidocaine	Analgesic-Antinflammatory
76-99-3	Methadone	Analgesic-Antinflammatory
532-03-6	Methocarbamol	Analgesic-Antinflammatory
76-57-3	Codeine	Analgesic-Antinflammatory
76-42-6	Oxycodone	Analgesic-Antinflammatory
68-88-2	Hydroxyzine	Analgesic-Antinflammatory
1665-48-1	Metaxalone	Analgesic-Antinflammatory
125-29-1	Hydrocodone	Analgesic-Antinflammatory
57-27-2	Morphine	Analgesic-Antinflammatory
130-95-0	Quinine	Anti-malarial
723-46-6	Sulfamethoxazole	Antibiotic
738-70-5	Trimethoprim	Antibiotic
114-07-8	Erythromycin	Antibiotic
50-48-6	Amitriptyline	Antidepressant
34911-55-2	Bupropion	Antidepressant
59729-33-8	Citalopram	Antidepressant
93413-62-8	Desvenlafaxine	Antidepressant
54910-89-3	Fluoxetine	Antidepressant
79617-96-2	Sertraline	Antidepressant
93413-69-5	Venlafaxine	Antidepressant
116539-59-4	Duloxetine	Antidepressant
148-79-8	Thiabendazole	Antifungal
86386-73-4	Fluconazole	Antifungal
132-22-9	Chlorpheniramine	Antihistamines
147-24-0	Diphenhydramine	Antihistamines
83799-24-0	Fexofenadine	Antihistamines
79794-75-5	Loratadine	Antihistamines
136470-78-5	Abacavir	Antiviral
59277-89-3	Acyclovir	Antiviral
134678-17-4	Lamivudine	Antiviral
196618-13-0	Oseltamivir	Antiviral
18559-94-9	Albuterol	Asthma Relief
58-55-9	Theophylline	Asthma Relief
29122-68-7	Atenolol	Beta blocker
51384-51-1	Metoprolol	Beta blocker
525-66-6	Propranolol	Beta blocker
42399-41-7	Diltiazem	Cardiovascular Care
486460-32-6	Sitagliptin	Cardiovascular Care
396-01-0	Triamterene	Cardiovascular Care
52-53-9	Verapamil	Cardiovascular Care
81-81-2	Warfarin	Cardiovascular Care
29385-43-1	Methyl-1H-benzotriazole	Corrosion inhibitor
486-56-6	Cotinine	Degradate
611-59-6	1,7-Dimethylxanthine	Degradate
64520-05-4	10-Hydroxy-amitriptyline	Degradate
86408-45-9	Desmethyldiltiazem	Degradate
141-83-3	Guanylurea	Degradate
67018-85-3	Norverapamil	Degradate
56161-73-0	Norfluoxetine	Degradate
87857-41-8	Norsertraline	Degradate
657-24-9	Metformin	Diabetes care

Chemical classes		
CAS	**Chemical**	**Class**
51481-61-9	Cimetidine	H2 Antagonists
76824-35-6	Famotidine	H2 Antagonists
66357-35-5	Ranitidine	H2 Antagonists
1912-24-9	Atrazine	Herbicide
60142-96-3	Gabapentin	Neurochemical Modulation
57-53-4	Meprobamate	Neurochemical Modulation
298-46-4	Carbamazepine	Neurochemical Modulation
57-41-0	Phenytoin	Neurochemical Modulation
28981-97-7	Alprazolam	Neurochemical Modulation
1088-11-5	Nordiazepam	Neurochemical Modulation
439-14-5	Diazepam	Neurochemical Modulation
54-11-5	Nicotine	OTC
125-71-3	Dextromethorphan	OTC
73590-58-6	Omeprazole + Esomeprazole	OTC
51-03-6	Piperonyl butoxide	Pesticide
846-50-4	Temazepam	Sedative
80474-14-2	Fluticasone	Steroid
58-08-2	Caffeine	Stimulant
300-62-9	Amphetamine	Stimulant
50-98-6	Pseudoephedrine + Ephedrine	Stimulant

Table A3. Total concentrations (μg/L) of detected chemicals by class at the effluent site in January and May 2018.

Total concentrations at the effluent site (μg/L)		
Class	**January**	**May**
Antidepressant	3.193	4.15165
Antihistamines	2.31013	3.38293
Degradate	2.0855	1.58053
Diabetes care	1.49	1.6
Analgesic, Anti inflammatory	1.38575	1.14895
Neurochemical Modulation	1.23741	1.10477
Antibiotic	0.9924	0.3907
Beta blocker	0.98	0.701
Corrosion inhibitor	0.713	0.267
H2 Antagonists	0.3529	0.9173
Antiviral	0.3268	0.84117
OTC	0.23546	0.117
Antifungal	0.2072	0.2513
Cardiovascular Care	0.1467	0.23843
Stimulant	0.0965	0.0575
Sedative	0.0454	0.0423
Anti-malarial	0.0302	0.0207
Pesticide	0.0118	0.00844
Asthma Relief	0.0109	0.00997
Herbicide	0	0.0118
Steroid	0	0.00032

Appendix B

Table of Contents

Table B.1. Bioactivity data from the ToxCast database was used for alternative formulations of chemicals detected in the analytical chemistry dataset as shown below.

Analytical chemistry dataset **Chemical Name**	**CASRN**	*ToxCast Database* **Chemical Name**	**CASRN**
Amitriptyline	50-48-6	Amitriptyline hydrochloride	549-18-8
Bupropion	34911-55-2	Bupropion hydrochloride	31677-93-7
Chlorpheniramine	132-22-9	Chlorpheniramine maleate	113-92-8
Clonidine	4205-90-7	Clonidine hydrochloride	4205-91-8
Codeine	76-57-3	Codeine hydrochloride	1422-07-7
Dextromethorphan	125-71-3	Dextromethorphan hydrobromide monohydrate	6700-34-1
Diphenhydramine	147-24-0	Diphenhydramine hydrochloride	147-24-0
Duloxetine	116539-59-4	Duloxetine hydrochloride	136434-34-9
Pseudoephedrine + Ephedrine	299-42-3	Ephedrine hydrochloride	50-98-6
Erythromycin	114-07-8	Erythromycin estolate	3521-62-8
Citalopram	59729-33-8	Escitalopram oxalate	219861-08-2
Fadrozole	102676-47-1	Fadrozole hydrochloride	102676-31-3
Fexofenadine	83799-24-0	Fexofenadine hydrochloride	153439-40-8
Fluoxetine	54910-89-3	Fluoxetine hydrochloride	56296-78-7
Hydrocodone	125-29-1	Hydrocodone phosphate (2:3) monohydrate	NOCAS_47802
Hydroxyzine	68-88-2	Hydroxyzine hydrochloride	1244-76-4
Propoxyphene	469-62-5	Levopropoxyphene napsylate	5714-90-9
Metformin	657-24-9	Metformin hydrochloride	1115-70-4
Methadone	76-99-3	Methadone hydrochloride	1095-90-5
Morphine	57-27-2	Morphine sulfate pentahydrate	6211-15-0
Oseltamivir	196618-13-0	Oseltamivir tartrate	NOCAS_45954
Phenazopyridine	94-78-0	Phenazopyridine hydrochloride	136-40-3
Promethazine	60-87-7	Promethazine hydrochloride	58-33-3
Propranolol	525-66-6	Propranolol hydrochloride	318-98-9
Quinine	130-95-0	Quinine hydrochloride dihydrate	6119-47-7
Ractopamine	97825-25-7	Ractopamine hydrochloride	90274-24-1
Raloxifene	84449-90-1	Raloxifene hydrochloride	82640-04-8
Sertraline	79617-96-2	Sertraline hydrochloride	79559-97-0
Tamoxifen	10540-29-1	Tamoxifen citrate	54965-24-1
Tiotropium	186691-13-4	Tiotropium bromide	136310-93-5
Tramadol	27203-92-5	Tramadol hydrochloride	36282-47-0
Valacyclovir	124832-26-4	Valacyclovir hydrochloride	124832-27-5
Venlafaxine	93413-69-5	Venlafaxine hydrochloride	99300-78-4
Verapamil	52-53-9	Verapamil hydrochloride	152-11-4

Table B.2 Chemical-assay combinations excluded from consideration in generation of EAR values. *indicates assays that were removed from consideration across all chemicals.

CAS	Chemical	Endpoint
		Tanguay_ZF_120hpf_ActivityScore*
		TOX21_TSHR_wt_ratio*
31677-93-7	Bupropion hydrochloride	TOX21_RT_HEPG2_FLO_40hr_ctrl_viability
31677-93-7	Bupropion hydrochloride	TOX21_RT_HEPG2_FLO_24hr_viability
31677-93-7	Bupropion hydrochloride	TOX21_RT_HEPG2_FLO_00hr_ctrl_viability
78-44-4	Carisoprodol	TOX21_RT_HEK293_GLO_40hr_viability
76824-35-6	Famotidine	TOX21_RT_HEK293_FLO_40hr_viability
153439-40-8	Fexofenadine hydrochloride	TOX21_RT_HEPG2_FLO_00hr_ctrl_viability
60142-96-3	Gabapentin	TOX21_RT_HEPG2_FLO_08hr_viability
60142-96-3	Gabapentin	TOX21_RT_HEPG2_FLO_16hr_ctrl_viability
532-03-6	Methocarbamol	TOX21_RT_HEK293_FLO_24hr_viability
532-03-6	Methocarbamol	TOX21_RT_HEK293_FLO_08hr_viability
54-11-5	Nicotine	TOX21_RT_HEK293_FLO_16hr_viability
54-11-5	Nicotine	TOX21_RT_HEK293_FLO_24hr_viability
73590-58-6	Omeprazole	TOX21_ERb_BLA_Antagonist_viability
73590-58-6	Omeprazole	TOX21_PR_BLA_Antagonist_viability
73590-58-6	Omeprazole	TOX21_PR_BLA_Agonist_viability
66357-35-5	Ranitidine	TOX21_RT_HEK293_FLO_08hr_viability
66357-35-5	Ranitidine	TOX21_RT_HEK293_FLO_40hr_viability
723-46-6	Sulfamethoxazole	TOX21_RT_HEK293_GLO_16hr_viability
148-79-8	Thiabendazole	NHEERL_MHC_MHCvCellCount_dn
29385-43-1	Tolyltriazole	TOX21_RT_HEK293_FLO_32hr_viability
29385-43-1	Tolyltriazole	TOX21_RT_HEK293_FLO_24hr_viability
29385-43-1	Tolyltriazole	TOX21_RT_HEK293_FLO_16hr_viability
66357-35-5	Ranitidine	TOX21_RT_HEK293_FLO_00hr_viability
66357-35-5	Ranitidine	TOX21_RT_HEK293_FLO_16hr_viability
66357-35-5	Ranitidine	TOX21_RT_HEK293_FLO_24hr_viability
66357-35-5	Ranitidine	TOX21_RT_HEK293_FLO_32hr_viability
137-58-6	Lidocaine	TOX21_RT_HEK293_GLO_08hr_viability
137-58-6	Lidocaine	TOX21_RT_HEK293_GLO_16hr_viability
137-58-6	Lidocaine	TOX21_RT_HEK293_GLO_24hr_viability
137-58-6	Lidocaine	TOX21_RT_HEK293_GLO_32hr_viability
137-58-6	Lidocaine	TOX21_RT_HEK293_GLO_40hr_viability
137-58-6	Lidocaine	TOX21_RT_HEPG2_FLO_00hr_ctrl_viability
137-58-6	Lidocaine	TOX21_RT_HEPG2_FLO_08hr_viability
137-58-6	Lidocaine	TOX21_RT_HEPG2_FLO_16hr_ctrl_viability
137-58-6	Lidocaine	TOX21_RT_HEPG2_FLO_24hr_viability
137-58-6	Lidocaine	TOX21_RT_HEPG2_FLO_32hr_ctrl_viability
147-24-0	Diphenhydramine hydrochloride	NVS_GPCR_hM3
18559-94-9	Albuterol	TOX21_p53_BLA_p5_ratio
318-98-9	Propranolol hydrochloride	TOX21_RT_HEK293_FLO_08hr_viability
147-24-0	Diphenhydramine hydrochloride	ACEA_AR_agonist_AUC_viability
532-03-6	Methocarbamol	TOX21_RT_HEPG2_FLO_40hr_ctrl_viability
532-03-6	Methocarbamol	TOX21_RT_HEK293_FLO_00hr_viability

Table B.3. Chemical-endpoint combinations that generated an EAR>0.001 from at least one sampling event over the seven months analyzed (January-August 2018, excluding March)

Chemical	Endpoints	Biological target	Gene target
Acetaminophen	NVS_NR_hPR,	Steroidal	PGR
	BSK_LPS_CD40_down	Inflammatory Factor	CD40
Carisoprodol	TOX21_RT_HEK293_FLO_16hr_viability	Cytotoxicity	
Methadone hydrochloride	NVS_GPCR_rOpiate_NonSelective	Rhodopsin-Like Receptor	OPRM1
	NVS_TR_rSERT	Neurotransmitter Transporter	SLC6A4
Fluconazole	NVS_ADME_hCYP2C19	Xenobiotic Metabolism	CYP2C19
Thiabendazole	CLD_CYP1A2_48hr	Basic Helix-Loop-Helix Protein	CYP1A2
	NVS_ENZ_hPPP2CA	Serine/Threonine Phosphatase	PPP2CA
	CLD_CYP1A1_48hr	Basic Helix-Loop-Helix Protein	CYP1A1
	CLD_CYP1A2_24hr	Basic Helix-Loop-Helix Protein	CYP1A2
	CLD_CYP1A1_24hr	Basic Helix-Loop-Helix Protein	CYP1A1
Chlorpheniramine maleate	TOX21_RT_HEPG2_FLO_16hr_ctrl_viability	Cytotoxicity	
	TOX21_RT_HEPG2_FLO_32hr_ctrl_viability	Cytotoxicity	
	TOX21_RT_HEPG2_FLO_40hr_ctrl_viability	Cytotoxicity	
Diphenhydramine hydrochloride	NVS_GPCR_hM5	Rhodopsin-Like Receptor	CHRM5
	NVS_ADME_hCYP2D6	Xenobiotic Metabolism	CYP2D6
	NVS_GPCR_p5HT2C	Rhodopsin-Like Receptor	HTR2C
	NVS_GPCR_hM1	Rhodopsin-Like Receptor	CHRM1
	NVS_TR_gDAT	Neurotransmitter Transporter	SLC6A3
	NVS_GPCR_hM4	Rhodopsin-Like Receptor	CHRM4
	NVS_GPCR_gH2	Rhodopsin-Like Receptor	Hrh2
	NVS_GPCR_gMPeripheral_NonSelective	Rhodopsin-Like Receptor	CHRM3
	NVS_GPCR_hM2	Rhodopsin-Like Receptor	CHRM2
	NVS_GPCR_h5HT7	Rhodopsin-Like Receptor	HTR7
	NVS_TR_hDAT	Neurotransmitter Transporter	SLC6A3
	NVS_GPCR_bH1	Rhodopsin-Like Receptor	HRH1
	NVS_GPCR_hH1	Rhodopsin-Like Receptor	HRH1
Acyclovir	TOX21_DT40_657	DNA Repair	
	TOX21_DT40	DNA Repair	
	TOX21_DT40_100	DNA Repair	
Lamivudine	TOX21_RT_HEK293_FLO_24hr_viability	Cytotoxicity	
	TOX21_RT_HEK293_FLO_32hr_viability	Cytotoxicity	
Albuterol	TOX21_TSHR_Agonist_ratio		TSHR
Theophylline	NVS_GPCR_hAdoRA2a	Rhodopsin-Like Receptor	ADORA2A
	OT_AR_ARELUC_AG_1440	Steroidal	AR
Tolyltriazole	TOX21_RT_HEK293_FLO_08hr_viability	Cytotoxicity	
17-Dimethylxanthine	NVS_ENZ_rMAOAC	Monoamine Oxidase	Maoa
	NVS_GPCR_hAdoRA1	Rhodopsin-Like Receptor	ADORA1
Cotinine	TOX21_p53_BLA_p3_viability	Cytotoxicity	
	TOX21_RT_HEPG2_GLO_24hr_ctrl_viability	Cytotoxicity	
Metformin hydrochloride	TOX21_RT_HEPG2_FLO_08hr_viability	Cytotoxicity	
	TOX21_GR_BLA_Agonist_ratio	Steroidal	NR3C1
	TOX21_AR_LUC_MDAKB2_Agonist	Steroidal	AR
Ranitidine	OT_AR_ARELUC_AG_1440	Steroidal	AR
Atrazine	NVS_ENZ_hPDE4A1	Phosphodiesterase	PDE4A
Carbamazepine	ACEA_AR_agonist_80hr	Steroidal	AR
Diazepam	TOX21_RT_HEK293_FLO_40hr_viability	Cytotoxicity	
	TOX21_RT_HEK293_FLO_00hr_viability	Cytotoxicity	
	TOX21_RT_HEK293_FLO_08hr_viability	Cytotoxicity	
	TOX21_RT_HEK293_FLO_24hr_viability	Cytotoxicity	
Nicotine	NVS_LGIC_rNNR_BungSens	Ligand-Gated Ion Channel	Chrna7
	NVS_LGIC_hNNR_NBungSens	Ligand-Gated Ion Channel	CHRNA2

Chemical	Endpoints	Biological target	Gene target
Omeprazole	TOX21_RT_HEK293_FLO_32hr_viability	Cytotoxicity	
	TOX21_RT_HEK293_GLO_24hr_viability	Cytotoxicity	
	TOX21_RT_HEK293_FLO_40hr_viability	Cytotoxicity	
	TOX21_AP1_BLA_Agonist_ratio	Basic Leucine Zipper	FOS|JUN
Piperonyl butoxide	NVS_ADME_hCYP3A4	Xenobiotic Metabolism	CYP3A4
	NVS_ADME_hCYP2J2	Xenobiotic Metabolism	CYP2J2
Fluticasone propionate	TOX21_GR_BLA_Agonist_ratio	Steroidal	NR3C1
	TOX21_AR_LUC_MDAKB2_Agonist_3uM_Nilutamide	Steroidal	AR
	TOX21_AR_LUC_MDAKB2_Agonist	Steroidal	AR
Caffeine	NVS_GPCR_bAdoR_NonSelective	Rhodopsin-Like Receptor	ADORA1
	ATG_Sox_CIS_up	HMG Box Protein	SOX1
	TOX21_RT_HEK293_FLO_32hr_viability	Cytotoxicity	
	TOX21_RT_HEK293_FLO_24hr_viability	Cytotoxicity	
	TOX21_ARE_BLA_agonist_ratio	Basic Leucine Zipper	NFE2L2
	NVS_GPCR_hAdoRA2a	Rhodopsin-Like Receptor	ADORA2A

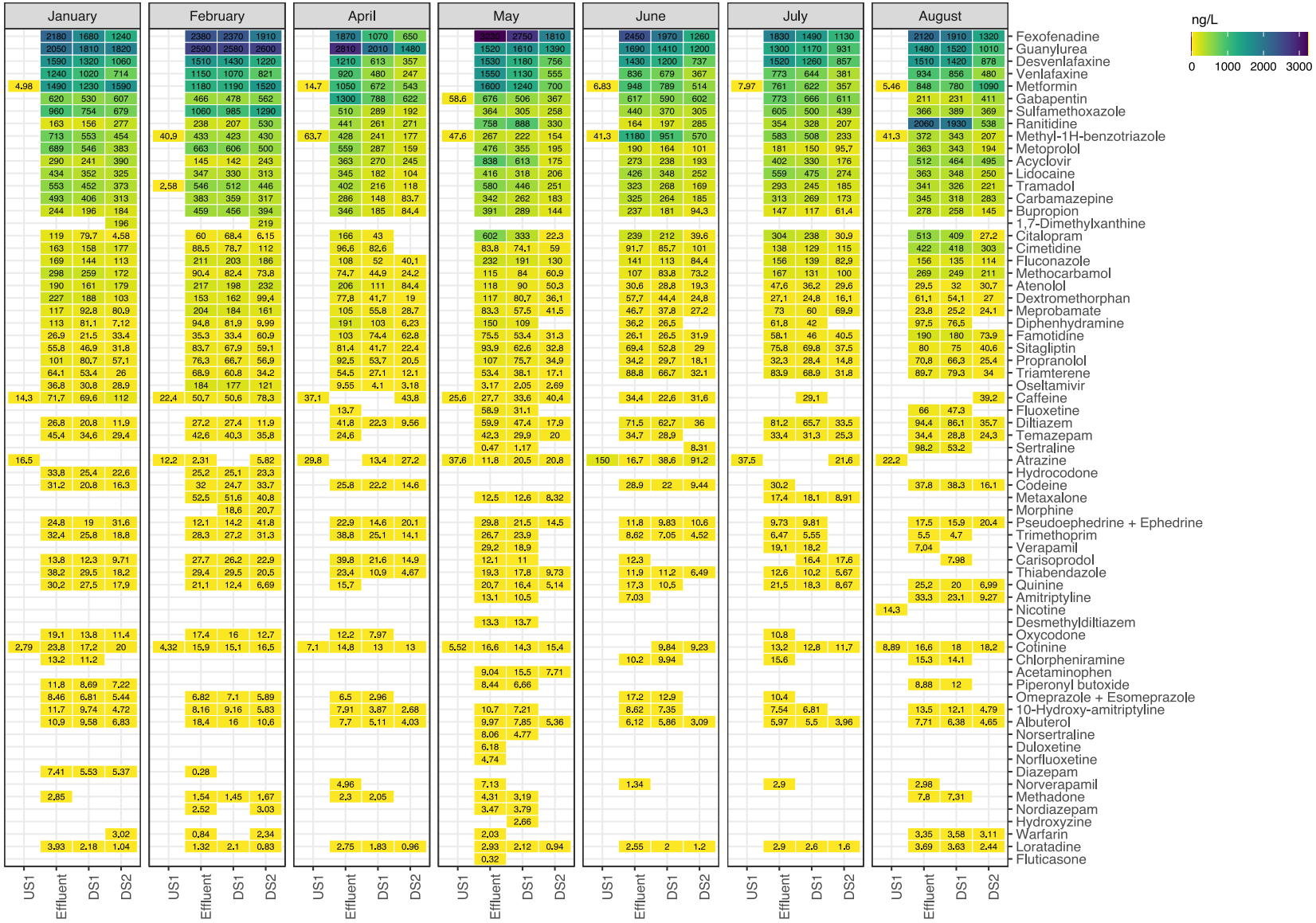

Figure B.1. Chemical measurements in ng/L for the 113 pharmaceuticals and CECs detected in Muddy Creek January-August 2018.[111]